COMPARATIVE PROTEOMICS: ASSESSING THE VARIATION IN MOLECULAR PHYSIOLOGY WITHIN THE ADDUCTOR MUSCLE BETWEEN *MYTILUS GALLOPROVINCIALIS* AND *MYTILUS TROSSULUS* IN RESPONSE TO ACUTE HEAT STRESS

A Thesis
Presented to
The Faculty of California Polytechnic State University,
San Luis Obispo

In Partial Fulfillment
of the Requirements for the Degree
Master of Science in Biological Sciences

By
Joshua Scott Mier
March 2018

COMMITTEE MEMBERSHIP

TITLE:	Comparative proteomics: assessing the variation in molecular physiology within the adductor muscle between *Mytilus galloprovincialis* and *Mytilus trossulus* in response to acute heat stress.
AUTHOR:	Joshua Scott Mier
DATE SUBMITTED:	March 2018
COMMITTEE CHAIR:	Lars Tomanek, Ph.D. Professor of Biology
COMMITTEE MEMBER:	Kristin Hardy, Ph.D. Associate Professor of Biology
COMMITTEE MEMBER:	Sandra Clement, Ph.D. Associate Professor of Biology

ACKNOWLEDGMENTS

Although this project required significant personal investment and tested the limits of my own stress tolerance, none of it would have ever been possible without the contributions and support from many admirable friends, family and colleagues. So many thanks are in order.

I would like to begin by thanking my committee members, Kristin Hardy and Sandra Clement for their patience and cooperation with the finalizing of my thesis. This experience would also not have been possible without the guidance from my advisor, Lars Tomanek and I would like to personally thank him for his mentorship, enthusiasm and patience with this endeavor. My experience within the Environmental Proteomics Lab would not have been complete, or nearly as entertaining without the camaraderie shared with my lab mates including Marcus Zuzow, Hayley Chilton, Cory Elowe, Talia Head, Aubrie Fowler, Christina Vasquez, Melissa May, Jackie Campbell, Alycia Uyeoka, Melissa Voisinet, Holland Elder, Michael Garland and James Koman. The Cal Poly Biological Sciences department faculty and staff have also been instrumental to my success and I would like to thank Ellen Calcagno, Melanie Gutierrez, Kristin Reeves, Alice Hamrick, Dave Clendenen, Eduardo Valle and Mike Curto for their assistance. Thank you all for making the department such a welcoming and vibrant atmosphere to be a part of.

I would also like to take this opportunity to thank my family for their enduring spirit and unwavering confidence in me. It has always been a foundation of strength from which I could draw upon, and I'm eternally grateful for everything you all have done. I may be biased in this particular instance, but I consider myself truly blessed to have such an amazing family.

Finally, although it took me a little longer than I would have initially anticipated, the Cal Poly Biological Sciences department has been somewhat of a home for me over the past several years. During that time, I've had the privilege of being introduced to some of the most inspiring,

talented and amiable people. Although the list is too long to thank each person individually, I would just like to say that I consider many of these people like family as well. Thanks for making graduate school so much fun to be a part of and also so hard to leave! Much obliged.

This work was funded by the National Science Foundation grant IOS-1145840 to Lars Tomanek and by Cal Poly College based fees.

TABLE OF CONTENTS

LIST OF TABLES

II. MANUSCRIPT

LIST OF FIGURES

I. INTRODUCTION

ABSTRACT

Increases in seawater temperatures have imposed physiological constraints which are partially thought to contribute to recently observed shifts in biogeographic distribution among closely related intertidal ectotherms. For instance, *Mytilus galloprovincialis* an introduced warm-adapted species from the Mediterranean, has displaced the native cold-adapted congener, *M. trossulus*, over large latitudinal expanses off the California coast. Several comparative physiological studies have revealed interspecific differences in thermal tolerance, including variation in aerobic metabolism and gape behavior, which suggest the invasive congener is better adapted to acclimate to increasing seawater conditions as predicted due to climate change. However, current analyses seek to discover the cellular process which contribute to thermal plasticity at the level of the whole organism in response to temperature stress. Since proteins represent the primary molecular machinery capable of responding to thermal stress, we quantified the proteomic response of the adductor muscles (AM) of *M. galloprovincialis* and *M. trossulus* to acute heat stress. After acclimation to 13°C, we exposed mussels to 24°C, 28°C and 32 °C (at a heating rate of 6C/h), kept mussels at the temperature for 1 h and then added a 24-h recovery period. Posterior adductor muscle samples were then excised and utilized for proteomic analysis. We were able to detect 273 protein spots within *M. galloprovincialis* and 286 protein spots within *M. trossulus.* Roughly 33% of these protein spots exhibited significant changes in abundance in response to heat stress within *M. trossulus* as compared to only 19% in *M. galloprovincialis.* In both data sets, most proteins changing abundance are part of the cytoskeleton or proteins controlling actin thin filament dynamics and stress fiber formation. Specifically, *M. galloprovincialis* increased the abundance of proteins involved in thin filament stabilization and cytoskeletal maintenance. In contrast, *M. trossulus* increased proteins involved

in thin filament destabilization and filament turnover. In addition, only *M. trossulus* increased proteins involved in the cellular stress response at the highest temperature, suggesting its AM proteome is more thermolabile. In return, our results suggest that cytoskeletal architecture is more thermally stable in *M. galloprovincialis*. The differences in the proteomic responses suggest that *M. galloprovincialis* is capable of protecting itself from heat stress through valve closure at a higher temperature due to the increase in actin stabilizing proteins.

.

Keywords: thin-filament, heat stress, contractile, adductor muscle, Proteomics.

I. INTRODUCTION

Overview

Recent increases in carbon emissions have resulted in precipitous changes in climate, culminating in a steady increase in global surface temperatures over the past half-century (Burrows et al., 2011; Doney et al., 2012). The world's oceans have retained a portion of this heat content (Levitus et al., 2012), resulting in increasing annual sea surface temperatures (IPCC, 2014). These temperature increases are of particular concern, as they often impose constraints among many coastal ectotherms adaptive capacity to respond to environmental perturbation (Bernhardt and Leslie, 2013; Pörtner, 2012; Somero, 2012). For instance, heat stress has been shown to be energetically taxing towards intertidal invertebrates, as it imposes limitations towards oxygen availability and decreases aerobic scope (Pörtner, 2009; Lockwood and Somero, 2011; Pörtner, 2012). Active thermal tolerance may be accomplished through behavioral modifications or primary physiological response mechanisms such as the attenuation of cardiocirculatory rates and aerobic metabolism (Somero, 2012; Tomanek, 2011; Pörtner, 2012). However, when exposure to temperature ranges exceeds thermal tolerance thresholds, the cellular stress response may result in the activation of compensatory molecular mechanisms, e.g., upregulation of molecular chaperones, to promote passive tolerance and mitigate the effects of thermally induced macromolecular damage (Kültz 2005; Pörtner, 2012; Tomanek, 2015). If these stress-induced compensatory mechanisms are insufficient to sustain passive tolerance, further temperature increases can expose susceptible species to critical temperatures beyond which may drastically affect individual fitness and performance (Pörtner, 2012). Furthermore, increasing sea temperatures affect the ecological resilience of coastal marine environments by increasing the frequency of disturbances, e.g., seasonal temperature extremes, which may ultimately lead to

shifts in species distribution (Perry et al., 2005; Harley et al., 2006; Sorte et al., 2011; Sunday et al., 2012), and favor the latitudinal expansion of warm-adapted species (Stillman, 2002; Tomanek, 2008; Somero, 2010). Since many intertidal ectotherms have been postulated to live near their respected thermal tolerance ranges (Pörtner and Knust, 2007; Tomanek, 2008; Tomanek, 2009; Somero, 2010), a strong emphasis in recent research comparing the effects of climate change on coastal marine ecology has been to establish potential causative links between environmental stress and the underlying physiological mechanisms which govern thermal tolerance (Somero, 2010; Tomanek, 2012). Specifically, these studies aim to gain a better understanding of which organisms are more likely to cope with environmental fluctuations in order to better predict future shifts in biogeographic distributions facilitated by climate change (Somero, 2010; Somero, 2012).

The intertidal zone represents a unique environment to study adaptive responses to environmental stress, as exposure to thermal extremes can influence patterns in species distribution even over small spatial scales (Helmuth et al., 2006; Schneider and Helmuth, 2007; Petes et al., 2007). For example, mussels occupying the mid to high intertidal exhibit cyclic changes in body temperature (T_b) which mirror monthly average peaks in both sea and air temperatures in correspondence with tidal heights (Helmuth 2009). Other studies involving intertidal mussels have also shown correlations between increased expressions of gene transcripts involved in the cellular stress response including those involved in molecular chaperoning, protein degradation, cell cycle suppression and apoptosis among high-site intertidal mussels as compared to subtidal mussels (Gracey et al., 2008). Therefore, invertebrates occupying higher vertical positions along the intertidal are exposed to greater temperature ranges which may elicit moderate to severe levels of thermal stress (Helmuth et al., 2006). This notion

is further supported from evidence comparing the heat shock responses (HSR) of several closely related species of limpets (genus *Chlorostoma*) which vary depending upon intertidal vertical location (Tomanek and Somero, 1999). In this context, several congeners exhibited similar responses in the onset temperature (T_{on}) of heat shock protein (Hsp) synthesis, when acclimated to common garden temperatures of 13°C and 24°C respectively. However, only the mid-intertidal congener exhibited the highest cessation temperature of Hsp synthesis as compared to the two-subtidal species. As such, high-intertidal organisms have been postulated to live near their physiological tolerance thresholds, and the induction of the heat shock response may represent the upper limits of thermal tolerance (Tomanek, 2008; Tomanek, 2009). These studies suggest intertidal invertebrates occupying highly variable thermal environments possess unique physiological adaptations towards dealing with their ecological niches. In addition, given the potential for increased frequencies of thermal disturbances, many aquatic organisms occupying the intertidal may be limited in their capacity to respond to climate change. Therefore, investigations into the physiological mechanisms which govern thermal tolerance within intertidal invertebrates may provide valuable insights into the adaptive mechanisms possibly contributing to biogeographical changes in response to climate change.

In this regard, mussels within the genus *Mytilus* have been studied extensively as sentinel species to monitor the impacts of environmental stress on broad scale changes in population distribution (Lockwood and Somero, 2011; Tomanek, 2011; Somero, 2012), and have even been used as baseline species to investigate ecological resilience within biomonitoring programs (Campos et al., 2012; Jarque et al., 2014: Rocher et al., 2015). Due to their sessile nature and persistence within a variety of habitats, these marine bivalves make for ideal candidates to study thermal adaptations in response to climate change, as they are relatively tolerant ectotherms

which are completely reliant upon ambient conditions for growth and survival (Lockwood and Somero, 2011). Furthermore, Blue mussels within the *M. edulis* complex are postulated to have only recently diverged evolutionarily (Seed, 1992), yet exhibit staunch differences in thermal tolerance (Braby & Somero, 2006; Schneider and Helmuth, 2007; Schneider, 2008). Since several *Mytilus* congeners experience distributional overlap in which biogeographic regions are being contested (Geller, 1999; Jones et al., 2010; Lockwood and Somero, 2011), current studies seek to identify key physiological parameters which may attribute to shifts in biogeographic ranges (Somero, 2011). Given the technical difficulties and inherent complexities associated with the integration of external stimuli in combination with the regulation of multiple stress response networks, it is difficult to quantitate the acute changes occurring at the cellular level which translate to whole-organism physiological responses of intertidal organisms during exposure to environmental stress (Tomanek, 2015). Therefore, proteomics represents a powerful tool to investigate complex regulatory mechanisms, as it comprises the full complement of proteins present within a given tissue and characterizes the molecular phenotype implemented during the thermal stress response (Tomanek, 2011; Diz et al., 2012).

In this study, we examine the proteomic responses within the posterior adductor muscle between two closely related species of Blue mussel, *M. galloprovincialis* and *M. trossulus*, in response to acute heat stress. Many omics studies investigating the differential responses of both species have focused on utilizing the gill tissue given its involvement in respiration and feeding (Tomanek and Zuzow, 2010; Lockwood and Somero, 2011; Fields et al., 2012). However, by comparing the abundance of proteins within the muscle tissue primarily responsible for controlling gape behavior, we may be able to discover potential causative links between contractile regulation and acclimation to thermal stress. In addition, the investigation into the

response of muscle tissue may compliment studies involving the gill, as it will allow for greater interpretation by providing a broader system based perspective into the potential mechanisms governing thermal tolerance. To begin, I will address the following in the preceding sections to summarize the current literature involving: I) *Mytilus* spp. natural history, uses as a model organism and current research involving physiological and molecular responses to environmental stressors, II) adductor muscle form and function and the contractile regulation involved in invertebrate muscle, and finally III) the proteomic workflow associated with the identification of novel cellular mechanisms involved during responses to environmental perturbation. I will conclude the chapter with the study goals and experimental objectives.

***Mytilus* species as a study organism**

Natural history of Mytilus spp.

M. galloprovincialis and *M. trossulus* are closely related species of Blue mussels within the *M. edulis* complex (McDonald and Koehn, 1988). The latter species, *M. trossulus*, is postulated to be the ancestral species and is thought to have given rise to *M. edulis* within the North Atlantic, following migratory shifts from Northern Pacific populations of *M. trossulus* over the past several million years (Seed, 1992). After a series of subsequent migration and geographic isolation events, *M. edulis* is thought to have given rise to *M. galloprovincialis* within the Mediterranean Sea (Seed, 1992). Given their widespread distribution and similar morphological characteristics, many researchers were led to believe that each of these species constituted a single cosmopolitan species, i.e., *M. edulis*. However, following analysis of alloenzymes and comparisons of sequence

data between common genetic loci, *M. galloprovincialis* and *M. trossulus* were confirmed as separate species from *M. edulis* (McDonald and Koehn, 1988).

Both species of Blue mussel exhibit widespread latitudinal distributions across a variety of temperate marine climates found around the globe (Figure 1; Santaclara et al., 2006; Gaitán-Espitia et al., 2016). For instance, *M. galloprovincialis*, a native to the Mediterranean Sea, displays biogeographic ranges spanning across the Northern and Southern hemispheres, including parts of East Asia, Southern Australia, New Zealand, and South Africa as well as the Southern Pacific Coast of North America (Fig. 1). In contrast, *M. trossulus*, a native to the Pacific Northwest, can be found in more Northerly latitudes such as the Baltic Sea, portions of the Northwest Atlantic, the North-Eastern Coasts of Japan and Russia and along the entire Pacific Coast of North America ranging from Baja California to Alaska (Fig. 1). Their widespread latitudinal distribution along with the capacity to develop sympatric populations in different regions where endemic species of mussels co-exist have classified the former species, *M. galloprovincialis*, as one of the top 100 invasive animal species in the world (Branch and Steffani, 2004; Lowe et al., 2000).

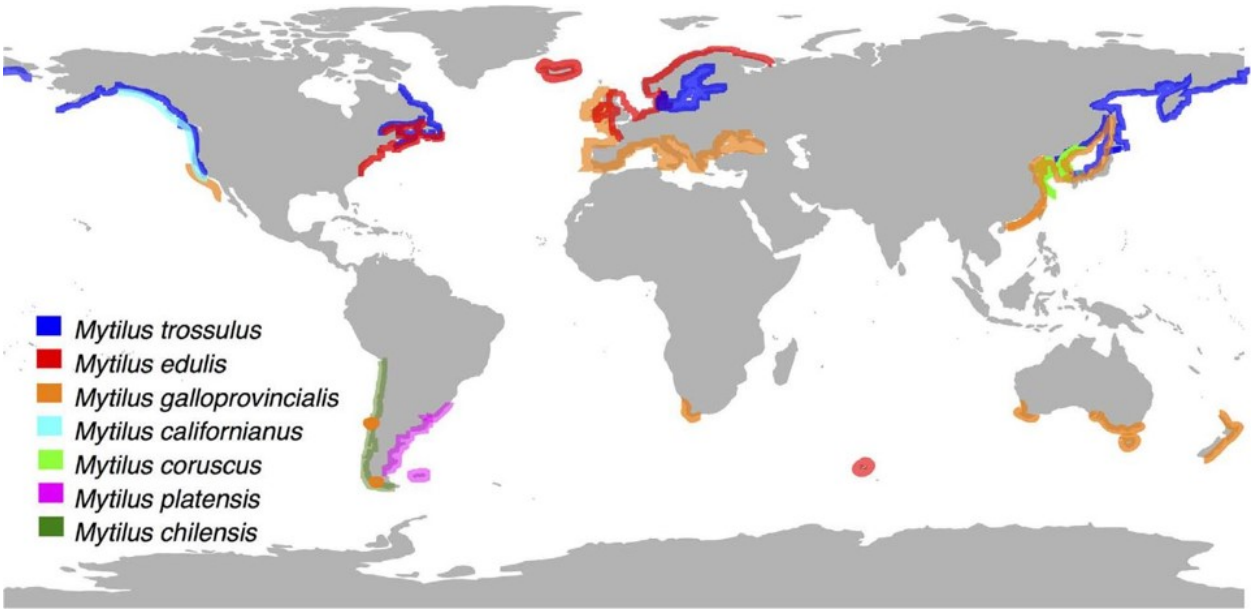

Figure 1. Global distributions and biogeographic ranges of different mussel species within the genus *Mytilus* (Gaitán-Espitia et al., 2016).

Given the relative success of the invasive congener at colonizing a variety of marine habitats, *M. galloprovincialis* has garnered notoriety as a topic of interest towards investigating the physiological mechanisms which facilitate biological invasion (Braby and Somero, 2005; Hilbish et al., 2010; Lockwood and Somero, 2011). Specifically, a large focus of research has centered on the California coast where certain contested regions of *M. galloprovincialis* and *M. trossulus* overlap (Fig. 2; Lockwood and Somero, 2011). *M. galloprovincialis* was most likely transported to the California Coast via ship ballast water sometime in the past half-century, and has since overtaken southerly portions of the *M. trossulus* former historic range (Geller, 1999). Since the introduction of the invasive species, *M. trossulus* has been displaced to regions North of Bodega Bay, California (Fig. 2). There is evidence of hybridization in regions where both species occur, although alternative evidence suggests these hybrids are infertile (Elliot et al., 2008; Lockwood and Somero, 2011). However, in regions where both species occur, *M.*

galloprovincialis and the corresponding hybrids have been observed to be larger, more abundant and even outcompete *M. trossulus* in both subtidal and intertidal habitats (Elliott et al., 2008; Shinen and Morgan, 2009). This distributional paradigm, in addition to the recent increases in sea temperatures and extreme weather events facilitated by climate change, has led to several hypotheses suggesting temperature and salinity may be two of the most influential abiotic factors driving recent shifts in species distribution along the California coast (Braby and Somero, 2005). Therefore, *M. galloprovincialis* appears to be expanding its latitudinal range at the expense of the displaced *M. trossulus* (Braby and Somero, 2005; Lockwood and Somero, 2011). Since both species share recent common evolutionary history (Seed, 1992), physiological comparisons between these two species represent a unique modeling system to investigate interspecific competition and species-specific variation in thermal tolerance which may influence changes in biogeography in response to climate change (Lockwood and Somero, 2011).

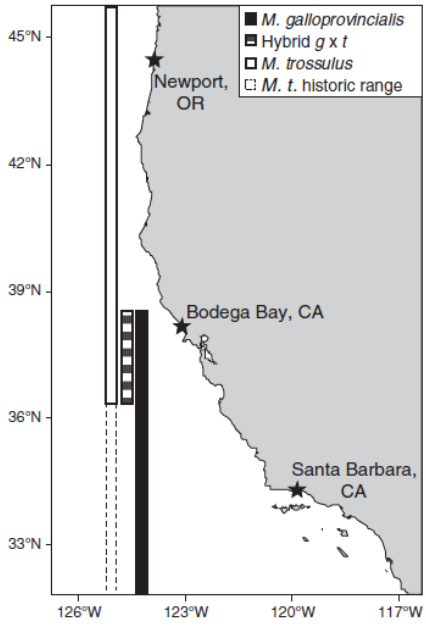

Figure 2. Distribution of *Mytilus galloprovincialis*, *M. trossulus* and respective hybrids along the California coast (Lockwood and Somero, 2011).

Comparative Physiological Responses between M. galloprovincialis & M. trossulus in Response to Temperature Stress

Many of the physiological comparisons between these species seek to ascertain the variation evident in both environmental thermal tolerance and the corresponding physiological constraints which may explain the recent changes in biogeographic distribution (Lockwood and Somero, 2011; Tomanek 2012). One of the first major interspecific differences discovered was variation in the thermal sensitivity of the enzyme cystolic malate dehydrogenase (cMDH) (Fields et al., 2006). These authors concluded that the cMDH ortholog of *M. trossulus* displayed a more thermally sensitive Michaelis-Menten constant, i.e., substrate affinity, as compared to the *M. galloprovincialis* (Fields et al., 2006). Interestingly, the biochemical differences in substrate affinity was found to be attributed to two amino-acid substitutions within the cMDH ortholog of *M. trossulus*, suggesting that enzyme kinetics could be subjected to natural selection (Fields et al., 2006). Other studies noted that relative levels of both heat-shock protein 70 (Hsp70) and ubiquitin conjugates were higher among *M. trossulus* than *M. galloprovincialis* during exposure to increases in seawater temperatures, suggesting a higher rate of thermally-induced protein denaturation occurring within the *M. trossulus* during acute heat stress (Hofmann and Somero, 1996). Subsequent experiments found that Hsp synthesis within *M. trossulus* was also induced between temperature ranges of 20°-23°C, which was much lower as compared to *M. galloprovincialis* (Buckley et al., 2001). In addition, although there have been reported acclimation effects in which both species exhibit increases of molecular chaperones at higher temperature ranges (Buckley et al., 2006), *M. trossulus* was still observed to increase the production of heat shock proteins at lower temperature ranges as compared to *M. galloprovincialis* (Tomanek and Zuzow, 2010; Fields et al.., 2012). Therefore, the interspecific differences in enzyme kinetics and regulation of molecular chaperones appear to support

adaptive differences favoring *M. galloprovincialis* in response to heat stress. However, these results do not provide specific mechanistic explanations which require further physiological comparisons to establish links between thermal adaptation and changes in species distribution.

One such study investigated the variation in heart rates between both species in response to temperature acclimation, and found that changes in cardiac output, i.e., critical heart rates or H_{crit}, are correlated with the temperature ranges to which each species is normally exposed (Braby and Somero, 2006). For instance, *M. trossulus* displayed greater tolerance to colder temperatures, as it was capable of sustaining cardiac function at temperatures lower than 14°C as compared to *M. galloprovincialis* (Braby and Somero, 2006). However, *M. galloprovincialis* appeared to display greater heat tolerance, as H_{crit} values were much higher compared to *M. trossulus* when temperatures began to exceed 21°C (Braby and Somero, 2006). These authors also assessed survivorship in response to heat stress and found that *M. trossulus* exhibited significant increases in mortality following exposure to temperatures exceeding 21°C (Braby and Somero, 2006). Therefore, heart rate also appears to be a function of physiological tolerance to heat stress, in which *M. galloprovincialis* is able to remain closed for longer durations when temperatures approach respective H_{crit} values.

Given the acclamatory ability of *M. galloprovincialis* in response to temperature increases, other studies have focused on behavioral responses to temperature stress, specifically on the opening and closing of the valve (Anestis et al., 2007; Nicastro et al., 2010). For instance, *M. galloprovincialis* reported a nearly six-fold increase in repeated valve closure events during exposure to seawater temperatures exceeding 24°C or higher as compared to conspecifics exposed to similar temperature ranges (Anestis et al., 2007). These results suggest that *M. galloprovincialis* is able to remain closed for longer durations during heat stress which may

confer increased survivorship (Anestis et al., 2007). Interestingly, links between mortality and the capacity to maintain valve closure have been reported when comparing *M. galloprovincialis* to another mussel species endemic to the Southern Hemisphere (Nicastro et al., 2010). In one instance, *M. galloprovincialis* was able to maintain valve closure for longer durations as compared to the temperate Brown mussel (*Perna perna*), which exhibited increased ventilation rates when exposed to higher emersion temperatures (Nicastro et al., 2010). These authors also observed increased desiccation stress and mortality occurring within the Brown mussel, possibly due to a limited capacity to maintain valve closure (Nicastro et al., 2010). Taken together, these results suggest *M. galloprovincialis* also displays behavioral modifications which allow them to better cope with increasing temperatures in either air or seawater as compared to other temperate mussel species.

There have also been behavioral comparisons made between *M. galloprovincialis* and *M. trossulus* in response to temperature increases reflecting fluctuations in tidal rhythmicity (Schneider, 2008; Dowd and Somero, 2013). For instance, Schneider analyzed the variation in thermal tolerance between the congeners by simulating exposure to aerial heat stress which may occur during periods of low tide (Schneider, 2008). In this context, *M. galloprovincialis* displayed higher survivorship as compared to *M. trossulus* in response to increasing emersion temperatures, regardless of immersion status (Schneider, 2008). In perhaps a more rigorous study, the variation in gape behavior and survivorship were compared between species during periods of elevated body temperature in both air and seawater over acute and chronic time courses (Dowd and Somero, 2013). In all circumstances, *M. galloprovincialis* was able to maintain valve closure for longer periods during both aerial emersion and seawater immersion as compared to *M. trossulus* (Dowd and Somero, 2013). In addition, *M. trossulus* displayed

significantly higher mortality rates as compared to *M. galloprovincialis* for each temperature treatment applied over the course of the trial period (Dowd and Somero, 2013). Together, these studies support the notion that there are potential links between physiological and behavioral modifications associated with heat stress, which may increase the mortality of the more susceptible *M. trossulus* while providing a competitive advantage for *M. galloprovincialis* (Schneider 2008; Dowd and Somero, 2013).

As further progress has been made identifying interspecific differences in physiology and behavior which may influence distributional patterns between both species in response to climate change, researchers studying this system of have become increasingly interested in attempting to link molecular changes which translate into whole-organismal responses by examining the processes occurring at the cellular level during heat stress. Many of these approaches are able to investigate the cellular mechanisms by integrating the various cellular stress response networks upregulated within various tissues during exposure to environmental stress (Joyce and Palsson, 2006; Tomanek, 2011). One of the first studies to incorporate this methodology, utilized a transcriptomic approach to investigate the variation in thermal tolerance between *Mytilus* congeners by assessing the regulation involved among thousands of mRNA transcripts during heat stress (Lockwood et al., 2010). These authors found that 31% of the transcriptome within both species exhibited temperature-dependent changes in gene expression within the gill tissue (Lockwood et al., 2010). However, only a negligible amount of gene transcripts exhibited species-specific responses including those involved cytoskeletal rearrangement, oxidative stress, molecular chaperoning and proteolysis (Lockwood et al.., 2010). Since gene transcripts do not reflect variation in protein abundance, this methodology was unable to quantify the molecular changes occurring within the proteome (Tomanek, 2011). As such, a

collaborative effort was done using the same experimental design but using a proteomics approach instead to visualize the changes in protein abundance occurring within the gill tissue in response to heat stress (Tomanek and Zuzow, 2010). In both experiments, *M. trossulus* exhibited increased expression and upregulation of molecular chaperones at lower temperature ranges as compared to *M. galloprovincialis* (Lockwood et al., 2010; Tomanek and Zuzow, 2010). However, in the proteomics experiment, *M. trossulus* also exhibited upregulation of proteasome subunits at lower temperatures as compared to *M. galloprovincialis* (Tomanek and Zuzow, 2010). Thus, both omic approaches were able to quantify changes in specific cellular processes which suggest a higher degree of proteolysis and protein denaturation occurring within the gill tissue of *M. trossulus* as compared to *M. galloprovincialis* during heat stress (Lockwood et al., 2010; Tomanek and Zuzow, 2010). Another key takeaway using the proteomics approach was that both species appeared to upregulate metabolic pathways to increase the production of antioxidants and reducing equivalents during exposure to the highest temperature ranges, suggesting oxidative stress is a costressor to temperature stress (Tomanek and Zuzow, 2010). Therefore, proteomics represents a powerful approach to provide insight into the cellular mechanisms which may confer thermal sensitivity within the gill tissue in response to heat stress.

Although these experiments provide insights into the interspecific differences in cellular processes which may be thermally adaptive, there are still gaps in current knowledge regarding the coordinated cellular responses of multiple tissues which translate to changes for the whole organism in response to heat stress. For instance, both omic experiments analyzed the changes in gene expression and protein abundance within the gill tissue (Lockwood and Somero, 2010; Tomanek and Zuzow, 2010). This tissue represents an ideal choice for experimental analysis, as the gills serve dual functional roles in feeding and respiration (Dahlhoff et al., 2002). However,

given the variation observed in gape behavior observed between the congeners (Schneider, 2008; Dowd and Somero, 2013) and the importance of the behavior in regulating both ventilation and particle exchange (Gosling, 2015), it is important to consider the regulation involved within the primary muscle responsible for controlling gape behavior.

Adductor Muscle Form, Function and Contractile Regulation

Adductor Muscle Structure and the Catch Response

Blue mussels display bilateral symmetry and retain two adductor muscles essential for controlling the opening and closing of the valve (Galtsoff, 1964; Howard et al., 2004). These muscles attach to the interior portions of the shell, and connect the shells in a transverse direction (Howard et al., 2004). The posterior muscle is much more pronounced in bivalves, as the anterior muscle may be somewhat reduced or disappears shortly after larval attachment (Galtsoff, 1964). In terms of microscopic structure, adductor muscle fibers are separated into white and translucent or obliquely-striated muscle fibers which innervate with connective tissue attached to the shell (Galtsoff, 1964). Rigidity of the muscle is retained during the development of tension within the contractile fibers and their anchorage points to connective tissue (Galtsoff, 1964). These fibers consist primarily of thick and thin filamentous structures (Philpott et al., 1960), and tension development is facilitated through the sliding-filament mechanism of actomyosin crossbridges (Millman, 1967).

Some of the earliest work done on invertebrate musculature revealed adductor muscle fibers, like many other bivalve muscles controlling gape behavior, retained the capacity to sustain tension development even after the cessation of contractile stimulation (Twarog, 1967).

This mechanism has been referred to as the catch response and describes the maintenance of tension and resistance to stretch are due to the formation of passive linkages between adjacent myosin thick filaments and actin thin filaments within the contractile apparatus during tonic activation-relaxation cycles (Hooper et al., 2008; Galler, 2008). The catch mechanism is postulated to be regulated by a large protein present on paramyosin thick filaments called twitchin (Galler, 2008, Hooper et al., 2008). Upon contractile stimulation, intracellular calcium levels increase within the smooth muscle which activate calcium-dependent phosphatases leading to the dephosphorylation of twitchin, thus allowing the protein to form passive linkages between adjacent thick and thin filaments and activate the catch response (Fig. 3; Funabara et al., 2005). The catch state is terminated when the concentration of intracellular cAMP levels increases, activating cAMP-dependent protein kinases which phosphorylate twitchin (Fig. 3; Funabara et al., 2005). The phosphorylation of twitchin severs the passive linkages between the thick and thin filaments, causing relaxation of the adductor muscle (Funabara et al., 2005). This unique property of Molluscan smooth muscle allows bivalves to retain tension within the muscle with minimal energy expenditure when exposed to external pressures (Galler, 2008). However, temperature has been shown to inversely affect Molluscan smooth muscle as increasing temperatures significantly decrease the latent period, reduces relaxation time and limits peak tension in prepared *Mytilus* smooth muscle (Linehan, 1981). In fact, when temperatures exceed 30°C, catch tension may be abolished (Twarog, 1967) and relaxation may become spontaneous (Linehan, 1981). Therefore, increasing temperatures may negatively affect the response of the adductor muscle in *Mytilus* species.

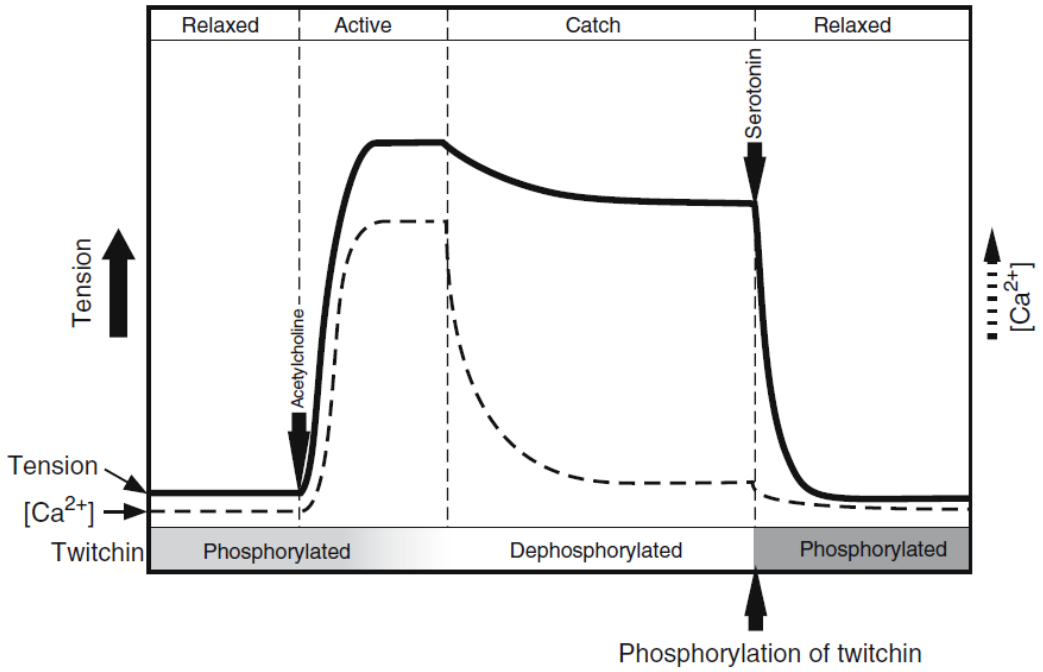

Figure 3. The relationship between the development of tension, intracellular calcium levels and phosphorylation status of twitchin within Molluscan smooth muscle (Funabara et al., 2005; Galler, 2008).

Smooth Muscle Contractile Regulation

In terms of contractile regulation and molecular structure, Molluscan smooth muscles display similar characteristics to vertebrate smooth muscle (Hooper et al., 2008). Nerve elements within visceral ganglia innervate with the adductor muscle and control tonic contraction through excitation of muscle fibers (Lowy, 1953). Release of acetylcholine from these nerve elements triggers contraction by causing an influx of calcium into the muscle cell (Fig. 3; Funabara et al., 2005; Hooper et al., 2008). The increase in intracellular calcium levels initiates actomyosin cross-bridge cycling leading to the development of muscle tension (Funabara et al., 2005; Hooper et al., 2008). During active contraction, calcium binds to actin regulatory proteins, e.g.,

troponin, which then expose myosin binding sites along the actin thin filament strand by inducing conformational changes to the thin filament stabilizing protein tropomyosin (Hooper et al., 2008). Conformational changes of myosin heads during the hydrolysis of ATP by myosin ATPase's then allow for myosin heads to attach, pull and release actin filaments causing thick and thin filaments to slide across one another resulting in tension development (Millman, 1967; Hooper et al., 2008). Relaxation occurs when the muscle is stimulated by serotonin which increases intracellular concentrations of cAMP and activates cAMP-dependent kinases (Funabara et al., 2005; Galler, 2008). These cAMP-dependent kinases phosphorylate twitchin which severs passive linkages between thick and thin filaments causing smooth muscle relaxation (Funabara et al., 2005; Galler, 2008).

Although Molluscan smooth muscle contraction is dependent upon the interactions between thick and thin filaments, there are alternative regulatory process postulated to control contractile dynamics (Hooper et al., 2008). Molluscan thin filaments contain different troponin protein isoforms (I, T & C), which together form a trimeric protein complex which functions to regulate the conformational status of tropomyosin and expose myosin binding sites on actin subunits along the filament strand during contractile impulses (Hooper et al., 2008). Molluscan smooth muscle thin filaments also contain the protein calponin, but not caldesmon, suggesting the adductor muscle exhibits differential regulatory responses to increasing concentrations of calcium (Dobrzhanskaya et al., 2013). The length of the thin filament also effects contractile dynamics and is tightly regulated by thin filament stabilizing and destabilizing factors, such as tropomyosin and profilin (Hooper et al., 2008). The variation in filamentous structures between different invertebrate smooth muscles primarily involves the structure of the thick filament which is primarily composed of paramyosin, myorod, myosin and the regulatory protein twitchin

(Hooper and Thuma, 2005; Funabara et al., 2005; Hooper et al., 2008; Galler, 2008). The contractile activity of the adductor muscle is also regulated by the phosphorylation status of myosin regulatory light chains which activate or inhibit myosin cross-bridge activity depending on the concentration of intracellular calcium (Hooper et al., 2008).

Although there has been extensive research into the structure of Molluscan muscle and the regulation surrounding the catch-state (Hooper et al., 2008; Galler, 2008; Funabara et al., 2005), much of the research involving contractile signaling pathways have focused on vertebrate smooth muscle (Gunst and Zhang, 2008; Lehman and Morgan, 2012). Smooth muscle cells are capable of undergoing dynamic conformational changes during contractile stimulation (Gunst and Zhang, 2008). Much of these dynamic structural changes are attributed to the asymmetric distribution of contractile filaments (Fig. 4; Gunst and Zhang, 2008; Galler, 2008). As such, smooth muscle contractile networks are subdivided into specific contractile domains, namely the contractile apparatus and the cortical cytoskeletal domain (Lehman and Morgan, 2012). The contractile apparatus consists of actin thin filaments, myosin thick filaments and cytosolic dense bodies located towards the interior of the cell, which serve as attachment points connecting the contractile apparatus to the membrane (Fig. 4; Gunst and Zhang; Galler, 2008). The cortical cytoskeletal domain consists of submembranous actin thin filaments and myosin filaments located near the periphery of the cell, and is tightly regulated by an assortment of thin filament regulatory proteins (Gunst and Zhang, 2008). This structural dichotomy surrounding cytoskeletal domains allows for the integration of external stimuli to facilitate active contraction through the dynamic restructuring of actin thin filaments within the cortical actin cytoskeleton (Fig. 4; Gunst and Zhang, 2008). Thus, tension development can be regulated through the dynamic remodeling of cortical cytoskeleton without involving the restructuring of actomyosin cross-bridges located

within the contractile apparatus towards the interior of the cell (Gunst and Zhang, 2008; Lehman and Morgan, 2012).

The dynamic rearrangement of cortical actin thin filaments involves the formation of macromolecular junctions, known as adhesion complexes (Fig. 4; Gunst and Zhang, 2008). During mechanical or contractile stimulation, many actin-regulatory proteins assemble within these adhesion complexes and induce the recruitment of accessory actin-binding proteins to restructure cortical actin thin filaments (A) Kim et al., 2008). Although the degree of cytoskeletal remodeling depends upon the stimulus, many of the downstream mediators activated within these pathways include signaling proteins within the Rho-family of GTPases (A) Kim et al., 2008; Gunst and Zhang, 2008; Lee and Dominguez, 2010). These downstream contractile mediators can induce post-translational modifications to proteins located within adhesion complexes, or serve as signaling scaffolds to further recruit and localize actin binding proteins to promote dynamic restructuring of cortical thin filaments (Gunst and Zhang, 2008; Lee and Dominguez, 2010; Lehman and Morgan, 2012). In addition, this can lead to the formation of dorsal actin stress fibers which can increase the number of connections between the cortical actin cytoskeleton and the contractile apparatus which further strengthens cytoskeletal integrity (Tojkander et al., 2012). Thus, smooth muscle contractile dynamics are highly dynamic and involve tight regulation surrounding actin thin filaments (Gunst and Zhang, 2008; Lee and Dominguez, 2010; Lehman and Morgan, 2012).

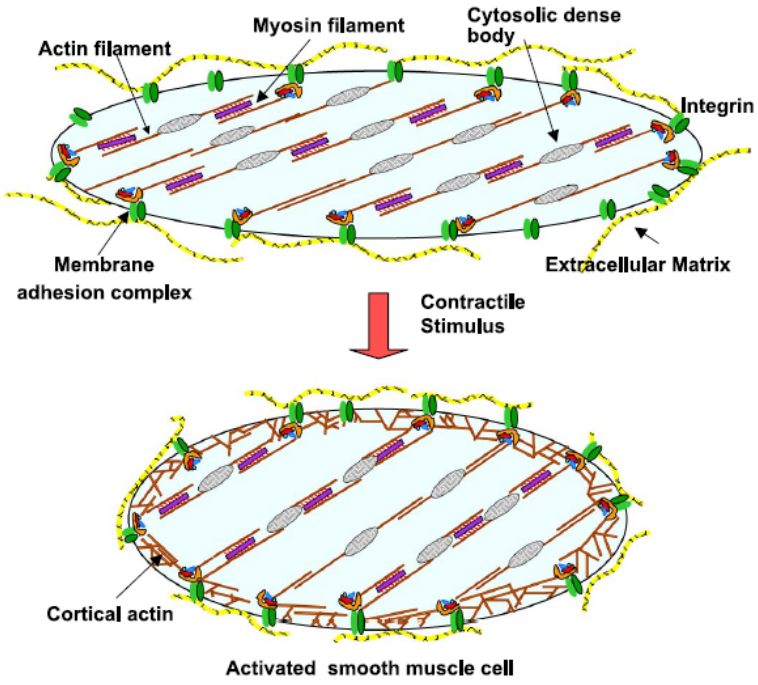

Figure 4. Hypothesized model for integrated smooth muscle contraction. Figure adapted from Gunst and Zhang, 2008.

Proteomics

Overview

Proteomics provides a holistic approach towards the investigation and analysis of the proteome, or the characterization of the entire complement of proteins expressed within a given cell (Lovrić, 2011). This technique represents a sub-discipline of various systems biological approaches, e.g., genomics, transcriptomics, metabolomics, which attempt to articulate the complex interactions occurring at the cellular level that translate into whole-organism physiological responses (Draghici, et al., 2007). These processes are very important to studying organismal responses to environmental disturbances, as they establish a conceptual framework to the cellular stress response by allowing researchers to investigate multiple cellular processes at

once, allowing for the integration of cellular processes which govern physiological organization and reestablish homeostasis following stress exposure (Tomanek, 2012; Campos et al., 2012).

A primary benefit of these high throughput technologies is that many result in the generation of substantially large data sets (Joyce and Palsson, 2006). For instance, the development of genomic sequencing methods for representative species has enabled researchers to study comprehensive patterns and interactive networks through the analysis of hundreds of different cellular components at once (Joyce and Palsson, 2006). Thus, many genomic methods including DNA microarrays and DNA barcoding have discovered evolutionary relationships between species using relatively small environmental samples (Shokralla et al., 2012). However, there are technical limitations associated with DNA amplification (Shokralla et al., 2012), and genomics does not encompass the processing of downstream gene products nor does it articulate the regulation involved in gene translation (Evans, 2015). Another major omic technology, transcriptomics, has also made significant strides linking variation in gene expression to physiological responses associated with environmental change (Lockwood et al., 2015). For instance, studies comparing the abundance of gene transcripts among mussel species within the genus *Mytilus* suggest certain factors, i.e., heat stress and tidal rhythmicity, exert substantial and robust changes within the transcriptome (Lockwood et al., 2010; Connor and Gracey, 2011). These approaches compare thousands of mRNA transcripts using high throughput sequencing techniques such as transcript microarrays or sequence analysis of gene expression (SAGE) methods (Joyce and Palsson, 2006). However, large scale changes in gene transcripts also do not necessarily equate to changes in organismal fitness and may not reflect alterations to protein activity (Evans, 2015). In addition, transcriptomic analyses fail to assess the variation associated

with post-transcriptional regulation, RNA splicing and protein modifications (Joyce and Palsson, 2006).

Although each sub-discipline offers its own suite of advantages, proteomic approaches may provide greater resolution towards the functional integration surrounding cellular networks. For instance, analysis of the proteome allows for detection of the end-products of gene expression while detecting potential post-translational modifications and protein interactions which influence cellular activity (Joyce and Palsson, 2006; Tomanek, 2011). Many proteins are also highly dynamic, e.g., metabolic enzymes and signaling proteins, and exist in a constant state of flux to detect acute changes occurring within the external environment (Tomanek, 2011). Thus, proteins represent the biochemical machinery capable of promoting rapid responses that are in tune with physiological requirements and represent the functional molecular phenotype subjected to natural selection (Tomanek, 2011; Diz et al., 2012). Proteomics can also compare patterns of protein abundance and assign specific cellular functional categories to groups of upregulated proteins, e.g., energy metabolism, which provides a greater interpretive spectrum towards the broad-scale changes occurring at the cellular level in response to stress exposure (Tomanek, 2011; Rocher, 2015). Therefore, proteomic studies have the potential to complement transcriptomic and genomic data sets by building an integrative platform to compare and contrast the different stages of regulation surrounding the molecular phenotype.

Although there are many benefits to using this multifaceted approach which aid in our understanding of cellular adaptation to external factors, there are some analytical drawbacks which limit our interpretation. For instance, this approach primarily focuses on changes in protein abundance, which may be attributed to many complicated processes including differential synthesis rates, protein degradation, cellular localization, protein-protein interactions, isoform

expression and post-translational modifications (Lovrić, 2011). As a result, it is difficult to discern the exact mechanisms occurring in response to stress exposure, without incorporating additional tests such as Western blots (Lovrić, 2011). The physiochemical properties of proteins also suggest the possibility of a multi-dimensional proteome which hinders drawing conclusions from changes in protein abundance patterns (Larance and Lomond, 2015). Next-generation proteomic techniques, including mass-spectrometry based approaches, also require sequenced genomes in order to compare experimental peptide sequences against theoretical sequences within large databases to obtain accurate protein identifications (Lovrić, 2011; Altelaar et al., 2012). Therefore, greater resolution and higher identification rates are expected if the study species in question has had its genome annotated, as attempts to quantify proteins in non-model organisms is dependent upon the availability of genetic information from sister taxa (Dowd, 2012; Altelaar et al., 2012). Even if these techniques are successful, high-throughput technologies have the potential to generate substantially large datasets containing hundreds and potentially thousands of data points (Lovrić, 2011; Altelaar et al., 2012). Therefore, interpretation requires robust statistical analyses and extensive literature research to compartmentalize changes in protein expression patterns and generate hypotheses concerning the integration of protein networks (Tomanek, 2015).

Nevertheless, proteomic approaches have a high degree of potential to enhance our understanding of cellular networks and how they contribute to organismal function in response to environmental perturbation. Therefore, in the preceding sections, I will attempt to summarize the major steps involving in the proteomic workflow utilized in our study. These sections characterize the sequence of steps required for the processing of biological samples for proteomic analysis following the experimental procedure. Briefly, these involve I) protein

separation using two-dimensional gel electrophoresis (2DGE), II) protein quantification using 2D gel analytical software and III) protein identification using tandem-mass spectrometry followed by bioinformatic searches for peptide sequence homology. For clarity, statistical representation assessing the variation in protein abundance between experimental treatments is determined using the 2D-gels and the 2D-gel analytical software (See Protein Quantification).

Protein Separation

Many experimental designs utilizing the proteomic workflow allow treated organisms to rest for a brief period under baseline conditions, to allow for protein synthesis following experimental conditions (Lovrić, 2011). Immediately following the recovery period, respective tissues to be analyzed are immediately flash-frozen in liquid nitrogen and held at exceedingly low temperatures, e.g., -80°C, to prevent protein degradation and denaturation until samples are ready to be processed (Berth et al., 2007). In this manner, flash-freezing the sample provides a snapshot of the cellular pathways induced following experimental procedure. However, careful attention to detail must be considered prior to sample preparation, as this step represents possibly one of the biggest challenges and limiting elements of proteomic analyses (Lovrić, 2011). For instance, the cell type must be taken into account as many organisms, i.e., bacteria and yeast, retain stiff cellular walls which make protein extraction difficult (Lilley et al., 2001). Other sample preparation issues include preventing protein digestion from active enzymes within the tissue, e.g., proteases, and limiting alterations such as post-translational modifications which occur during the extraction process (Lovrić, 2011). Given these issues, careful attention to detail must be considered during protein isolation techniques, otherwise the researcher risks losing a significant portion of the proteins within the sample (Lovrić, 2011). Therefore, the methods used

for sample preparation must take into account several prerequisite criteria prior to protein isolation: (1) sample should retain as many of the original and intact proteins as possible, (2) all other biological components extracted but not concerning the tissue of interest, e.g., extracellular proteins, lymph and blood, must be removed, (3) protein modifications must remain intact and finally (4) the sample composition must be compatible with all subsequent analytical steps within the proteomic method chosen (Lovrić, 2011).

The first step concerning protein extraction consists of utilizing a lysis buffer containing a high concentration of chaotropic compounds, e.g., urea and thiourea, and strong detergents, e.g., sodium dodecyl sulfate (SDS) or 3-[(3-cholamidopropyl) dimethylamine]-2-hydroxy-1-propanesulfate (CHAPS), to break open the cellular membrane and solubilize intracellular proteins (Lovrić, 2011). The chaotropic compounds present within these lysate solutions denature proteins by disrupting bonds between amino acids within tertiary structures and are also essential to inhibit the activity of proteases or other enzymes which may degrade or alter proteins within the sample (Wiśniewski et al., 2009). Other chemical components of the lysis buffer include zwitterionic detergents, e.g., amidosulfobetaine-14 (ASB14), Triton-X100 or carbonate, which disrupt hydrophobic interactions and aid in solubilizing membrane proteins (Bodzon-Kulakowska et al., 2007). Additionally, reducing agents such as dithiothreitol and dithioerythritol are needed to disrupt disulfide bridges between cysteine residues and further denature proteins into their primary state (Bodzon-Kulakowska et al., 2007). Furthermore, some compounds are added to the solution, i.e., ampholytes, which stabilize pH gradients and assist in protein migration during isoelectric focusing (Bodzon-Kulakowska et al., 2007). Although all of these compounds within lysis solutions aid in the separation and solubilization of proteins, the specific composition depends on the biological tissue being used (Lovrić, 2011). Finally, the

buffer procedure is conducted in a timely manner and kept at low temperatures as to minimize the chances of artificial changes to protein composition within the sample (Lovrić, 2011).

In addition to the lysis buffer, cells are further disrupted through a process known as homogenization (Bodzon-Kulakowska et al., 2007). There are several methods of homogenization used in proteomic procedures, but the primary categories involve mechanical breakdown, ultrasonic cellular lysis, pressure homogenization, freeze-thaw, detergent based cell lysis and using osmotic pressure gradients (Bodzon-Kulakowska et al., 2007). Once the cells have been thoroughly disrupted, cellular contaminants need to be removed in order to prevent protein aggregation which would impede protein migration during isoelectric focusing (Lovrić, 2011). For instance, lipids and salts interact and complex with proteins, thus altering their structure and reducing their solubility within the buffer solution (Bodzon-Kulakowska et al., 2007). Other contaminants, such as polysaccharides and nucleic acids interact with carrier ampholytes and can impede 2D separation, resulting in potential streaking of gels (Shaw and Reiderer, 2003; Bodzon-Kulakowska et al., 2007). Furthermore, even the relative protein concentration within the sample can impede 2D gel resolution, as abundant proteins within biological samples can limit the possibility of detecting proteins which occur in lower abundance (Bodzon-Kulakowska et al., 2007; Lovrić, 2011). Therefore, many proteomic analyses include a protein precipitation step, e.g., tricarboxylic-acid/acetone or chloroform/methanol precipitation accompanied with cold centrifugation, which allows for contaminant elution followed by protein resuspension in buffer solution (Shaw and Reiderer, 2003; Bodzon-Kulakowska et al., 2007).

Once proteins within the sample have been concentrated and the potential contaminants have been removed, the precise protein content within the sample must be determined in order to ensure equivalent concentrations of proteins are loaded for first dimension separation (Lovrić,

2011). Typically, standard Bradford assays are sufficient to determine the relative concentrations of proteins within a sample (Lovrić, 2011). However, the chaotropic agents and detergents within the lysis buffer alter spectrophotometric readings (Lopez, 2007). Therefore, certain proprietary concentration assays are optimized for proteomic analyses, e.g., 2D Quant kits (GE Healthcare), in which copper ions are added to the sample solution and bind to the peptide backbones of proteins present within the solution (Weist et al., 2008). The resulting colorimetric reading is inversely related to the protein concentration, meaning that lower absorbance values indicate a higher total amount of protein within the sample (Weist et al., 2008). Determining the amount of protein within each sample is essential, as most guidelines for isoelectric focusing require between 100 μg-500 μg of protein loaded onto each immobilized pH gradient (IPG) strips (Görg et al., 2004). These IPG strips are very stable and provide a carrier matrix containing ampholytes to allow for separation of proteins based on the isoelectric points, or the pH range at which proteins exhibit a net neutral charge (Görg et al., 2009; Lovrić, 2011). Prior to isoelectric focusing (IEF), i.e., separation of proteins along a linear gradient, IPG strips are rehydrated in a solution containing iodoacetamide, glycerol, urea and dithiothreitol (DTT) to further aid in protein migration (Görg et al., 2009). Once the IPG strips have been rehydrated, the solubilized protein solution is then immersed in these IPG strips and proteins are separated during IEF through a series of running conditions in which a voltage and current gradients are applied (Görg et al., 2009). This process of IEF and applied voltages gradients is referred to as separation in the first dimension, and it is important to emphasize that each first-dimension protocol is optimized for the particular sample under investigation (Bodzon-Kulakowska et al., 2007; Weist et al., 2008). Therefore, the number of hours in which a voltage is applied, the voltage (V) and current (μA) ranges used, the type of IPG pH gradient strip used and the optimum focusing time are all

dependent upon the amount of protein loaded and the tissue type under investigation (Görg et al., 2009). Finally, once the proteins are separated in the first dimension, the IPG strips are kept at a very low temperature holding state, e.g., -20°C to -80°C, until samples are ready to be further processed.

After proteins are separated in IEF during first dimension, the IPG strips are then used to separate proteins further in a second dimension during gel electrophoresis (2DGE). The most commonly used procedure involves using sodium dodecylsulfate-polyacrylimide gel electrophoresis (SDS-PAGE) to separate proteins based on their apparent molecular weights (Lopez 2007; Friedman et al., 2009; Lovrić, 2011). SDS is an amphipathic molecule with a long hydrophobic tail and polar sulfate head group (Lovrić, 2011). These structural characteristics allow SDS molecules to readily bind to peptide backbones in a sequence ratio of one SDS molecule per two amino acids (Lovrić, 2011). This binding affinity also efficiently denatures proteins and gives them a strong net negative charge which is attributed to the negatively charged sulfate group of the SDS molecule, thus allowing denatured proteins within an aqueous solution to migrate towards the positively charged cathode when a constant current is applied (Lovrić, 2011). The polyacrylamide matrix serves as a chemically modified mesh network which separates the anionic SDS/peptide complexes based on molecular weight (in kilodaltons or kDa), in which smaller proteins are able to migrate further down the vertical axis of the gel (Lopez, 2007). The IPG strip is first loaded onto the top of the polymerized polyacrylamide matrix, along with a molecular weight standard to aid in the estimation of molecular weights (Lopez, 2007). The acrylamide percentage used in the gels determines the range of linear protein separation; however, the most commonly used acrylamide concentrations are between 10-12.5% which roughly separates proteins within a 15-150 kDa range (Lovrić, 2011). Most 2DGE procedures

use the standard Tris-chloride/Tris-glycine buffer system in which the running buffer consists of an aqueous solution of one mol/L of Tris-chloride and 20% SDS with the pH lowered to 8.4 (Lopez, 2007). The running buffer solution provides and electrical conduit when a voltage gradient is applied (Lovrić, 2011). Typically, the electrical field applied will be between 3 to 30V/cm, corresponding to an average run time of 90 minutes (Lovrić, 2011). Once the loading dye color marker, i.e., bromphenol blue, has reached the bottom of the gel, the proteins have finished migrating (Lovrić, 2011). Typical run times for 2DGE gels last between 45-60 minutes based on this process (Lovrić, 2011). Gels are promptly removed and the proteins are fixed within their relative positions with the aid of specific staining protocols. The type of staining protocol varies depending upon the proteomic analysis and the staining sensitivity, but most visualization procedures use either fluorescent, e.g., LavaPurple, SYPRO Ruby, or colorimetric stains, e.g., Silver Stain or Colloidal Coomassie Blue (CCB) (Lopez, 2007; Friedman et al., 2009; Lovrić, 2011). Most proteomic protocols utilize acidic CCB as the preferred staining procedure as it is considered one of the most sensitive staining methods, it is very specific to proteins as opposed to other biological macromolecules and is arguably one of the most compatible staining procedures used in tandem with mass spectrometry (Lopez, 2007; Lovrić, 2011).

Protein Quantification

One of the main goals in gel-based proteomic analyses involves determining the relative variation in protein abundance within samples following SDS-PAGE. In order to detect and accurately measure quantitative changes in protein abundance, gels have to be digitized with the aid of a camera or scanner (Lopez, 2007). Once scanned, digitized gel images are usually

converted into specific files, e.g., TIFF files, which provide adequate resolution for gel-image analysis software packages (Lopez, 2007; Lovrić, 2011). Adequate resolution also depends upon the quality of the gel (Lovrić, 2011). Gels displaying high resolution in protein expression are usually devoid of streaks, bubbles and other physical deformations (Lovrić, 2011). Also, quality gel images display a more precise noise-background ratio, in which there is a staunch contrast between the protein spots present within the gel image in relation to the background stain (Lovrić, 2011). Typically, this involves a washing step prior to scanning to remove as much of the unbound stain as possible from the background of the gel. However, this can also be achieved by altering the pixel density spectrum, i.e., dots per inch or dpi, within the TIFF image to create a higher contrast of protein spot visualization (Lovrić, 2011). Although, if researchers are going to incorporate the latter strategy into their proteomic workflow, they must apply the chosen dpi setting to every gel within the experiment, otherwise it could increase the chances of identifying proteins which are false positives during image analysis (Lovrić, 2011).

Analysis of SDS-PAGE gel images and changes in protein abundance following digitization requires sophisticated software programs, as 2D gels can separate up to several thousand protein spots at once (Berth et al., 2007). There are multiple commercially available programs, but the two of the most commonly used, i.e., Delta 2D (DECODON; Greifswald, Germany) and Z3 software (Compugen), superimpose gel images to create and compare spot boundaries between gels of various treatment groups (Berth et al., 2007). Protein spot positions may change based on the running conditions and techniques used during 2DGE, and other issues surrounding spot matching can make comparing spot patterns between samples difficult (Berth et al., 2007). However, these issues can be solved by applying a gel-warping strategy which utilizes an algorithm to combine the all the spots from each of the samples to create a representative

image for the entire experiment (Fig(s) 5A, 5B & 5C; Luhn et al., 2003). This representative image, also referred to as the fusion image or proteome map, is used to generate a consensus spot pattern which defines the average spot boundaries for all the individual protein spots represented within each sample (Fig. 5D; Berth et al., 2007). Once the consensus spot pattern is generated within the fusion image, it is then transferred back to all gel images for the experiment, and the variation in protein abundance is quantified by measuring differences in mean spot volumes between treatment groups (Berth et al., 2007). The response variable measured in the context of spot volumes is pixel density, and algorithms are then used to detect changes in pixel density and quantify changes in abundance by averaging the pixel densities within the spot boundaries for each gel (Fig(s). 5E & 5F Berth et al., 2007). Each pixel, with respect to the software package being used, equates to roughly about 0.1 mm in total volume (Lovrić, 2011). Alterative variables for equating changes in mean abundance may compare pixel size or area, intensity of the pixels within the protein spot or the sharpness of the spot (Lovrić, 2011).

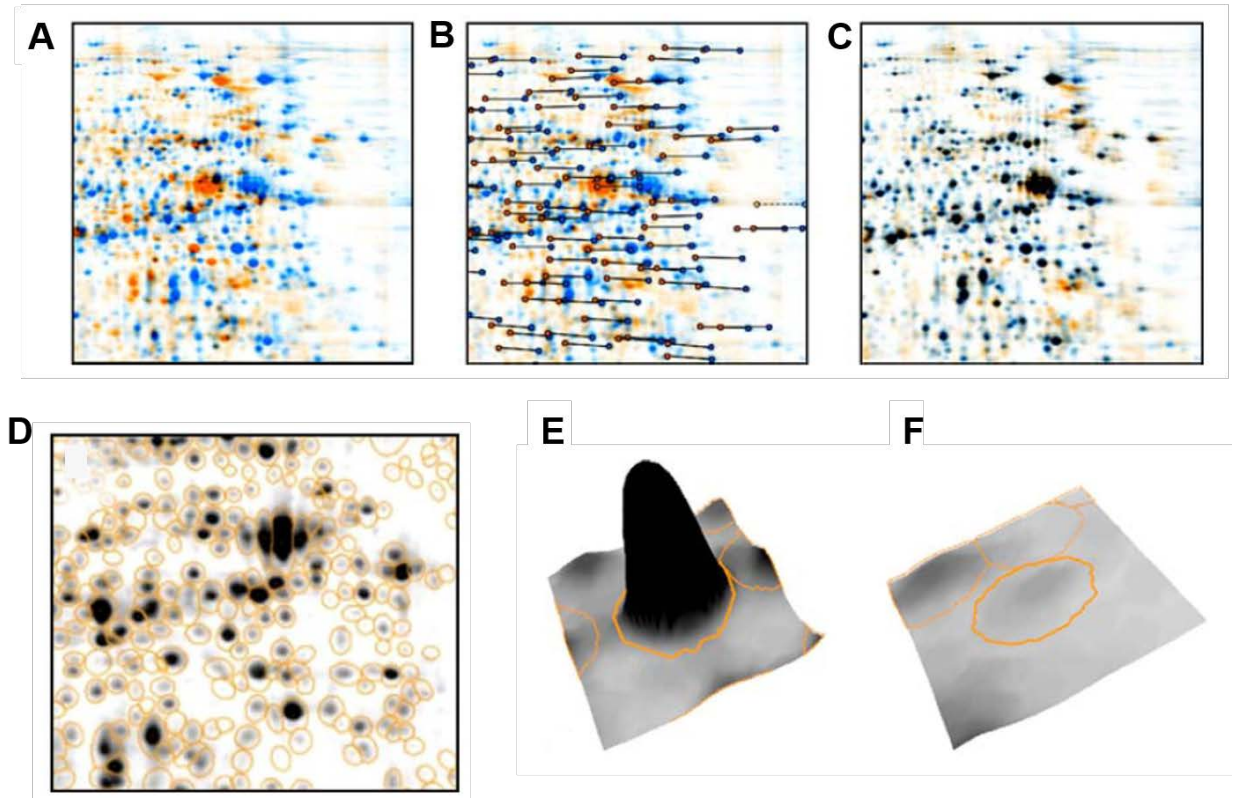

Figure 5. Software analysis of protein spots from two-dimensional gels using Delta 2D (DECODON; Greifswald, Germany). A) Two gels depicted by color. The orange gel represents a sample from an experimental treatment which is to be warped onto a control gel represented in blue. B) Vectors are used to align equivalent protein spots on both gels. C) Following a warping strategy, the gels are superimposed upon one another. Portions of the protein spots which overlap along the gel are highlighted in black, whereas portions which do not overlap and exhibit unique spot boundaries are highlighted in orange. D) Fusion image displaying the consensus spot pattern. Examples of protein abundance: E) high abundant spot displaying a high average pixel density or normalized spot volume; F) low abundant spot. Figure modified from Berth et al., 2007.

Prior to performing statistical analyses, all spots volumes must be normalized. The technique is used to minimalize differences between the gel images attributed to methodical approaches (Berth et al., 2007). Normalization uses the raw data from all the protein spot

volumes to gain a reliable measure of spot quantity, spot outline, position of the spot center and spot quality (Berth et al., 2007). It is important to note the process of protein spot volume normalization, as it helps reduce the propensity for higher abundant proteins to mute lower abundant proteins (Meunier et al., 2007). To compensate for this, some normalization methods involve dividing all the expression profiles by the maximum protein spot volume, or inducing a log transformation of the data (Meunier et al., 2007). However, one commonly used method is the logged ratio-based approach in which each individual spot volume is divided by the mean of all the existing values for that particular protein spot within all the gel samples of the experiment (Meunier et al., 2007). The logged ratio-based approach can be optimized even further by performing a logarithmic transformation. In this context, each gel sample or protein spot volume can be compared to a respective synthetic mean value for greater comparison: samples which display a zero-value exhibit no differences between the means, whereas deviations of +/- one or two exhibit plus or minus orders of magnitude higher or lower abundance (Meunier et al., 2007). This is a commonly used normalization approach used in large quantity proteomic data sets, and can be even further optimized within displaying microarrays by assigning color patterns to indicate higher or lower abundance changes (Berth et al., 2007; Meunier et al., 2007).

Once all spots have been normalized, changes protein abundance between the treatments can be assessed. Since 2DGE has the capability of producing thousands of potential protein spots, it important to realize that the false discovery rate could potentially lead to a high concentration of false positives (Lovrić, 2011). One method to mitigate the false discovery rate in proteomic analyses is to include a more stringent alpha value (Berth et al., 2007). Another issue which may arise when comparing changes in mean abundance is that gel image analyses usually do not support some of the assumptions of an analysis of variance test, including the

prerequisites of normal distribution and equal variance of the residuals (Meunier et al., 2007). Therefore, an alternative approach to this problem involves the use of a permutation test, which calculates the probability of getting a value equal to or more extreme than an observed value of a test statistic under the null hypothesis by recalculating the test statistic following random shuffling, i.e., permutations, of the data (Anderson, 2001). In this context, the number of random shuffling events depend upon the chosen alpha-value, however, the general rule is at least 1,000 permutations given an alpha value of 0.05 (Anderson, 2001). Therefore, permutation analysis of variance tests allows for the recalculation of a statistical distribution by obtaining a new value for the *F*-statistic (Anderson, 2001). The permutation analysis of variance tests is particularly useful for large data sets and are used in many biological and ecological applications (Anderson, 2001; Berth et al., 2007)

Following a permutation test for analysis of variance, the computer software program determines the number and specific protein spots which exhibit significant increases or decreases in mean spot volume with respect to treatment. However, biologists are more concerned with the relative pattern of proteins changing abundance in response to experimental treatment and are conflicted with the issue of having to analyze up to thousands of proteins at once (Berth et al., 2007; Meunier et al., 2007). Therefore, a common solution is to group together proteins which exhibit similar changes in protein abundance, i.e., patterns of upregulation or downregulation, and cellular function to organize their interpretation in a biological context (Berth et al., 2007). The primary unit of these analyses are heat maps, i.e., hierarchical clusters (HCA), which are visual graphics displaying the changes in protein abundance by grouping proteins which exhibit similar correlated patterns of abundance in response to treatment (Berth et al., 2007). The precise grouping of these expression profiles depends upon the clustering methodology, but it primarily

involves processing the data matrices into an HCA by calculating a distance and linkage metric (Meunier et al., 2007). Some of the most commonly used distance metrics used in proteomics are the Euclidean metric or the Pearson Correlation metric (Meunier et al., 2007). Both of these require normalization of spot volumes, i.e., to mitigate the effects of more strongly abundant proteins (Meunier et al., 2007). However, the Pearson correlation has been noted as one of the more popular procedures, as it is considered less sensitive to the scale of protein spot volumes (Meunier et al., 2007). Following application of the distance metric, proteins are assembled into horizontal dendrograms, in which groups of proteins displaying similar patterns of abundance are clustered together into specific groups (Meunier et al., 2007). Generally, gels samples are included along the top axis which separates each sample replicate into individual columns according to treatment group (Meunier et al., 2007). Finally, a standardized abundance range depicting deviations in mean abundance is given as a color indicator to visualize which proteins exhibit either increased or decreased abundance responses (See Results and Discussion section of Manuscript Chapter for details; Meunier et al., 2007).

Although HCA's are a valuable interpretative tool to assess the patterns of significant changes in protein abundance in response to treatment, it does not determine specifically which proteins exhibit the greatest changes towards the differences separating the particular treatment groups. It also does not determine whether individual proteins specifically exhibit significant increases in abundance in response to a given treatment. The HCA's are primarily used to develop hypotheses regarding the patterns of protein expression in response to experimental treatment (Meunier, et al., 2007). Therefore, alternative statistical test provides even greater interpretive strength to proteomic data sets. One commonly used statistical tool in the proteomic arsenal includes principal component analysis (PCA). The PCA's can be done for proteins or gel

samples, but gel samples are typically of greater use for biological interpretation as they may offer a greater explanation towards the separation and or overlap between treatment groups (Berth et al., 2007). Essentially, PCA's project changes in protein abundance into a multidimensional plane in which the variation in the data is preserved and principal components are directions or axes along which the variation in protein changes is maximal (Berth et al., 2007; Ringnér, 2008). There may be many different components, however, the top two components explain the greatest proportion of the variation in protein abundance and are then plotted along a two-dimensional plane (Ringnér, 2008). All gel samples are considered vectors and are plotted within the plane according to the spot intensities within the gels (Berth et al., 2007). The spot intensities or spot volumes, therefore, serve as coordinate points for each of the gel samples (Berth et al., 2007). All spots are included in the PCA 'coordinate point cloud' and gels are aligned according to the changes in protein abundance of the corresponding tissue sample (Ringnér, 2008). Then the analyst determines whether experimental groups exhibit similar or differential responses to treatment by assessing the relative overlap of the gel samples; those samples which exhibit overlap share similar responses in terms of protein abundance to treatment, whereas samples which exhibit a high degree of separation are considered to exhibit substantially different responses to treatment (Ringnér, 2008). Finally, in order to determine how individual proteins, change in abundance in response to treatment, *post-hoc* analysis of expression profiles may be conducted using Tukey's pairwise comparison analysis of variance (Berth et al., 2007; Tomanek & Zuzow, 2010). This method allows the researcher to determine whether individual proteins exhibit significant changes in proteins abundance to specific experimental treatment groups (Tomanek & Zuzow, 2010).

Protein Identification

The ability to identify proteins and describe potential modifications to their structure in response to external perturbations is a central theme of proteomics (Domon and Aebersold, 2006; Bensimon et al., 2012). The identification of proteins not only provides a principle link between the genome and cellular physiology, but it also provides a unique perspective into the complex molecular mechanisms and regulatory networks which govern the molecular phenotype (Tyers and Mann, 2003; Domon and Aebersold, 2006; Gstaiger and Aebersold, 2009; Diz et al., 2012). Prior to the discovery of genomic techniques and other high throughput technologies to analyze large scale changes in biological systems, biochemical analysis of polypeptide sequences was an arduous and labor-intensive process, often involving the stepwise chemical digestion of amino acid residues followed by residue detection via fluorescent spectroscopy (Domon and Aebersold, 2006). However, given the recent expansions in genomic sequence databases in addition to the advances in mass spectrometry (MS) techniques, comprehensive quantification of the full complement of proteins within a biological sample has become more readily accessible (Domon and Aebersold, 2006; Gstaiger and Aebersold, 2009; Bensimon et al., 2012).

Mass spectrometers were limited in their early use as they were restricted to very small and thermostable compounds, owing to their incapacity of limiting excessive fragmentation of ionized molecules during transition from the condensed phase to the gas phases of the ionization process (Domon and Aebersold, 2006). However, the development of soft-ionization techniques allowed for molecular ions of biological macromolecules to remain intact, thus further perpetuating the incorporation of mass spectrometry into the analysis of polypeptides (Domon and Aebersold, 2006). Mass spectrometers tend to vary depending upon the initial peptide

separation process and ionization methods used (Aebersold and Mann, 2003). In general, however, all mass spectrometers principally consist of several main components: an ion source, a mass analyzer and an ion detector (Fig. 6A; Aebersold and Mann, 2003). Following ionization, charged particles are accelerated through a vacuum according to their relative molecular mass (Aebersold and Mann, 2003). This is referred to as the mass-to-charge ratio (*m/z*-value), which aids in the determination of the peptide sequence (Fig. 7B; Aebersold and Mann, 2003). The detector then registers the numbers of ions present at any given *m/z* value (Aebersold and Mann, 2003). The data resulting from the ionization of the accumulated peptides is then provided as a series of isotopic peaks or mass spectra, commonly referred to as the peptide mass fingerprint (PMF) (Fig.7B; Domon and Aebersold, 2006; Tomanek, 2011). Furthermore, selected peptides can be further fragmented by collision induced dissociation (CID) through tandem mass spectrometry (MS/MS), which generates a second mass-spectra known as the peptide fragmented fingerprint (PFF) (Fig. 7B; Domon and Aebersold, 2003; Suckau et al., 2003; Tomanek, 2011). The PFF is important towards interpreting the amino acid sequence and is therefore capable of detecting changes attributed to the protein structure (Suckau et al., 2003). Thus, tandem MS/MS has the capacity to determine both the identity of the protein as well as any additional protein interactions or potential post-translational modifications (Bensimon et al., 2012).

Currently, the two most common soft ionization techniques used in proteomic workflows to generate mass-spectra are electrospray ionization (ESI) and matrix assisted laser desorption/ionization (MALDI) (Fig(s). 6B & 6C; Aebersold and Mann, 2003). Both techniques efficiently sublimate peptides during the gas phase and all mass spectrometry techniques require proteins be digested prior to ionization, as large polypeptides are often indistinguishable and generate low quality isotopic peak patterns (Aebersold and Mann, 2003; Lovrić, 2011).

However, both MS techniques are optimized for proteomic workflows depending upon how the isolated proteins are prepared prior to ionization (Aebersold and Mann, 2003; Lovrić, 2011). ESI is used to analyze multiple peptides resulting from a complex biological solution, and therefore is used in tandem with liquid chromatography peptide elution procedures (Aebersold and Mann, 2003; Lovrić, 2011). In contrast, MALDI ionizes peptides which have been isolated within a solid crystalline matrix (Aebersold and Mann, 2003; Lovrić, 2011). ESI is considered to be the more efficient ionization technique (Lovrić, 2011). However, ESI is also said to be more susceptible to potential contaminants accumulated during the separation process, which can impede upon isotopic peak detection (Lovrić, 2011). In addition, MALDI is the preferred option when analyzing isolated peptides originating from 2D gels (Aebersold and Mann, 2003). Since the ionization method utilized in this study was a MALDI tandem time-of-flight mass spectrometer (MALDI-TOF/TOF MS), I will focus on this method for the remainder of the review.

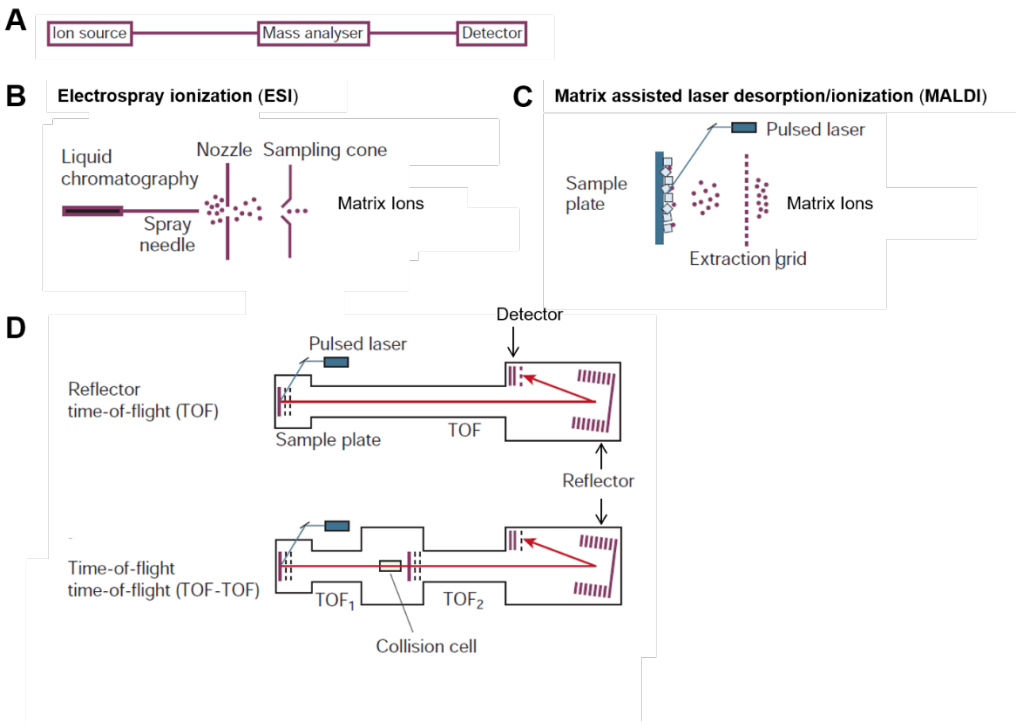

Figure 6. Basic principles involved in commonly used mass spectrometers in proteomic research. A) All mass spectrometers generally consist of an ion source, mass analyzer and a detector. The two most commonly used techniques in MS to ionize and measure proteins are B) electrospray ionization (ESI) and C) matrix-assisted laser desorption/ionization (MALDI). D) In time-of-flight (TOF) analyzers, the mass-charge ratio (m/z) is determined by the flight time it takes for ionized particles to move through the specified length of the vacuum tube within the first quadrupole (Domon and Aebersold, 2006). In tandem time-of-flight (TOF-TOF), or MS/MS mode, the selected ions are further fragmented in a collision cell using collision-induced dissociation, and are then detected during the second time-of-flight (TOF_2). Figure adapted and modified from Aebersold and Mann, 2003.

In order to prepare isolated peptides for MALDI-TOF-TOF MS, proteins have to first be excised from the 2D gels of origin and separated from the resulting gel spots. After the proteins have been eluted from the acrylamide matrix, they are subsequently digested into peptides by proteases which cleave peptides as specified amino acid residues (Aebersold and Mann 2003;

Domon and Aebersold, 2006; Lovrić, 2011). Protein digestion is usually performed by the enzyme trypsin, which cleaves proteins at C-terminal lysine and arginine residues (Lovrić, 2011). The digested peptide solutions are then precipitated and a matrix solution is added to the mixture (Fig. 7A). Although there are many different available matrix solutions, the most commonly used matrix in MALDI-MS is α-Cyano-4-hydroxycinnamic acid (CCA), as it slightly more sensitive than alternative matrices and it complements well during MS/MS analysis (Lovrić, 2011). Following the addition of the matrix solution, the resulting matrix/peptide mixture is then aliquoted and saturated onto a MALDI steel target plate using a hydrophobic solvent such as acetonitrile. Once the peptide matrices have dried within the target plate, the plate is loaded into a high vacuum and a point laser delivers pulsed wavelengths of about 370 nm, i.e., around the maximum absorption range of the matrix chosen, at the target sites which generates a plume of charged analytes and matrix ions (Fig. 6D; Aebersold and Mann, 2003 Lovrić, 2011). The matrix is important as it assists in the protonation of ionized peptides, thus providing a net positive charge which aids in ion acceleration (Lovrić, 2011). It also helps keep the fragmented peptide ions stable during laser-induced sublimation (Suckau et al., 2003). The ionized peptides are then accelerated through the mass analyzer facilitated by a series of voltage plates (Fig. 6D; Aebersold and Mann, 2003; Lovrić, 2011).

The mass-to-charge ratio (*m/z*) of ionized peptides is deduced by the flight time taken through specified length of the vacuum, which is registered at the mass analyzer (Fig. 6D; Aebersold and Mann, 2003; Domon and Aebersold, 2006). Typically for MALDI based MS analysis, linear TOF mass analyzers are used as they compensate for size variation between similarly charged peptide ions, as smaller ions are detected before larger ones (Lovrić, 2011). During the first round of peptide ionization (MS), peptide fragments are detected according to

their *m/z*-values in mass spectra, with the intensity of the isotopic peaks indicating the relative abundance of a particular peptide (Aebersold and Mann; Lovrić, 2011). The resulting MS spectra or PMF can then be uploaded to sequence databases to identify proteins by matching them to theoretical peptide spectra (Aebersold and Mann, 2003; Domon and Aebersold, 2006). In this instance, theoretical spectra from sequence databases are processed *in silico* to quantify the corresponding peptide sequences which would occur following trypsin digestion (Lovrić, 2011). Following MS and PMF analysis, certain peptide ions can be further fragmented using collision induced dissociation (CID) (Fig. 7A; Lovrić, 2011). This process otherwise referred to as tandem MS (MS/MS) produces a second mass spectra or PFF, which displays further information regarding the amino acid sequence (Fig. 7B; Aebersold and Mann, 2003). Therefore, MALDI TOF-TOF MS/MS represents a powerful analytical technique which can identify proteins and possible modifications to peptide structure (Lovrić, 2011).

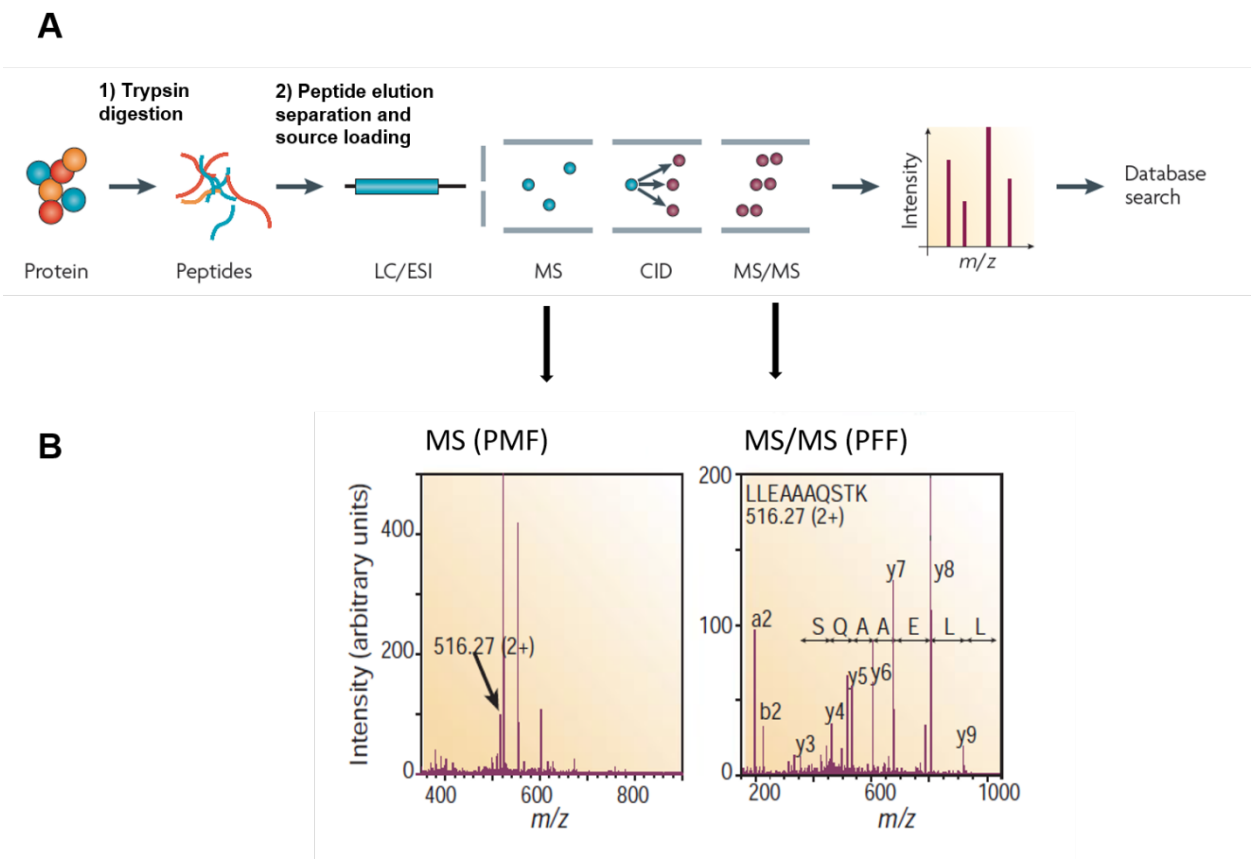

Figure 7. Principle steps involved in the preparation of peptide mixtures for mass spectrometry based analysis. A) Protein mixtures are enzymatically degraded; digestion usually occurs by the protein trypsin, which cleaves proteins at specifically known amino acid residues (Lovrić, 2011; Tomanek, 2011). B) Example of experimental mass spectra or the peptide mass fingerprint (PMF) displaying m/z ratios of ionized peptides. Selected peptides may be further fragmented to show potential differences in amino-acid sequences through analysis of a peptide fragmented fingerprint (PFF). Figure adapted and modified from Aebersold and Mann, 2003 & Gstaiger and Aebersold, 2009.

Although tandem mass spectrometers have the capacity to generate thousands of reliable fragmented peptide spectra, MS/MS generated spectra have to be aligned with the correct peptide spectra during bioinformatics searches (Lovrić, 2011). This represents unique logistical issues involved with data processing, as the sheer volume of potential data generated from MS analysis

requires advanced computational and analytical software tools (Nesvizhskii et al., 2007). In general, the assigning of spectra can be separate into three subcategories: I) Database searching, in which experimental MS/MS ion spectra are compared to theoretical predicted ion spectra within chosen sequence database libraries; II) *De novo* sequencing, in which the experimental MS/MS ion spectra serve as the template for translation of the peptide sequences; and III) Hybrid or sequence tag approaches, in which partial sequences generated from experimental MS/MS ion spectra are limited to databases which contain the partial sequence extrapolated from the experimental MS/MS spectra (Nesvizhskii et al., 2007). However, the majority of large-scale proteomic strategies utilize the database searching approach (Lovrić, 2011).

Sequence databases vary in terms of their overall completeness, sequence redundancy and sequence quality; however, there are several common sequence databases available for MS/MS spectra interpretation (Nesvizhskii et al., 2007). These include the Entrez database from the US National Center for Biotechnology Information (NCBI), RefSeq (NCBI), Swiss-Prot, TrEMBL and the International Protein Index (IPI) (Nesvizhskii et al., 2007). If the proteomic studies involve organisms whose genome has not been fully annotated, i.e., non-model organisms, or if peptide sequence information is not available on any current database, then genomic databases or translated expressed sequence tag (EST) libraries can also be used for protein identification (Nesvizhskii et al., 2007). However, the use of non-model organisms as study species offers its own unique sort of challenges as it limits the scope of available databases due to the lack sequence annotation (Tomanek, 2011). These issues can hamper coverage of the proteome leading to a decrease in protein identification rates (Dowd, 2012). In addition, alternative challenges to database searching for large proteomic data sets can impede upon downstream biological interpretation by increasing the false discovery rate (FDR), including the

statistical methods chosen for MS/MS peptide analysis (Nesvizhskii et al., 2007). In order to account for these limitations, scoring schemes are usually incorporated to the database searches in which candidate peptides from theoretical spectra are ranked and sorted according to a computed score (Nesvizhskii et al., 2007). There are different scoring scheme methods, but many measure the level of confidence associated with a positive peptide match by calculating the probability that the experimental match and the theoretical match within the sequence database is based on chance (Perkins et al., 1999). In this context, the significance threshold is usually predetermined ($\alpha < 0.05$) and the potential peptide match with the lowest probability is purported to be the best match candidate (Perkins et al., 1999). Therefore, protein identification via database searching requires a robust search engine tool which is also capable of incorporating a stringent scoring scheme to ensure confidence in positive protein identification (Nesvizhskii et al., 2007).

Although there have been many programs developed, one of the most commonly used and publically available database search engine tools are MASCOT (Matrix Science Inc., Boston, MA, USA) (Nesvizhskii et al., 2007). This software uses a molecular weight search engine (MOWSE) score, which determines protein sequences based on a probability-based scoring algorithm (Perkins et al., 1999). The significant match also depends upon the database, but significant hits ($p < 0.05$) with a MOWSE score higher than 45 indicate a positive match (Perkins et al., 1999; Tomanek & Zuzow, 2010). We also incorporated a more stringent approach towards peptide identification, by limiting positive identifications to two matched peptides regardless of MOWSE score (Tomanek and Zuzow, 2010). In this study, MASCOT was used to search the following databases: *Mytilus* protein (7,844 sequences), *Mytilus* EST (409,254 sequences), *Mytilus edulis* EST (447,720 sequence), Mollusca EST (1,147,871 sequences), and

NCBI Metazoa (last update: April 2016; 9,560,026 sequences). Since MASCOT also contains sequences of non-model organisms, we also used a Basic Local Alignment Search Tool (BLAST) to identify proteins based on sequence homology from annotated genomes of closely related invertebrates.

Study Objectives

As climate change continues to increase the frequency of environmental disturbances within marine ecosystems (Harley et al., 2006; Burrows et al., 2011; Doney et al., 2012), it is important to establish mechanistic links between environmental tolerance and the physiological constraints which govern patterns of species distribution (Helmuth, 2009; Tomanek, 2011; Somero, 2012; Pörtner, 2012). In this regard, *Mytilus* congeners represent a unique comparative study system to investigate the potential effects of environmental stress on shifts in biogeographic ranges given their recently observed differential responses in survivability (Schneider, 2008; Dowd and Somero, 2013), behavior (Dowd and Somero, 2013), cardiac function (Braby and Somero, 2006), enzymatic function (Lockwood and Somero, 2011), gene expression (Lockwood and Somero, 2010), protein expression (Tomanek and Zuzow, 2010) and temperature acclimation (Fields et al., 2012) to heat stress. However, none of these studies compared the molecular differences within the muscle primarily responsible for controlling gape behavior. Therefore, this study has the potential to provide a greater system based perspective, by incorporating the responses of muscle tissue to our current understanding of the gill's responsiveness to acute heat stress (Tomanek 2012). Given that episodes of moderate to severe stress decreases aerobic scope within marine invertebrates (Pörtner, 2010), primarily resulting in episodes of metabolic depression (Sokolova et al., 2012), we expect to changes in protein abundance which would indicate a downregulation of aerobic metabolism during temperature

increases in both species. In addition, given the observed variation in thermal tolerance between the congeners, we expect to see evidence of the cellular stress response, i.e., upregulation of molecular chaperones and oxidative stress proteins, which would indicate that the adductor muscle within *M. trossulus* is more-susceptible to increases in temperature as opposed to the warm-adapted *M. galloprovincialis*. Finally, given the adductor muscles primary role as a contractile tissue, we expect the greatest variation in protein abundance exhibited between the congeners to surround regulation surrounding thick and thin filaments within the cytoskeleton. Specifically, we expect to see an increased abundance of cytoskeletal regulatory proteins within the muscle tissue of the *M. galloprovincialis*, which would indicate the maintenance of cytoskeletal structural integrity occurring at the higher temperature ranges as opposed to *M. trossulus.*

References

Aebersold, R., and Mann, M. (2003). Mass spectrometry-based proteomics. *Nature* **422**, 198-207.

Altelaar, A. F. Maarten., Munoz, J., and Heck, A. J. R. (2012). Next-generation proteomics: towards an integrative view of proteome dynamics. *Nature Review Genetics*. **3356**, 1-14.

Anderson, M. J. (2001). Permutation tests for univariate or multivariate analysis of variance and regression. *Can. J. Fish. Aquat. Sci.* **58**, 626-639.

Anestis, A., Lazou, A., Pörtner, H. O., Michaelidis, B. (2007). Behavioral, metabolic, and molecular stress responses of marine bivalve *Mytilus galloprovincialis* during long-term acclimation at increasing ambient temperature. *Am. J Physiol. Regul. Integr. Comp. Physiol.* **293**, R911-R921.

Bensimon, A., Heck, A. J. R., Aebersold, R. (2012). Mass spectrometry-based proteomics and network biology. *Annu. Rev. Biochem.* **81**, 379-405.

Bernhardt, J. R., and Leslie, H. M. (2013). Resilience to climate change in coastal marine ecosystems. *Annu. Rev. Mar. Sci.* **5**, 371-392.

Berth, M., Moser, F. M., Kolbe, M. Bernhardt, J. (2007). The state of the art in the analysis of two-dimensional gel electrophoresis images. *Applied Microbiology Biotechnology*. **76**, 1223-1243.

Bodzon-Kulakowska, A., Bierczynska-Krysik, A., Dylag, T., Drabik, A., Suder, P., Noga, M., Jarzebinska, J., and Silberring, J. (2007). Methods for samples preparation in proteomic research. *Jour of Chromatography*. **84**, 1-31

Braby, C. E., and Somero, G. N. (2005). Ecological gradients and relative abundance of native (Mytilus trossulus) and invasive (Mytilus galloprovincialis) blue mussels in the California hybrid zone. *Mar. Bio*. **148**, 1249-1262.

Braby, C. E., and Somero, G. N. (2006). Following the heart: temperature and salinity effects on heart rate in native and invasive species of blue mussels (genus *Mytilus*). *Jour. Exp. Bio*. **209**, 2554-2566.

Branch G. M., and Steffani, C. N. (2004). Can we predict the effects of alien species? A case-history of the invasion of South Africa by *Mytilus galloprovincialis* (Lamarck). *Jour. Exp. Mar. Bio. & Ecol.* **300**, 189-215.

Buckley, B. A., Owen, M. E., and Hofmann, G. E. (2001). Adjusting the thermostat: the threshold induction temperature for the heats hock response in intertidal mussels (genus *Mytilus*) changes as a function of thermal history. *Jour. Exp. Bio.* **204**, 3571-3579.

Burrows, M. T., Schoeman, D. S., Buckley, L. B., Moore, P., Poloczanska, E. S., Brander, K. M., Brown, C., Bruno, J. F., Duarte, C. M., Halpern, B. S., Holding, J., Kappel, C. V., Kiessling, W., O'Connor, M. I., Pandolfi, J. M., Parmesan, C., Schwing, F. B., Sydeman, W. J., Richardson, A. J. (2011). The pace of shifting climate in marine and terrestrial ecosystems. *Science*. **334**, 652-655.

Campos, A., Tedesco, S., Vasconcelos, V. and Cristobal, S. (2012). Proteomic research in bivalves: Towards the identification of molecular markers of aquatic pollution. Journal of Proteomics **75**, 4346–4359.

Connor, K. M., and Gracey, A. Y. (2011). Circadian cycles are the dominant transcriptional rhythm in the intertidal mussel *Mytilus californianus*. *Proc. Natl. Acad. Sci.* **108**, 16110-16115.

Dahlhoff, E. P., Stillman, J. H., and Menge, B. A. (2002). Physiological community ecology: variation in metabolic activity of ecologically important rocky intertidal invertebrates along environmental gradients. *Integr. Comp. Biol.* **42**, 862-871.

Diz, A. P., Martínez-Fernández, M., and Rolán-Alvarez, E. (2012). Proteomics in evolutionary ecology: linking the genotype with the phenotype. *Mol. Ecology* **21**, 1060-1080.

Dobrzhanskaya, A., Vyatchin, I. G., Lazarev, S. S., Matusovsky, O. S., Shelud'ko, N. S. (2013). Molluscan smooth catch muscle contains calponin but not caldesmon. *J. Muscle Res. Cell Motil.* **34**, 23-33

Domon, B., and Aebersold, R. (2006). Mass spectrometry and protein analysis. *Science.* **312**, 212-217.

Doney, S. C., Ruckelshaus, M. J., Duffy, E., Barry, J. P., Chan, F., English, C. A., Galindo, H. M., Grebmeier, J. M., Hollowed, A. B., Knowlton, N., Polovina, J., Rabalais, N. N., Sydeman, W. J., and Talley, L. D. (2012). Climate change impacts on marine ecosystems. *Annu. Rev. Mar. Sci.* **4**, 11-37.

Dowd, W. W. (2012). Challenges for biological interpretation of environmental proteomics data in non-model organisms. *Integr. Comp. Biol*. **52**, 705-720.

Dowd, W. W., and Somero, G. N. (2013). Behavior and survival of *Mytilus* congeners following episodes of elevated temperature in air and seawater. *Jour. Exp. Biol.* **216**, 502-514.

Draghici, S., Khatri, P., Tarca, A. L., Amin, K., Done, A., Voichita, C., Georgescu, C., and Romero, R. (2007). A systems biology approach for pathway level analysis. *Genome Research*. **17**, 1537-1545.

Elliott, J., Holmes, K., Chambers, R., Leon, K., and Wimberger, P. (2008). Differences in morphology and habitat use among the native mussel *Mytilus trossulus*, the non-native *M. galloprovincialis*, and their hybrids in Puget Sound, Washington. *Mar. Biol* **156**, 39-53.

Evans, T. G. (2015). Considerations for the use of transcriptomics in identifying the 'genes that matter' for environmental adaptation. *Jour. Exp. Biol.* **218**, 1925-1935.

Fields, P. A., Rudomin, E. L., and Somero, G. N. (2006). Temperature sensitivities of cytosolic malate dehydrogenases from native and invasive species of marine mussels (genus *Mytilus*): sequence–function linkages and correlations with biogeographic distribution. *Jour. Exp. Bio.* **209**, 656-667.

Fields, P. A., Zuzow, M. J., and Tomanek, L. (2012). Proteomic responses of blue mussel (*Mytilus*) congeners to temperature acclimation. *Jour. Exp. Bio.* **215**, 1106-1116.

Friedman, D. B., Hoving, S., and Westermeier. (2009). Chapter 30 isoelectric focusing and two-dimensional gel electrophoresis. *Methods in Enzymology.* 463: 515-540.

Funabara, D., Kanoh, S., Siegman, M. J., Butler, T. M., Hartshorne, D. J., and Watabe, S. (2005). Twitchin as a regulator of catch contraction in molluscan smooth muscle. *Jour. Mus. Res. Cell Mot.* **26**, 455-460.

Gaitán-Espitia, J. D., Quitero-Galvis, J. F., Mesas, A., and D'Elia, G. (2016). Mitogenomics of southern hemisphere blue mussels (Bivalvia: Pteriomorphia): Insights into the evolutionary characteristics of the *Mytilus edulis* complex. *Sci Rep* **6**, 1-10.

Galler, S. (2008). Molecular basis of the catch state in molluscan smooth muscles: a catchy challenge. *J. Muscle. Res. Cell. Motil.* **29**, 73-99.

Galtsoff, P. S. (1964). The American oyster *Crassostrea virginica*. *Fishery Bulletin.* **64**: 152-157.

Geller, J. B. (1999). Decline of a native mussel masked by sibling species invasion. *Conservation Biology* **13**, 661-664.

Görg, A., Weiss, W., Dunn, M. J. (2004). Current two-dimensional electrophoresis technology for proteomics. *Proteomics*. **4**, 3365-3685.

Görg, A., Drews, O., Lück, C., Weiland, F., Weiss, W. (2009). 2-DE with IPGs. *Electrophoresis.* **30**, 1-11.

Gosling, E. (2015). *Marine Bivalve Molluscs*. Second Ed., Wiley-Blackwell.

Gracey, A. Y., Chaney, M. L., Boomhower, J. P., Tyburczy, W. R., Conner, K., and Somero, G. N. (2008). Rhythms of gene expression in a fluctuating intertidal environment. *Current Biology*. **18**, 1501-1507.

Gstaiger, M., and Aebersold, R. (2009). Applying mass spectrometry-based proteomics to genetics, genomics and network biology. *Nat. Rev. Gen.* **10**, 617-627.

Gundry, R. L., White, M. Y., Murray, C. I., Kane, L., A., Fu, Q., Stanley, B. A., Van Eyk. J. E. (2009). Preparation of proteins and peptides for mass spectrometry analysis in a bottom-up proteomics workflow. *Curr. Protoc. Mol. Biol.* 1-29.

Gunst, S. J., and Zhang, W. (2008). Actin cytoskeletal dynamics in smooth muscle: a new paradigm for the regulation of smooth muscle contraction. *Am. J. Physiol Cell Physiol.* **295**, C576-C587.

Harley, C. D. G., Hughes, A. R., Hultgren, K. H., Miner, B. G., Sorte, C. J. B., Thornber, C. S., Rodriguez, L. F., Tomanek, L., and Williams, S. L. (2006). The impacts of climate change in coastal marine ecosystems. *Ecology Letters* **9**, 228-241.

Helmuth, B., Broitman, B. R., Blanchette, C. A., Gilman, S., Halpin, P., Harley, C. D. G., O'Donnell, M. J., Hofmann, G. E., Menge, B., and Strickland, D. (2006). Mosaic patterns of thermal stress in the rocky intertidal zone: implications for climate change. *Ecological Monographs*. **76**, 461-479.

Helmuth. B. (2009). From cells to coastlines: how can we use physiology to forecast the impacts of climate change. *Jour. Exp. Bio*. **212**,753-760.

Hilbish, T. J., Brannock, P. M., Jones, K. R., Smith, A. B., Bullock, B. N., and Wethey, D. S. (2010). Historical changes in the distribution and endemic marine invertebrates are contrary to global warming predictions: the effects of decadal climate oscillations. *J. Biogeogr*. **37**, 423-431.

Hofmann, G. E., and Somero, G. N. (1996). Interspecific variation in thermal denaturation of proteins in the congeneric mussels *Mytilus trossulus* and *M. galloprovincialis:* evidence from the heat-shock response and protein ubiquitination. *Marine Bio.* **126**, 65-75.

Hooper, S. L., and Thuma, J. B. (2005). Invertebrate muscles: muscle specific genes and proteins. *Physiol. Rev*. **85**, 1001-1060.

Hooper, S. L., Hobbs, K. H., and Thuma, J. B. (2008). Invertebrate muscles: Thin and thick filament structure; molecular basis of contraction and its regulation, catch and asynchronous muscle. *Progress in Neurobiology*. **86**, 72-127.

Howard, W. D., Lewis, E. J., Keller, B. J., and Smith, C. S. (2004) Histological techniques for marine bivalve mollusks and crustaceans. NOAA Technical Memorandum. NOS NCCOS 5: 218 pp.

IPCC, 2014: *Climate Change 2014: Synthesis Report*. Contribution of working groups I, II and III to the fifth assessment report of the Intergovernmental panel on climate change [Core Writing Team, R.K. Pachauri and L.A. Meyer (Eds.)]. IPCC, Geneva, Switzerland, 151 pp.

Jarque, S., Prats, E., Olivares, A., Casado, M., Ramón, M., Piña, B. (2014). Seasonal variations of gene expression biomarkers in *Mytilus galloprovincialis* cultured populations: Temperature, oxidative stress and reproductive cycle as major modulators. *Sci. Total. Env.* **499**, 363-372.

Jones, S. J., Lima, F. P., Wethey, D. S. (2010). Rising environmental temperatures and biogeography: poleward range contraction of the blue mussel, *Mytilus edulis* L., in the western Atlantic. *J. Biogeogr*. **37**, 2243-2259.

Joyce, A. R., and Palsson, B. Ø. (2006). The model organism as a system: integrating 'omics' data sets. *Nature Reviews Molecular and Cell Biology*. **7**, 198-210.

A) Kim, H. R., Appel. S., Vetterkind, S., Gangopadhyay, S. S., and Morgan, K. G. (2008). Smooth muscle signaling pathways in health and disease. *J. Cell. Mol. Med.* **12**, 2165-2180.

B) Kim, H. R., Gallant, C., Leavis, P. C., Gunst, S. J., and Morgan, K. G. (2008). Cytoskeletal remodeling in differentiated vascular smooth muscle is actin isoform dependent and stimulus dependent. *Am. J. Physiol. Cell Physiol.* **295**, C768-C778.

Kültz, D. (2005). Molecular and evolutionary basis of the cellular stress response. *Annu. Rev. Physiol.* **67**, 225-257.

Larance, M., and Lamond, A. I. (2015). Multidimensional proteomics for cell biology. *Nature Rev. Mol. Cell Bio.* **16**, 269-280.

Lee, S. H., and Dominguez, R. (2010). Regulation of actin cytoskeleton dynamics in cells. *Mol. Cells* **29**, 311-325.

Lehman, W., Morgan, K. G. (2012). Structure and dynamics of the actin-based smooth muscle contractile and cytoskeletal apparatus. *J. Muscle Res. Cell Motil*. **33**, 461-469.

Levitus, S., Antonov, J. I., Boyer, T. P., Baranova, O. K., Garcia, H. E., Locarnini, Mishonov, A. V., Reagan, J. R., Seidov, D., Yarosh, E. S., and Zweng, M. M. (2012). World ocean heat content and thermosteric sea level change (0-2000 m), 1955-2010. *Geophysical research letters.* **39**, L10603.

Lilley, K. S., Razzaq, A., and Durpee, P. (2001). Two-dimensional gel electrophoresis: recent advances in sample preparation, detection and quantification. *Current Opinion in Chemical Biology.* **6**, 46-50.

Linehan, C. M. (1982). The effect of temperature on the tension responses of the anterior byssal retractor mussel (ABRM) of *Mytilus edulis*. *J. exp. Biol*. **97**: 375-384.

Lockwood, B. L., Sanders, J. G., and Somero, G. N. (2010). Transcriptomic responses to heat stress in invasive and native blue mussels (genus Mytilus): molecular correlates of invasive success. *Jour. Exp. Bio.* **213**, 3548-3558.

Lockwood, B. L., and Somero, G. N. (2011). Invasive and native blue mussels (genus Mytilus) on the California coast: The role of physiology in a biological invasion. *Jour. Exp. Mar. Bio. and Ecol.* **400**, 167-174.

Lockwood, B. L., Connor, K. M., and Gracey, A. Y. (2015). The environmentally tuned transcriptomes of *Mytilus* mussels. *Jour. Exp. Biol*. **218**, 1822-1833.

Lopez, J. L. (2007). Two-dimensional electrophoresis in proteome expression analysis. *Journal of Chromatography B.* **849**, 190-202.

Lovrić, J. (2011). Introducing proteomics: from concepts to sample separation, mass spectrometry and data analysis. John Wiley & Sons. West Sussex, UK.

Lowe, S., Browne, M., Boudjelas, S., and De Poorter M., (2000). 100 of the world's worst invasive alien species. A selection from the global invasive species database. Auckland, New Zealand: The Invasive Species Specialist Group (ISSG).

Lowy, J. (1953). Contraction and relaxation in the adductor muscles of *Mytilus edulis*. *J. Physiol.* **120:** 129-140.

Luhn, S., Berth, M., Hecker, M., Bernhardt, J. (2003). Using standard positions and image fusion to create proteome maps of two dimensional gel electrophoresis images. *Proteomics*. **3**, 1117-1127.

McDonald, J. H., and Koehn, R. K. (1988). The mussels *Mytilus galloprovincialis* and *M. trossulus* on the Pacific coast of North America. *Marine Biology*. **99**, 111-118.

Meunier, B., Dumas, E., Piec, I., Béchet, D., Hébraud, M., and Hocquette J. F. (2007). Assessment of hierarchical clustering methodologies for proteomic data mining. *Jour. of the Proteome.* **6**, 358-366.

Millman, B. M. (1967). Mechanism of contraction in molluscan muscle. *Am. Zoologist.* **7**: 583-591.

Nesvizhskii, A. I., Vitek, O., and Aebersold, R. (2007). Analysis and validation of proteomic data generated by tandem mass spectrometry. *Nature Methods*. **4**, 787-797.

Nicastro, K. R., Zardi, G. I., McQuaid, C. D., Stephens, L., Radloff, S., and Blatch, G. L. (2010). The role of gaping behavior in habitat partitioning between coexisting intertidal mussels. *BMC ecology*. **10**, 17.

Perkins, D. N., Pappin, D. J. C., Creasy, D. M., and Cottrell, J. S. (1999). Probability-based protein identification by searching sequence databases using mass spectrometry data. *Electrophoresis.* **20**, 3551-3567.

Perry, A. L., Low, P. J., Ellis, J. R., and Reynolds, J. D. (2005). Climate change and distribution shifts in marine fishes. *Science* **308**, 1912-1915.

Petes, L. E., Menge, B. A., and Murphy, G. D. (2007). Environmental stress decreases survival, growth, and reproduction in New Zealand mussels. *Jour. Exp. Mar. Bio. and Ecol.* **351**, 83-91.

Philpott, D. E., Kahlbrock, M., and Szent-Gyorgyi, A. G. (1960). Filamentous organization of molluscan muscles. *J. Ultrastruct. Res.* **3**: 254-269.

Pörtner, H. O., and Knust. R., (2007). Climate change affects marine fishes through the oxygen limitation of thermal tolerance. *Science* **315**, 95-97.

Pörtner, H. O. (2010). Oxygen-and capacity-limitation of thermal tolerance: a matrix for integrating climate-related stressor effects in marine ecosystems. *Journal of Exp. Biol.* **213**, 881-893

Pörtner, H. O. (2012). Integrating climate-related stressor effects on marine organisms: unifying principles linking molecule to ecosystem-level changes. *Mar. Ecol. Prog. Ser.* **470**, 273-290.

Ringnér, M. (2008). What is principal component analysis? *Nature Biotechnology*. **26**, 303-304.

Rocher, B., Bultelle, F., Chan, P., Le Foll, F., Letendre, J., Monsinjon, T., Olivier, S., Péden, R., Poret, A., Vaudry, D., and Knigge, T. (2015). 2-DE mapping of the blue mussel gill proteome: the usual suspects revisited. *Proteomes*. **3**, 3-41.

Schneider, K. R. (2008). Heat stress in the intertidal: comparing survival of an invasive and native mussel under a variety of thermal conditions. *Biol. Bull.* **215**, 253-264.

Schneider, K. R., and Helmuth. B. (2007). Spatial variability in habitat temperature may drive patterns of selection between an invasive and native mussel species. *Mar. Ecol. Prog. Ser.* **339**, 157-167.

Seed, R. (1992). Systematics evolution and distribution of mussels belonging to the genus *Mytilus*: an overview. *Am. Malacological Bulletin* **9**, 123-137.

Shaw, M. M., and Riederer, B. M. (2003). Sample preparation for two-dimensional gel electrophoresis. *Proteomics* **3**, 1408-1417.

Shinen, J. S., and Morgan, S. G. (2009). Mechanisms of invasion resistance: competition among intertidal mussels promotes establishment of invasive species and displacement of native species. *Mar. Ecol. Prog. Series.* **383**, 187-197.

Shokralla, S., Spall, J. L., Gibson, J. F., and Hajibabaei, M. (2012). Next-generation sequencing technologies for environmental DNA research. *Mol. Ecology* **21**, 1794-1805.

Sokolova, I. M., Frederich, M., Bagwe, R., Lanning, G., Sukhotin, A. A. (2012). Energy homeostasis as an integrative tool for assessing limits of environmental stress tolerance in aquatic invertebrates. *Mar. Env. Res*. **79**, 1-15.

Somero, G. N. (2010). The physiology of climate change: how potentials for acclimatization and genetic adaptation will determine 'winners' and 'losers.' *Jour. Exp. Biol.* **213**, 912-920.

Somero, G. N. (2012). The physiology of climate of global climate change: linking patterns to mechanisms. *Annu. Rev. Mar. Sci.* **4**, 39-61.

Sorte, C. J. B., Jones, S. J., and Miller, L. P. (2011). Geographic variation in temperature tolerance as an indicator of potential population responses to climate change. *Jour. Exp. Mar. Bio and Ecol.* **400**, 209-217.

Stillman. J. H. (2002). Causes and consequences of thermal tolerance limits in rocky intertidal porcelain crabs, genus *Petrolisthes*. **42**,790-796.

Suckau, D., Resemann, A., Schuerenberg, M., Hufnagel, P., Franzen, J., Holle, A. (2003). A novel MALDI LIFT-TOF/TOF mass spectrometer for proteomics. *Anal. Bioanal. Chem* **376**, 952-965.

Sunday, J. M., Bates, A. E., Dulvy, N. K. (2012). Thermal tolerance and the global redistribution of animals. *Nature Climate Change* **2**, 686-690.

Tomanek, L., and Somero, G. N. (1999). Time course and magnitude of synthesis of heat-shock proteins in congeneric marine snails (genus *Tegula*) from different tidal heights. *Physiological and Biochemical Zoology* **73**, 249-256.

Tomanek, L. (2008). The importance of physiological limits in determining biogeographical range shifts due to global climate change: the heat-shock response. *Physiological and Biochemical Zoology*. **81**, 709-717.

Tomanek, L. (2009). Variation in the heat shock response and its implication for predicting the effect of global climate change on species' biogeographical distribution ranges and metabolic costs. *Jour. Exp. Bio.* 213: 971-979.

Tomanek, L. (2011). Environmental proteomics: changes in the proteome of marine organisms in response to environmental stress, pollutants, infection, symbiosis and development. *Ann. Rev. Mar. Sci.* (3): 14.1-14.27.

Tomanek, L. (2012). Environmental Proteomics of the Mussel Mytilus: Implications for Tolerance to Stress and Change in Limits of Biogeographic Ranges in Response to Climate Change. *Integrative and Comparative Biology.* 1-17.

Tomanek, L. (2015). Proteomic response to environmentally induced oxidative stress. *Journal of Experimental Biology* 218: 1867-1869.

Twarog, B. M. (1967). Factors influencing contraction and catch in *Mytilus* smooth muscle. *J. Physiol.* 192: 847-856.

Tyers, M.., and Mann, M. (2003). From genomics to proteomics. *Nature.* 422: 193-197.

Weist, S., Eravci, M., Broedel, O., Fuxius, S., Eravci, S., Baumgartner, A. (2008). Results and reliability of protein quantification for two-dimensional gel electrophoresis strongly depend on the type of protein sample and the method employed. *Proteomics.* 8: 3389-3396.

Wiśniewski, J. R., Zougman, A., Nagaraj, N., and Mann, M. (2009). Universal sample preparation method for proteome analysis. *Nature Methods*. **6**, 359-362.

II. MANUSCRIPT

Abstract

Increases in seawater temperatures have imposed physiological constraints which are partially thought to contribute to recently observed shifts in biogeographic distribution among closely related intertidal ectotherms. For instance, *Mytilus galloprovincialis* an introduced warm-adapted species from the Mediterranean, has displaced the native cold-adapted congener, *M. trossulus*, over large latitudinal expanses off the California coast. Several comparative physiological studies have revealed interspecific differences in thermal tolerance, including variation in aerobic metabolism and gape behavior, which suggest the invasive congener is better adapted to acclimate to increasing seawater conditions as predicted due to climate change. However, current analyses seek to discover the cellular process which contribute to thermal plasticity at the level of the whole organism in response to temperature stress. Since proteins represent the primary molecular machinery capable of responding to thermal stress, we quantified the proteomic response of the adductor muscles (AM) of *M. galloprovincialis* and *M. trossulus* to acute heat stress. After acclimation to 13°C, we exposed mussels to 24°C, 28°C and 32 °C (at a heating rate of 6C/h), kept mussels at the temperature for 1 h and then added a 24-h recovery period. Posterior adductor muscle samples were then excised and utilized for proteomic analysis. We were able to detect 273 protein spots within *M. galloprovincialis* and 286 protein spots within *M. trossulus.* Roughly 33% of these protein spots exhibited significant changes in abundance in response to heat stress within *M. trossulus* as compared to only 19% in *M. galloprovincialis.* In both data sets, most proteins changing abundance are part of the cytoskeleton or proteins controlling actin thin filament dynamics and stress fiber formation. Specifically, *M. galloprovincialis* increased the abundance of proteins involved in thin filament

stabilization and cytoskeletal maintenance. In contrast, *M. trossulus* increased proteins involved in thin filament destabilization and filament turnover. In addition, only *M. trossulus* increased proteins involved in the cellular stress response at the highest temperature, suggesting its AM proteome is more thermolabile. In return, our results suggest that cytoskeletal architecture is more thermally stable in *M. galloprovincialis*. The differences in the proteomic responses suggest that *M. galloprovincialis* is capable of protecting itself from heat stress through valve closure at a higher temperature due to the increase in actin stabilizing proteins.

Introduction

Global climate change (GCC) has already resulted in increases in air and sea surface temperatures, which affect all levels of biological organization (IPCC 2014; Doney et al., 2012; Bernhardt and Leslie, 2013). The thermal stress imposed on intertidal ecosystems are particularly concerning as they affect organismal performance and may strongly influence large-scale shifts of invertebrate distributions (Harley et al., 2006; Doney et al., 2012; Bernhardt and Leslie, 2013). For instance, many intertidal ectotherms have exhibited contractions at the southern but expansions at the poleward end of their distribution in response to climate change (Harley et al., 2006; Helmuth et al., 2009; Jones et al., 2010; Drinkwater et al., 2010; Sunday et al., 2012). The ability of intertidal ectotherms to acclimate to temperature fluctuations is largely dependent upon their thermal tolerance window, which reflects the temperatures to which they are routinely exposed and describes the temperature range required to maintain optimal physiological performance (Somero, 2002; Hofmann and Todgham 2010, Pörtner, 2012). Although the intertidal is a highly dynamic thermal environment and intertidal ectotherms retain passive compensatory mechanisms to acclimatize to temperatures which exceed their thermal tolerance range, exposures to temperatures beyond these thermal thresholds for extended periods may

offset energy balances required to maintain homeostatic functions (Pörtner, 2012; Sokolova et al., 2012). Thus, any long-term exposures to temperatures exceeding an organism's thermal threshold can negatively affect physiological performance resulting in decreased aerobic scope, energy homeostasis and consequently survivorship during chronic stress (Pörtner, 2012; Dowd and Somero, 2013). Furthermore, these effects may be exacerbated near a species' range boundaries, as animals occupying these areas may be limited in their thermal capacity to respond further environmental change (Harley et al., 2006; Tomanek, 2008, Tomanek 2010).

In order to assess the temperature-dependent effects on physiological performance many studies have compared the responses to heat stress between the two closely related species of blue mussels, *Mytilus galloprovincialis* and *M. trossulus* (Braby and Somero, 2005; Hofmann and Todgeham, 2010, Lockwood & Somero, 2011; Tomanek, 2011). Over the last century, the warm-adapted *M. galloprovincialis*, an introduced species from the Mediterranean, has displaced the native *M. trossulus* from its southern range in California (McDonald & Koehn, 1988; Geller, 1999). Both species belong to the *Mytilus edulis* complex, and can form stable hybrids in regions where they overlap (Braby & Somero, 2006; Elliott et al., 2008). Within these regions, however, *M. galloprovincialis* is typically larger, more viable, and exhibits competitive interference by decreasing the abundance of the native *M. trossulus* (Elliott et al., 2008; Shinen and Morgan 2009; Lockwood and Somero, 2011). In addition, *M. trossulus* has been observed to display lower survivorship in response to temperature increases during both aerial emersion and seawater immersion as compared to *M. galloprovincialis* (Schneider, 2008; Dowd and Somero, 2013). Recent physiological comparisons have revealed interspecific differences including variation in enzyme kinetics, anaerobic metabolism and cardiac output, suggesting that *M. galloprovincialis* may have a competitive advantage over *M. trossulus* in response to temperature increases (Braby

and Somero, 2005; Fields et al., 2006; Lockwood and Somero, 2011). Thus, comparisons of congeners are particularly useful as they share a similar genome, life history patterns and environments and thus increasing the likelihood that any differences are adaptive in the context of different environments (Somero, 2010; Lockwood and Somero, 2011; Anacleto et al., 2014). However, in order to determine which thermally adaptive traits contribute to phenotypic plasticity and confer differential success towards warm-adapted species, further research is required to link the cellular mechanisms which translate into physiological processes occurring at the level of the whole organism.

To address these complex questions, recent analyses have utilized a proteomics approach, which attempts to characterize the acute changes in abundance of the entire complement of proteins occurring within a selected tissue in response to stress (Lovrić, 2011; Diz et al., 2012; Tomanek, 2012). All organisms retain a conserved set of stress response proteins, known as the minimal stress proteome, which functions to detect and mitigate damage to cellular macromolecules during stress exposure (Kültz, 2005). The regulatory patterns displayed by stress responsive proteins allows for greater interpretation towards the complex physiological processes involved during stress adaptation (Tomanek, 2014; Rocher et al., 2015), and since proteins represent the biochemical machinery capable of integrating external stimuli at the cellular level (Diz et al., 2012), any method capable of detecting changes in protein abundance has the capacity to discover the functional molecular phenotype induced during temperature stress (Lovrić, 2011; Diz et al., 2012; Tomanek, 2012). Therefore, a proteomics approach represents a powerful tool to investigate the complex regulatory processes and cellular mechanisms involved during the thermal stress response, as it characterizes the full complement of proteins upregulated within a given tissue during heat stress (Tomanek, 2011; Diz et al., 2012;

Tomanek, 2014). In addition, by comparing the proteomic responses of closely related species of varying thermal tolerance whose current biogeographical ranges are in flux, it is possible to discover novel molecular mechanisms which may confer competitive advantages to invasive species in response to climate change (Tomanek, 2011; Tomanek, 2012). Comparative proteomics may then provide a more comprehensive approach to better understand the cellular mechanisms driving adaptive variation at the level of the whole organism in response to increasing temperatures (Tomanek, 2014).

In this study, we utilized a comparative proteomics based approach to investigate the responses within the adductor muscles of *M. galloprovincialis* and *M. trossulus*, in response to acute heat stress. By attempting to characterize the proteomic differences within the muscle primarily responsible for controlling the opening and closing of the valve (Gosling, 2015), we may be able to provide a more conceptual framework for studies documenting variation in gape behavior between both species in response to thermal stress (Dowd and Somero, 2013). In addition, we complement previous work completed on gill tissue by providing a more systems-based perspective into the molecular mechanisms which translate into whole-organismal responses to temperature stress. Given the adductor muscles contractile function, we expect the variation in protein abundance patterns exhibited between *M. galloprovincialis* and *M. trossulus* in response to heat stress to primarily involve regulation surrounding the cytoskeleton. Specifically, this may entail regulation surrounding the contractile apparatus or actomyosin-based mechanics, which control cytoskeletal contractile activity within Molluscan smooth muscle (Hooper et al., 2008). Finally, we expect any variation in protein abundance of molecular chaperones and proteins involved in the cellular stress response to closely align with thermal tolerance thresholds previously outlined in other experiments (Buckley et al., 2001; Anestis et

al., 2007; Schneider, 2008; Lockwood and Somero, 2010; Tomanek and Zuzow, 2010; Tomanek, 2012). Specifically, we expect any interspecific differences in the abundance of proteins involved in molecular chaperoning, oxidative stress, energy metabolism and cell-signaling to closely mirror induction temperature ranges previously described within the gill tissue for both *M. galloprovincialis* and *M. trossulus* respectively (Tomanek and Zuzow, 2010).

Results and Discussion

In order to compare the proteomic responses of the adductor muscle between both *M. galloprovincialis* and *M. trossulus* to acute heat shock following acclimation to a common temperature of 13°C, we separated the results into several sections for clarity. First, we present the proteome maps with respect to each species, which depicts all detectable protein spot boundaries and highlights those spots that changed significantly (One-Way permutation ANOVA, $p<0.05$). Next, we illustrate the variation existent between the temperature treatments for each species through principal component analyses (PCA). We subsequently utilize protein component loading values provided by each PCA to determine which proteins were significantly contributing towards the variation existent between the temperature treatment groups (Table 1). After defining specific proteins with the greatest contributions towards the variation exhibited between temperature treatments, we precede to delineate between the protein abundance patterns represented within the hierarchical clusters, i.e., heat maps, to identify molecular mechanisms which may be induced. The final section includes protein expression profiles (Tukey's pairwise comparison's; $p<0.05$) of both significant and non-significantly identified proteins to compare the relative similarities and or differences of orthologous proteins between the two species. The latter section is also further separated by protein functional categories to define the interspecific

differences. Finally, we propose several hypotheses about the biochemical differences that distinguish the response to heat stress between the two species.

It is important to note that changes in protein abundance may occur through multiple processes including protein synthesis, post-translational modifications (PTMs) or protein degradation (Tomanek and Zuzow 2010; Fields et al., 2011; Garland et al., 2015). Thus, changes in protein abundance patterns may be facilitated by any of these processes, and so the total abundance of all isoforms of a given protein does not necessarily represent the full complement of isoforms which may be present within the adductor muscle (for further review see Tomanek 2011, 2014). Therefore, our interpretation involves generating hypotheses based on the specific subset of identified protein isoforms, which requires further clarification and validation. A number of proteins which were identified but did not significantly change in protein abundance are also presented in the Supplement for further reference (Table(s) S3 & S4).

Significant Changes in Total Protein Abundance in Response to Acute Heat Stress

Mytilus galloprovincialis

Following the aligned warping of all two-dimensional (2D) gel images, we generated a proteome map, i.e., composite image, representative of the average pixel density of all individual adductor muscle samples (N=24) across all treatments. We then determined protein spot boundaries and transferred these consensus spot patterns back to each individual gel image to determine significant changes in protein abundance based on pixel density or protein spot volume. This approach enabled us to detect a total of 273 individual protein spots represented within the adductor muscle of *M. galloprovincialis*. From this, 52 total proteins (or 19% overall) exhibited significant changes in abundance in response to acute heat shock (One-way

permutation ANOVA; $p<0.05$; Figure 1A). We were then able to successfully identify 31 of these 52 significant protein spots for a 60% identification rate using tandem mass spectrometry (MS/MS) (significant protein spots represented through highlighted spot boundaries, see Fig. 1A). Protein identifications and corresponding MS/MS data can be found in the supplement (See Table S1).

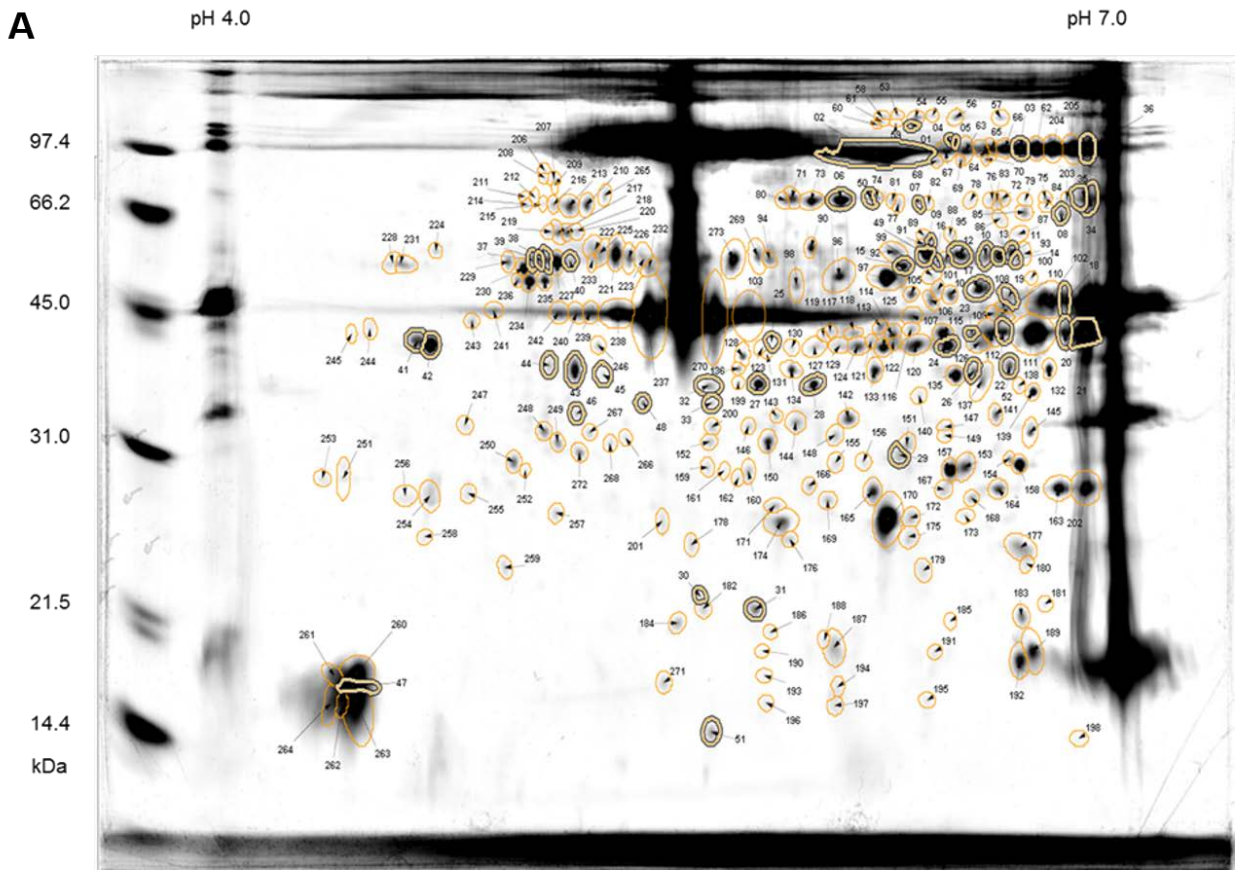

Figure 1A. An average composite gel image comprising all adductor muscle samples (N=24), depicting a total of 273 protein spots detected within the adductor muscle of *Mytilus galloprovincialis* in response to acute heat shock during immersion. Proteins are separated according to their respected isoelectric points (pI) along the horizontal axis, and by molecular weight (kDa) along the vertical axis. The fusion image represents the average normalized pixel volumes for each protein spot detected across all 24 gel images utilizing Delta 2D gel analysis software (version 4.3, Decodon, Greifswald, Germany). Highlighted spots, i.e., spot numbers 1-52, showed significant changes in abundance in response to acute heat shock (One-way permutation ANOVA; $p<0.05$). All protein spots were then excised and analyzed using tandem mass spectrometry for protein identification, regardless of whether they exhibited significant changes in abundance in response to treatment (See Table(s) S1 & S3).

Mytilus trossulus

We detected 286 distinct protein spots within the adductor muscle of *Mytilus trossulus*. Of the total detected spots, 97 protein spots (or 34% overall) exhibited significant changes in protein abundance in response to acute heat stress (One-way permutation ANOVA, $p<0.05$; Fig. 1B). From this, we were able to successfully identify roughly 60 proteins for a similar 62% success rate using MS/MS (significant protein spots represented through highlighted spot boundaries, see Fig. 1B). Protein identifications and corresponding MS/MS data can be found in the supplement (See Table S2).

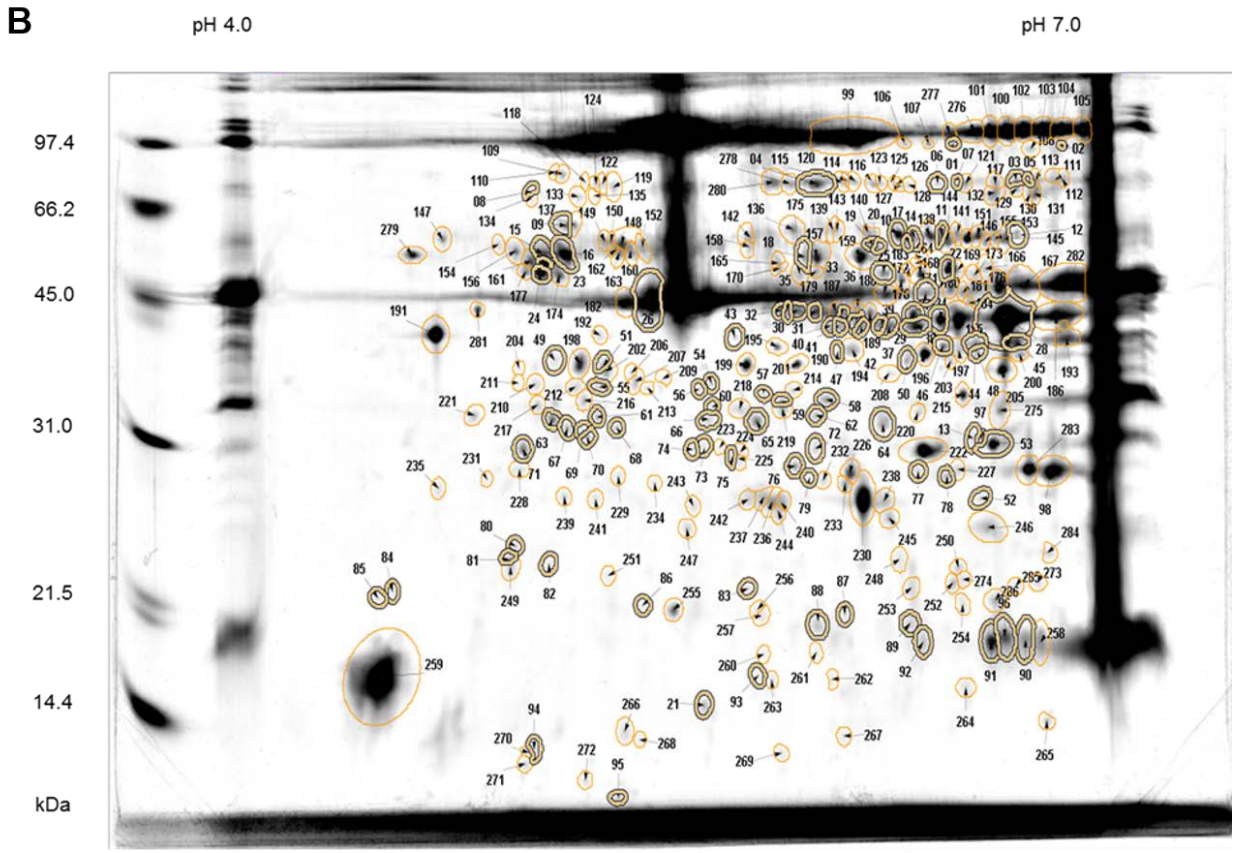

Figure 1B. An average composite gel image comprising all adductor muscle samples (N =24), depicting a total of 286 protein spots detected within the adductor muscle of *M. trossulus* in response to acute heat shock under sea water immersion. Highlighted spots, i.e., spot numbers 1-

97, exhibited significant changes in abundance in response to acute heat stress. For protein identifications, see Table(s) S2 & S4).

Principal Component Analyses

Due to the complexity associated with large biological networks, their analysis can be extremely difficult without the implementation of techniques utilized to compartmentalize multidimensional data sets (Raychaudhuri et al., 2000). Therefore, in order to investigate the contribution of protein abundance changes towards the relative separation of the temperature treatments, we conducted several principal component analyses (PCAs). This statistical technique utilizes all the protein spot intensities present within each individual gel image and combines them into a single vector per gel (Delta 2D version 3.6; Decodon, Greifswald, Germany). Each gel vector is then plotted along a multi-dimensional coordinate plane in which the two axes, i.e., principal components, explain the greatest proportion of the variability in terms of percent variation in protein abundance existent between the temperature treatments. These principal components are therefore linear transformations of the data, which attempt to reduce the dimensionality of all the spot intensities into two primary component axes to graphically represent the maximal percent variation in protein abundance (Ringnér 2008). Each temperature treatment is then clustered and defined by the proximity and overall perimeter grouping of their respected gel vectors (see Fig(s). 2A & 2B). Temperature clusters which share a high degree of overlap are interpreted to exhibit similar changes in protein abundance in response to thermal stress, whereas temperatures which exhibit greater separation are perceived to display distinctive proteomic response profiles.

Although these PCA's provided a visual characterization of the apparent separation existent between different temperatures, the principal components were further assessed through examination of principal component loading values (Table 1). These loading values, i.e., eigenvalues, provide further context as to the distinct differences observed in protein abundance, as proteins which exhibit high rankings are suggested to significantly contribute towards the separation of temperature clusters along the respected component axis (Fig(s) 2A & 2B). In this regard, proteins which exhibit high positive loading values contribute a greater proportion towards the separation of gel vectors located within the positive quadrant of the component axis. Conversely, proteins exhibiting negative loading values contribute a greater proportion towards gel vectors located along the negative component axis.

Table 1. Positive and negative component loading values for highest ranking proteins associated with the principal component analyses, with respect to species. Component loading values are numerically ranked, and the top ten rankings are shown. These proteins contribute the greatest proportion of variation towards the separation of gel vectors along the corresponding principal component axes (Fig(s). 2A & 2B), and were thus open for greater biological interpretation. For further analysis of all protein component values, see Table S5. *Post-hoc analysis, represents protein spots which exhibited significant changes in protein abundance (Tukey pairwise comparison; $p<0.05$; See Fig(s). 16-21). Note: component loading values for protein spots which were not identified via tandem MS/MS are not shown. For analysis of additional component loading values, see Table S5.

	Mytilus galloprovincialis		*Mytilus troussulus*	
Component Loading Rank	Protein (Spot ID)	Component Loading	Protein (Spot ID)	Component Loading
A) Positive component loadings for PC1				
1	Rab GDP-dissociation inhibitor β-subunit (17)*	1.684	Actin (67)*	1.924
2	Calponin (22)*	1.684	Whirlin (88)*	1.781
3	Calponin (12)*	1.614	Guanine nucleotide-binding protein β-subunit (52)*	1.775
4	Tropomyosin (41)*	1.478	14-3-3 protein (59)*	1.762
5	Aldehyde dehydrogenase, mitochondrial (15)*	1.421	Profilin (21)*	1.729
6	Calponin (13)*	1.407	Small heat shock protien (62)*	1.616
7	Guanine nucleotide-binding protein β-subunit (28)*	1.375	Small heat shock protien (65)*	1.560
8	Actin-2 (46)	1.323	Actin (43)	1.529
9	Troponin-T (24)	1.313	Small heat shock protein (61)*	1.482
10	Calponin (23)*	1.302	Actin (76)*	1.479
B) Negative component loadings for PC1				
1	Filamin-C (36)*	-1.174	Small heat shock protein (45)	-1.620
2	Filamin-C (3)*	-1.171	β-tubulin (15)*	-1.528
3	Calponin (21)*	-1.166	ATP synthase, F1 β-subunit (23)*	-1.359
4	Tropomyosin (42)*	-1.147	β-tubulin (16)*	-1.322
5	Calponin (20)*	-1.020	Calponin (34)*	-1.265
6	Calponin (18)*	-1.014	Calponin (28)*	-1.244
7	β-tubulin (39)	-0.673	Short chain collagen (55)*	-1.237
8	β-tubulin (37)	-0.601	Calponin (12)*	-1.125
9	β-tubulin (38)	-0.569	Troponin-T (31)*	-1.040
10	Myosin regulatory light chain (47)*	-0.459	Collagen α-VI chain (18)*	-1.006
C) Positive component loadings for PC2				
1	β-tubulin (38)	1.790	Gelsolin (24)*	2.098
2	β-tubulin (39)	1.774	Aldehyde dehydrogenase, mitochondrial (20)*	1.888
3	β-tubulin (37)	1.645	ATP synthase, F1 β-subunit (23)*	1.610
4	β-tubulin (40)	1.611	β-tubulin (16)*	1.600
5	Myosin regulatory light chain (47)*	1.600	Pyruvate dehydrogenase, E1 component β-subunit (54)*	1.299
6	Actin interacting protein 1 (8)*	1.041	Rab GDP dissociation inhibitor β-subunit (22)*	1.214
7	Apextrin-like protein (29)	0.694	β-tubulin (15)*	1.013
8	Calponin (31)*	0.447	Fascin (10)*	0.912
9	Rab GDP-dissociation inhibitor β-subunit (17)*	0.436	Purine nucleoside phosphorylase (60)*	0.874
10	NAD-dependent isocitrate dehydrogenase mitochondrial α subunit (25)	0.418	Calponin (49)*	0.676
D) Negative component loadings for PC2				
1	Calponin (20)*	-1.884	Actin (36)*	-2.505
2	Heat shock protein 70 (6)*	-1.841	Actin (41)*	-2.390
3	Calponin (18)*	-1.807	Heavy metal binding protein (47)*	-2.279
4	β-actin (7)	-1.441	Troponin-T (33)*	-2.261
5	Fascin (49)	-1.203	Actin-2 (40)*	-2.163
6	Filamin-C (36)*	-1.025	Troponin-T (39)*	-2.112
7	Filamin-C (3)*	-0.782	Cu-Zn Superoxide dismutase (92)*	-2.067
8	Aldehyde dehydrogenase mitochondrial (15)*	-0.647	Actin (35)*	-1.698
9	Troponin-T (24)*	-0.530	Troponin-T (31)*	-1.661
10	Tropomyosin (42)*	-0.501	F-actin capping protein α-subunit (46)*	-1.638

Mytilus galloprovincialis

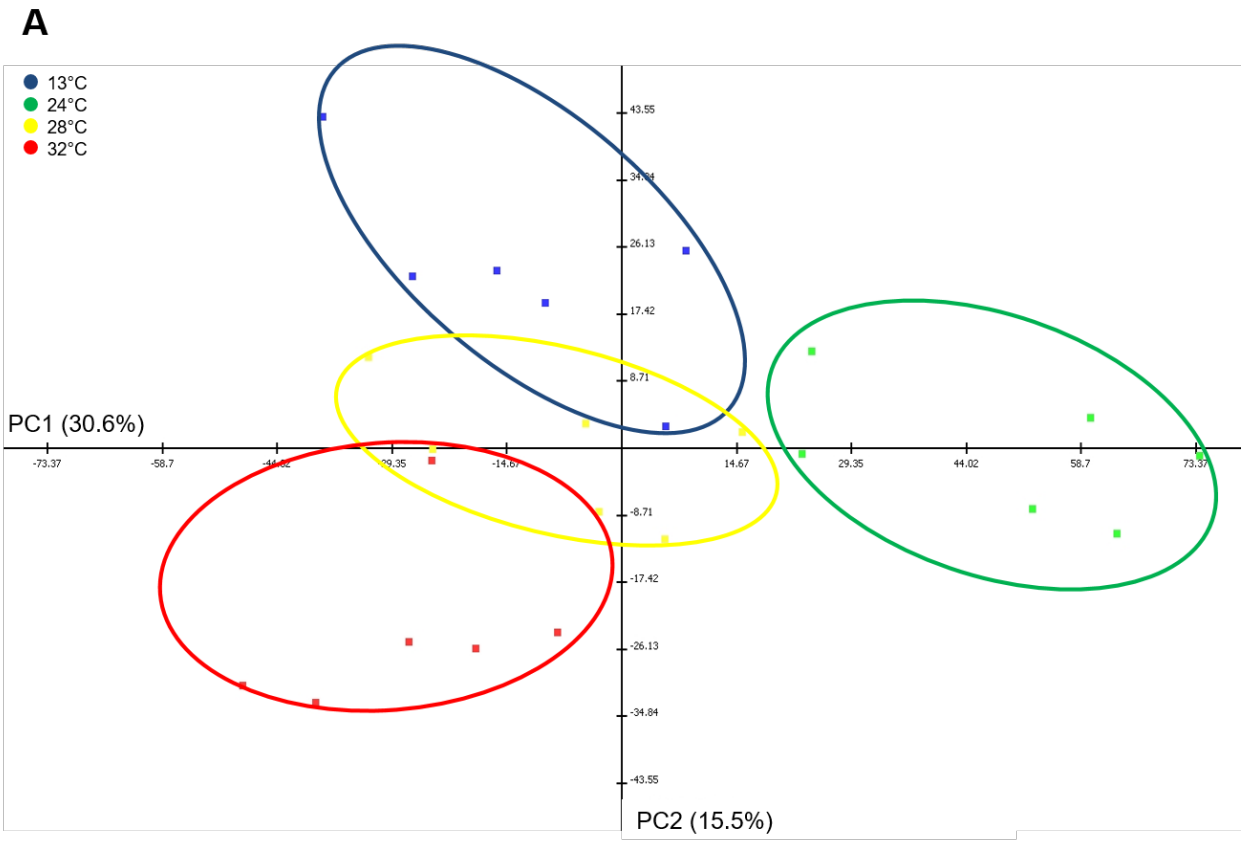

Figure 2A. Principal component analysis displaying all significant proteins within the adductor muscle of *M. galloprovincialis* in response to acute heat shock under sea water immersion. Each coordinate point displayed represents a gel vector with respect to temperature treatment (13°C, 24°C, 28°C & 32°C). All gel vectors are plotted along the principal components axes, PC1 & PC2, which attempt to explain the greatest proportion of the variation observed between temperature treatments in terms of protein abundance (for individual protein contributions, see Table(s) 1 & S5). In this context, 46.1% of the variation observed in protein abundance changes can be explained along the along the two provided component axes. Specifically, PC1 explains roughly 30.6% of the variation whereas PC2 explains 15.5% of the variation exhibited between temperature treatments.

The first PCA depicts all 52 significant proteins observed to change in abundance in response to acute heat stress within the adductor muscle of *M. galloprovincialis*, and explains roughly 45% of the total variation exhibited between temperature treatments (Fig. 2A). The first principal component explains 30.6% of the variation and separates the gel vectors into two

quadrants along a vertical axis. Specifically, this component isolates the 24°C treatment, suggesting a more varied response in protein abundance following 24°C heat shock as compared to all other temperatures. Proteins possessing high positive component loading values for PC1 were then used further to investigate this treatment isolation (Table 1). These included proteins involved in vesicular trafficking/signal transduction (Rab GDP-dissociation inhibitor β-subunit, guanine nucleotide-binding protein β-subunit), regulation of the acto-myosin complex (four isoforms of calponin, troponin-T) thin filament regulation (tropomyosin), oxidative stress (mitochondrial aldehyde dehydrogenase) and the cytoskeleton (actin-2) (Table 1). Conversely, the 13°C, 28°C and 32°C treatments were uniformly clustering around the same distance from the 24°C treatment, suggesting they all responded similarly in protein abundance changes with respect to PC1 (Fig. 2A). Proteins contributing to this arrangement include those involved in the cytoskeleton (four isoforms of β-tubulin) thin filament regulation (filamin-C and tropomyosin) and regulation about the acto-myosin complex (three isoforms of calponin and a myosin regulatory light chain). Together, it appears that exposure to higher temperatures changed the abundance of proteins primarily involved in cell signaling and thin-filament regulation, whereas exposure to the other temperatures caused changes in the abundance of microtubule subunits and proteins involved in both thick and thin filament regulation. Therefore, it appears acute mild heat stress may have resulted in substantial changes within the cytoskeleton of the adductor muscle.

Given the nature of these results and the thermal history of *M. galloprovincialis*, 24°C may represent a pivotal temperature in which the mussel may detect potential increases in temperature and respond accordingly through alterations to the actin cytoskeleton. Populations of *M. galloprovincialis* have exhibited increased mortality rates when acclimated to temperatures above 24°C, suggesting a decreased capacity to maintain extended valve closure when exposed

to high immersion temperatures for long periods (Anestis et al., 2007; Dowd and Somero, 2013). In addition, the heat shock response of *M. galloprovincialis* is readily induced within a finite temperature range between 23°C & 25°C, through increased abundance of molecular chaperones such as heat shock protein 70 (Hsp70) and the magnitude of heat shock protein expression increases proportionally in response to temperature exposures above 28°C (Hofmann and Somero, 1996; Tomanek and Zuzow 2010). These results indicate exposure to temperatures between 24°C and 32°C may increase the thermal denaturation of susceptible proteins. Interestingly, actin thin filaments are extremely heat sensitive as exposure to increasing temperatures has been shown to promote dissociation of ADP-bound nucleotides between F-actin subunits, which promote vital connections between of F-actin monomers along the length of the filament strand (Hartl et al., 2008). Therefore, the actin cytoskeleton may represent one of the most vulnerable domains to heat stress and subsequent heat shock expression following heat exposure may be in response to prevent aggregation of thermally destabilized thin filaments. Although we did not identify any molecular chaperones contributing to the separation of the 24°C treatment which would suggest thin filament destabilization, the contribution of multiple actin binding proteins suggest modifications to existing myofilaments.

Interestingly, the protein exhibiting the highest loading value separating the 24°C is Rab GDP-dissociation inhibitor (Rab GDI; Table 1). These proteins function primarily to recycle Rab GTPases, which are common mediators in membrane targeted vesicular transport (Stenmark and Olkkonen, 2001). Rab GDI has also been implicated in the RhoA-GTPase/Rho-kinase (RhoA/ROK) calcium sensitization pathway within vertebrate smooth muscle (Somlyo and Somlyo, 2003). Upon activation by heterotrimeric G-protein complexes, RhoA-GTPase is translocated to the membrane to activate Rho-kinase, which further amplifies the signal cascade

through phosphorylation of many downstream mediators including those involved in stress fiber formation (Somlyo and Somlyo, 2003; Tojkander et al., 2012). In this context, Rab-GDI is utilized to sequester RhoA and inhibit the signal by burying the hydrophobic tail of RhoA in order to prevent insertion and localization to the cystolic portion of the muscle cell membrane (Pfeffer, 1995). Thus, the net increase in Rab-GDI abundance at 24°C may perhaps be in response to inactivate RhoA causing quiescence of the RhoA pathway. Due to their relative low abundances, hydrophobic properties and lack of charged residues, membrane proteins are inherently difficult to identify through many conventional proteomic approaches (Helbig et al., 2010). Therefore, the identification of integral, transmembrane and lipid-anchored proteins, i.e., RhoA, within this study is rather limited. However, a portion of the heterotrimeric G-protein complex, i.e., guanine nucleotide binding protein β-subunit, also exhibited a high positive component ranking (Table 1), suggesting a high relative contribution towards the separation of the 24°C treatment. Interestingly, g-protein coupled receptors (GCPR's) and tyrosine kinases represent two of the primary receptors which initiate signal transduction within the RhoA-GTPase/Rho-kinase signaling pathway, and external stimuli which are known to activate these receptors have also been shown to induce actin polymerization and cytoskeletal remodeling within smooth muscle (Somylo and Somlyo 2003; Gunst and Zhang, 2008). Since both signaling proteins were upregulated at this temperature range, it could represent the attenuation of one signaling pathway and the upregulation of another. Therefore, given the isolation of 24°C and the contribution of the proposed signaling proteins in addition to the high number of actin binding proteins, it appears to suggest exposure to 24°C may prompt the reorganization of the actin cytoskeleton within the adductor muscle through activation of particular signaling pathways.

PC2 separated the treatments along a vertical axis and explained nearly 15.5% of the variation in protein abundance observed between the different temperatures (Fig. 2A). Along PC2, there is clear separation of both the 13°C and 32°C treatments within the positive and negative quadrants respectively. Both the 24°C and the 28°C temperatures, however, lie intermittent horizontally between the 13°C and 32°C suggesting similar changes in abundance profiles between these treatments with respect to the PC2 axis (Fig. 2A). Therefore, the major difference evident along PC2 is represented by the change in protein abundance between the control temperature 13°C and extreme temperature of 32°C. Analysis of positive component loading values for PC2, suggests proteins contributing towards the isolation of the 13°C control include those involved in regulation of the cytoskeleton (four isoforms of β-tubulin), thin filaments (actin interacting protein 1), the acto-myosin complex (myosin regulatory light chain, calponin), immune function (apextrin-like protein), vesicular traffic/signal transduction (Rab GDP-dissociation inhibitor β-subunit) as well as energy metabolism (NAD-dependent isocitrate dehydrogenase mitochondrial α-subunit) (Table 1). In contrast, the negative component loadings contributing to the separation of the 32°C treatment are due to proteins involved in regulation of the actomyosin complex (two isoforms of calponin, troponin-T), molecular chaperoning (heat shock protein 70), thin filament regulation (two isoforms of filamin-C, fascin, tropomyosin), the cytoskeleton (β-actin) and oxidative stress (aldehyde dehydrogenase mitochondrial).

Analysis of both protein subsets with respect to PC2 revealed staunch contrasts in the proteomic responses within *M. galloprovincialis* to the control and highest temperature ranges respectively. For instance, β-tubulin isoforms were previously included in the negative component loading values for PC1, which separated the 13°C, 28°C and the 32°C temperatures. However, the inclusion of the two high-ranking β-tubulin isomers, i.e., spot numbers 38 and 39,

within the positive component loadings for PC2 appears to suggest these proteins confer a greater contribution towards the overall separation of the 13°C control temperature (Table 1; Fig. 2A). Isoforms of β-tubulin assimilate towards the fast-growing ends of microtubule protofilaments, and the exchange of the GTP nucleotide within the β-tubulin monomer is crucial for microtubule assembly and disassembly rates (Akhmanova and Steinmetz, 2008). These protofilaments perform a variety of vital cellular functions including in the maintenance of cell morphology as well as assistance with cell motility, vesicular transport and cellular division (Dráber and Dráberová, 2012). In this context, the contribution of β-tubulin isomers may be due to a higher cytoplasmic pool of GTP-bound β-tubulin subunits, possibly as an indication of the active polymerization of microtubule structures at lower temperatures. Perhaps more notable, however, is that these protofilament isoforms do not contribute to the separation of any of the higher temperatures (Table 1). Interestingly, a decrease in β-tubulin gene transcripts in response to increasing immersion temperatures was also observed within muscle tissue of the goby fish, *Gillichthys mirabilis* (Buckley et al., 2006). These authors postulated the net decrease in β-tubulin gene transcripts was due to a downregulation of the cell cycle and suppression of cell proliferation within the muscle tissue. Therefore, the observed absence of β-tubulin subunits at higher temperatures may also indicate cell senescence. This may also provide a context for the observed contribution of the apextrin-like protein towards the separation of the 13°C control (Table 1). Apextrin has been described as a potential member of the membrane attack complex/perforin (MACPF) family (Rosado et al., 2008) and it has been shown to be strongly upregulated in response to bacterial infection of different species of bivalves (Dheilly et al., 2010; Estévez-Calvar et al., 2011), supporting a proposed role in the invertebrate immune response. Since apextrin also does not contribute towards the separation of the higher

temperatures, it may also be indicative of an attenuation of an immune response to increasing temperatures. Interestingly, proteins involved in suppression of the immune response, e.g., RAF kinase inhibitor protein and prostaglandin reductase, were also shown to increase in abundance in response to heat shock within muscle tissue of the porcelain crap, *Petrolishes cinctipes*, suggesting an attenuation of immune function during higher temperature exposure (Garland et al., 2015). Together, these results suggest heat shock possibly inhibits both cell proliferation and immune responses, possibly as a means of allocating resources towards alternative regulatory processes within the muscle cell.

Similar to the positive component loadings contributing to the separation of the 13°C, the negative component loading values with respect to PC2 aid in the sole separation of the 32°C highest temperature extreme (Fig. 2A). Whereas the proteins with positive loading values for PC2 appear to involve the downregulation of specific regulatory processes following exposure to 13°C, the negative component loading values contributing to the separation of 32°C primarily involve proteins which function in the cellular stress response as well as thin filament stabilization (Table 1). Two prominent proteins within this subset involved in the cellular stress response are Hsp70 and mitochondrial aldehyde dehydrogenase (mALDH). Hsp70 isoforms represent a class of molecular chaperones which are highly conserved and function to bind to nascent polypeptide chains of newly synthesized proteins, and promote proper substrate folding using energy released from ATP-hydrolysis (Mayer and Bukau, 2005). During stressful conditions, these chaperones maintain protein quality control within the cell through housekeeping functions designed to recognize misfolded proteins, which then bind to exposed hydrophobic residues in order to prevent further protein denaturation and aggregation (Buchberger et al., 2010). Hsp70 isoforms have been shown to increase in abundance within *M.*

galloprovincialis exposed to immersion temperatures ranging between 23°C & 25°C (Tomanek & Zuzow, 2010, Anestis et al., 2010). In addition, inducible Hsp70 gene transcripts have been observed to significantly increase in expression within *M. galloprovincialis* in response to acute heat exposure between immersion temperatures ranging from 24°C-32°C (Hofmann & Somero, 1996; Franzellitti & Fabbri, 2005; Lockwood et al., 2010). Although we did not quantify the peak temperature of Hsp synthesis, the contribution of the lone Hsp70 isoform towards the separation of the 32°C temperature, it may indicate that this temperature range most likely represents the upper physiological thermal tolerance range for *M. galloprovincialis*.

In addition, the presence of the mALDH isoform within this subset suggests moderate to severe thermal stress occurring within the adductor muscle at highest temperature range. ALDHs are represented in all three taxonomic domains and are upregulated in response to cellular stressors which are known to increase the production of reactive aldehydes (Marchitti et al., 2008; Singh et al., 2013). For instance, during oxidative stress-induced lipid peroxidation, reactive oxygen species (ROS) can interact with polyunsaturated double bonds located within the plasma membrane and produce reactive aldehydes (Ellis, 2007). As such, these aldehyde scavengers have also been shown to be upregulated in the gill tissue of *Mytilus* congeners in response to heat stress (Tomanek & Zuzow, 2010), temperature acclimation (Fields et al., 2012) and hyposalinity stress (Tomanek et al., 2012), suggesting multiple abiotic factors may influence the production of reactive aldehydes in mussels. Since oxidative stress has recently been described as a costressor of thermal stress due to the upregulation of ROS scavenging pathways during heat shock (Tomanek 2012; Tomanek 2015), the presence of both Hsp70 and mALDH in this context appears to support the occurrence of moderate to severe stress to the highest the temperature of 32°C.

Mytilus trossulus

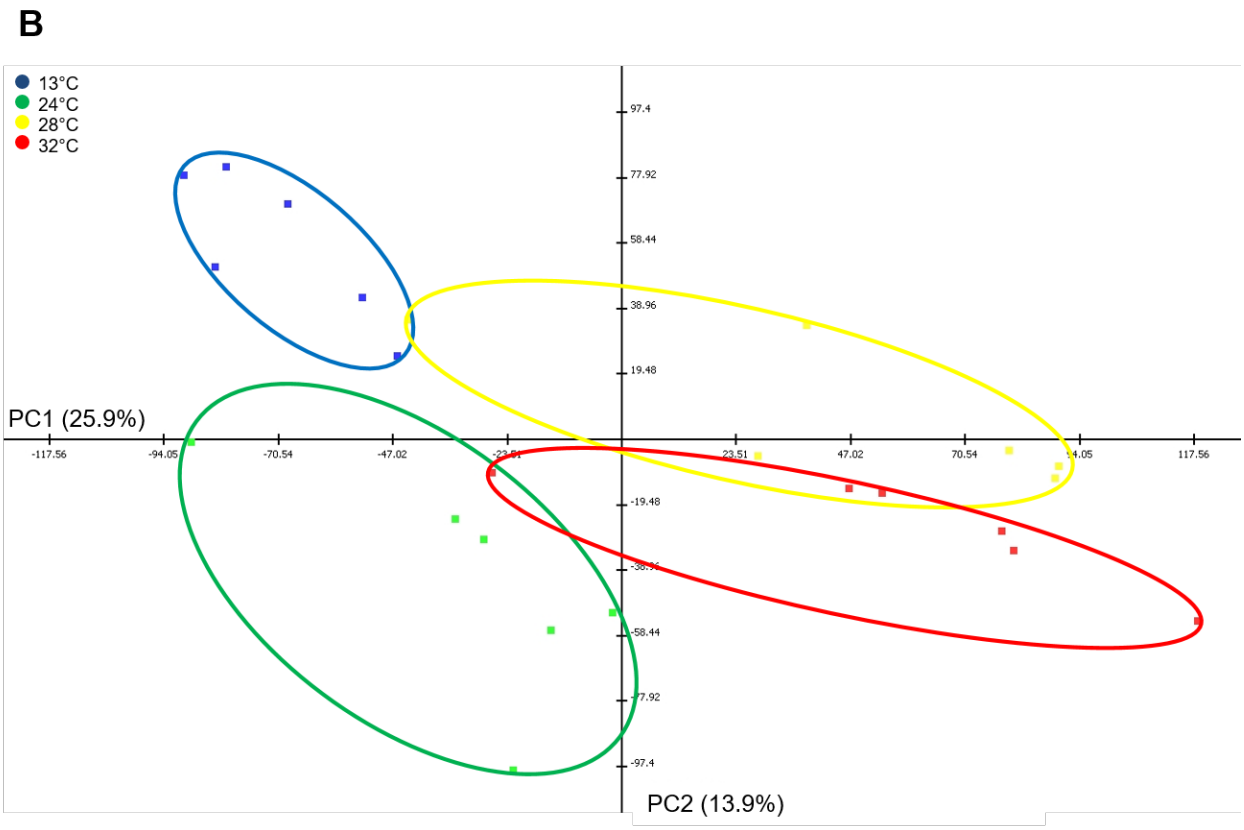

Figure 2B. Principal component analysis displaying all significant proteins within the adductor muscle of *M. trossulus* in response to acute heat shock under sea water immersion. The PCA explains 39.8% of the variation observed between temperature treatments in terms of protein abundance. Specifically, PC1 explains roughly 25.9% whereas PC2 explains 13.9% of the total variation respectively. For PC component loading values see Table(s) 1 & S5.

The second PCA depicts all 97 significant proteins which changed abundance in response to acute heat stress within the adductor muscle of *M. trossulus* (Fig 2B). Similar to *M. galloprovincialis*, the first two components explain roughly 40% of the variation exhibited between temperature treatments. The first component explained 26.9% of the variation in protein abundance and separated the higher temperatures of 28°C and 32°C from the lower 13°C control and 24°C temperatures. In contrast, the second component explained 13.9% of the variation in terms of protein abundance and separated the 13°C and 28°C treatments from the 24°C and 32°C

temperatures respectively (Fig. 2B). Perhaps the most intriguing and most prominent aspect of the overall PCA is the limited overlap between each of the four clusters. Therefore, it appears heat stress evoked distinctive proteomic profiles within the adductor muscle of *M. trossulus*, and these protein signatures were unique to each temperature as compared to *M. galloprovincialis* (Fig. 2A).

Proteins contributing towards the separation of the higher temperature extremes along PC1 include several isoforms of actin as well as proteins involved in cell signal transduction (guanine nucleotide-binding protein β-subunit, 14-3-3 protein), thin-filament regulation (profilin, whirlin) heat stress (three small heat shock protein isoforms) and the actin cytoskeleton (Table 1). The variation observed in actin isoforms appears to suggest remodeling of thin filament structures, given the additional contributions of the thin-filament regulatory proteins, e.g., profilin and whirlin, towards the observed separation of the higher temperatures (Table 1). Profilin promotes the exchange of ADP/ATP of G-actin monomers, which then bind to barbed ends of F-actin in order to promote microfilament assembly (Dos Remedios et al., 2003; Pollard and Borisy, 2003). By sequestering and forming complexes with ATP bound to G-actin, profilin increases the kinetic parameters favoring barbed end nucleation, thus increasing the rate of thin filament polymerization (Carlier and Pantaloni, 2007). Whirlin has also been suggested to assist in thin filament assembly by colocalizing near the growing end of actin filaments and forming complexes with myosin and other actin binding proteins near the apical membrane during stereocilia growth in cochlear hair cells (Rzadzinska et al., 2004; Mburu et al., 2006; Brown et al., 2008). Interestingly, these proteins are quintessential for regulating thin filament polymerization such that overabundance of whirlin can result in abnormally long hair cells (Prosser et al., 2008). Whirlin has also been postulated to ensure cytoskeletal integrity by acting

as a cytoskeletal scaffolding protein and aid in the structural integrity of the actin bundle network in hair cells and myelinated axons (Wang et al., 2011; Green et al., 2013). Given the nature of these proteins, it suggests higher temperatures influences active thin filament polymerization and coordination of actin treadmilling, possibly as a means to promote cytoskeletal structural integrity. However, perhaps the most intriguing aspect among this protein subset is the contribution of multiple small heat shock protein (sHsps) isoforms (Table 1). A primary function of these molecular chaperones is the prevention of F-actin aggregation, following thermally induced denaturation of actin thin filaments (Pivovarova et al., 2007). Therefore, given the combined contributions of proteins involved in regulation of thin filament elongation and prevention of thin filament aggregates, it appears higher temperatures destabilize thin filament structure and possibly induce the dynamic remodeling of actin thin filaments which may weaken the structural integrity of the cytoskeletal network within the adductor muscle of *M. trossulus*.

While the positive loading values for PC1 separate the higher temperatures, the negative loading values facilitate the separation of the lower temperatures of 13°C control and 24°C respectively (Fig 2B). The negative component loadings contributing to this separation include a molecular chaperone (sHsp), microtubule monomers (two β-tubulin subunits), a monomeric subunit of the F_1 portion of the mitochondrial ATP synthase (ATP synthase β-subunit), multiple thin and thick filament regulatory proteins (three calponin isoforms and troponin-T) and cytoskeletal proteins (short-chain collagen, actin and collagen α-VI chain) (Table 1). As mentioned previously, most of these proteins appear to indicate adaptive remodeling of the cytoskeletal architecture. However, perhaps one of the more intriguing aspects of this subset, is represented by the contribution of the sHsp isoform (Table 1). It is possible the upregulation observed in sHsp abundance may in fact reflect the onset threshold induction temperature for the

inducible heat-shock response within *M. trossulus*. The expression of heat-shock transcription factors (HSFs) has been shown to readily increase in this species between temperatures of 20-23°C (Buckley et al., 2001). Since a major housekeeping function of sHsp's is to stabilize the actin-based cytoskeleton (Sun and MacRae, 2005; Wettstein et al., 2012), this observation could possibly be indicative of increased thin filament destabilization within the cytoskeletal network. This coincides with previous observations, as several sHsp isoforms were found to significantly contribute towards the separation of the higher temperature treatments, suggesting thermal denaturation of thin filaments may readily occur within the adductor muscle at seawater temperatures approaching 24°C. Taken together, the observed contribution of multiple sHsp isoforms towards the separation of each of the higher temperatures appears to suggest the induction of the heat-shock response within the adductor muscle of *M. trossulus* may also coincide with thermal denaturation of actin microfilaments. Therefore, upregulation of sHsp's may be required to prevent further thin filament destabilization and the aggregation of denatured thin filament aggregates.

The second principal component explains nearly 14% of the variation among temperature treatments, and separates both the 13°C control & 28°C group from the 24°C and the 32°C temperatures along a vertical axis (Fig. 2B). A striking aspect of this component separation is the near complete separation of the 13°C control from all other temperature treatments. The positive component loading values for PC2 which contribute towards the near complete separation of the 13°C control from all higher temperature treatments, include several proteins involved in thin filament regulation (gelsolin and calponin), thin filament bundling (fascin), oxidative stress (mALDH), energy metabolism (pyruvate dehydrogenase E1 component β-subunit, ATP synthase F1 β-subunit and purine nucleoside phosphorylase), vesicular trafficking/signal transduction

(Rab-GDI) and cytoskeletal proteins (two isoforms of β-tubulin and an actin isoform) (Table 1). Given the high number of protein functional groups evident within this component subset, it suggests a multi-tiered cellular response upon the onset of increasing immersion temperature. As similarly seen in *M. galloprovincialis*, several proteins which contribute towards the sole separation of the 13°C control appear to be at low levels at the higher temperatures, alluding to the possible attenuation of certain cellular functions in response to heat stress. For instance, several metabolic proteins including pyruvate dehydrogenase, ATP synthase F1 β-subunit and purine nucleoside phosphorylase only contributed towards the separation of the 13°C temperature (Table 1). This appears to suggest downregulation of specific energetic pathways during higher temperature exposure. In previous studies, downregulation of certain glycolytic enzymes, e.g., pyruvate kinase (PK), among *Mytilus* congeners in response to acclimation temperatures higher than 24°C was suggested to facilitate a putative switch from aerobic to anaerobic metabolism (Anestis et al., 2007). This energetic shift was possibly in reference to extended valve closure and therefore a reduction in oxygen supply (Anestis et al., 2007). The proposed downregulation of energetic pathways in this context may also represent an alternative strategy to reduce the accumulation of ROS, as indicated by the presence of the ROS-scavenger mALDH (Table 1). However, perhaps the most notable aspect of this subset is indicated by the contribution of multiple actin-binding proteins (Table 1), further suggesting substantial changes to the actin cytoskeleton in response to temperature increases.

Finally, proteins with negative component loadings for PC2, which partially separates 28°C and completely separates 24°C and 32°C from the 13°C control (Fig. 2B), are involved in regulation of the acto-myosin complex (three isoforms of troponin-T), molecular chaperoning (sHsp), the cytoskeleton (three isoforms of actin), oxidative stress (Cu-Zn superoxide dismutase)

and heavy metal sequestration (heavy metal binding protein). Whereas the positive component loadings for PC2 exhibit a correlation towards thin-filament reorganization, the proteins included in the negative component loadings appear to suggest severe thermal stress impacting actin thin filament structure. Recent evidence has suggested increase in troponin-T (TnT) isoforms is due to irreversible proteolytic degradation of molecular contractile elements within multiple muscle types, and increased abundance of TnT isoforms has become a hallmark for detecting myocyte cell turnover, apoptosis and organ damage (Apple and Collinson, 2012, Lavatelli et al., 2014). The abundance of TnT isoforms also coincides with the contribution of the sHsp and Copper-Zinc superoxide dismutase isoforms (Cu-Zn SOD) towards the separation evident along PC2. Cu-Zn SOD belongs to a family of peroxidases and is one of the primary detoxifying agents which function to sequester accumulated intracellular ROS to prevent further cellular damage to macromolecules (Matés and Sánchez-Jiménez, 2000). Coincidentally, several peroxidase enzymes along with thioredoxin and ALDH were also identified in the gill tissue of *M. trossulus* in response to increasing temperature (Tomanek and Zuzow, 2010). However, Cu-Zn SOD isoforms were only identified in the gill tissue of *M. galloprovincialis* at both high and low temperatures. These authors suggested that the absence of Cu-Zn SOD within *M. trossulus* at the higher temperatures was due to incapacity to cope with oxidative stress in response high temperature exposure. Given the protective function of both sHsp and Cu-Zn SOD, it is possible the adductor muscle can respond to higher temperatures, but this response may be rather limited as indicated by the presence of the TnT isoforms and the correlations between increased rates of cell damage. Therefore, acute exposure to higher temperatures may evoke a severe cellular stress response within muscle cells of *M. trossulus*.

Hierarchical Clustering Analysis

Hierarchical clustering analysis is a preferred method for visualizing large data sets, which attempts to classify individual samples based on their global abundance profiles (Meunier et al., 2007). In this regard, each protein spot is normalized against the mean protein spot volume generated from the consensus spot pattern within the corresponding composite fusion image (Fig(s). 1A & 1B). These dendrograms link together proteins into distinct clusters via a correlational relationship, which then display similar patterns in abundance change across the temperature treatments. To this degree, each column within the dendrogram represents an individual adductor muscle sample, whereas each row illustrates the variance in abundance for a given protein spot in response to the different temperature (Fig(s) 3 & 4). Thus, individual protein spots can be compared across a standardized abundance range (Eisen et al., 1998). Here, we focus on which proteins were found to be significantly upregulated, i.e., exhibit increased abundance, or downregulated, i.e., exhibit decreased abundance, in response to temperature exposure.

Mytilus galloprovincialis

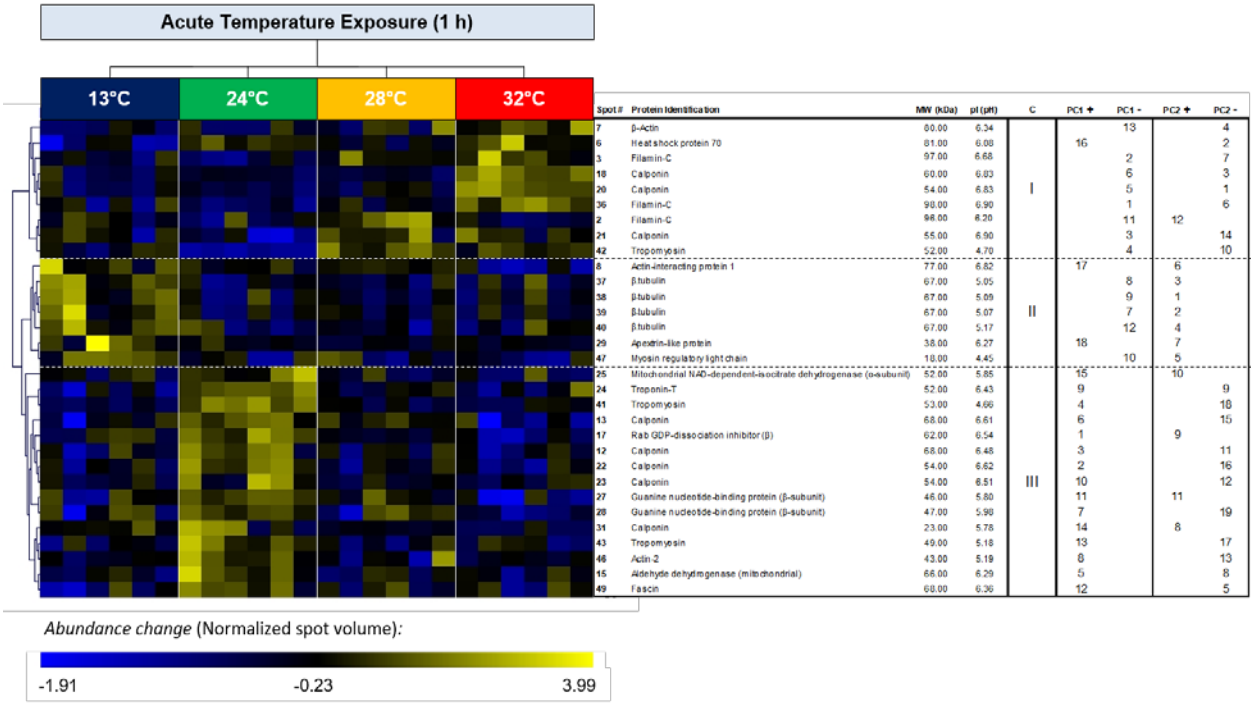

Spot #	Protein Identification	MW (kDa)	pI (pH)	C	PC1 +	PC1 -	PC2 +	PC2 -
7	β-Actin	80.00	6.34			13		4
6	Heat shock protein 70	81.00	6.08		16			2
3	Filamin-C	97.00	6.68			2		7
18	Calponin	60.00	6.83			6		3
20	Calponin	54.00	6.83	I		5		1
36	Filamin-C	98.00	6.90			1		6
2	Filamin-C	98.00	6.20			11	12	
21	Calponin	55.00	6.90			3		14
42	Tropomyosin	52.00	4.70			4		10
8	Actin-interacting protein 1	77.00	6.82		17		6	
37	βtubulin	67.00	5.05			8	3	
38	βtubulin	67.00	5.09			9	1	
39	βtubulin	67.00	5.07	II		7	2	
40	βtubulin	67.00	5.17			12	4	
29	Apextrin-like protein	38.00	6.27		18		7	
47	Myosin regulatory light chain	18.00	4.45			10	5	
25	Mitochondrial NAD-dependent-isocitrate dehydrogenase (α-subunit)	52.00	5.85			15	10	
24	Troponin-T	52.00	6.43			9		9
41	Tropomyosin	53.00	4.66			4		18
13	Calponin	68.00	6.61			6		15
17	Rab GDP-dissociation inhibitor (β)	62.00	6.54			1	9	
12	Calponin	68.00	6.48			3		11
22	Calponin	54.00	6.62			2		16
23	Calponin	54.00	6.51	III		10		12
27	Guanine nucleotide-binding protein (β-subunit)	46.00	5.80			11	11	
28	Guanine nucleotide-binding protein (β-subunit)	47.00	5.98			7		19
31	Calponin	23.00	5.78			14	8	
43	Tropomyosin	49.00	5.18			13		17
46	Actin-2	43.00	5.19			8		13
15	Aldehyde dehydrogenase (mitochondrial)	66.00	6.29			5		8
49	Fascin	68.00	6.36			12		5

Figure 3. Hierarchal clustering using Pearson's correlation depicting all significant spots identified within *M. galloprovincialis* in response to acute heat stress. Changes in protein abundance are provided in terms of normalized spot volume; blue denotes a lower than average protein abundance, whereas yellow indicates a greater than average protein abundance. The temperature treatments are labeled along the upper horizontal axis. Each column depicts an individual mussel sample, i.e., adductor muscle (n = 6 per treatment), whereas each row represents the standardized abundance pattern for an identified protein within each tissue sample across the varying temperature treatments. Clustering depicts three major groups of proteins (C), which exhibit similar changes in relative abundance patterns across temperature treatments. Molecular weights (kDa) and isoelectric points (pI) were determined through investigation of the relative locations within the fusion gel image (Fig. 1A). Note: Principal component loading values associated with each protein are presented in terms of numerical rank; lower numbers correspond to proteins which attribute greater contributions towards the separation between temperature treatments exhibited along the respected component axis (See Fig. 2A).

Hierarchical clustering analysis produced three major protein clusters (Fig. 3). The first cluster is characterized by the up-regulation of proteins in response to the two highest temperatures, i.e., 28°C and 32°C, as compared to the two lower temperatures, i.e., 13°C control and 24°C. In total, there were nine proteins which comprised this cluster. These included one large actin isoform (β-actin), along with several actin-binding protein isoforms such as calponin, filamin-C and tropomyosin (Fig. 3). The final protein within this subset corresponded to the molecular chaperone Hsp70. Interestingly, this Hsp70 isoform was the only significant molecular chaperone identified within the adductor muscle of *M. galloprovincialis* (Table S1). Since this isolated Hsp70 isoform only exhibited an increased abundance following exposure to the highest temperature range, it further suggests the heat shock response within the adductor muscle of *M. galloprovincialis* is possibly induced following exposure to immersion temperatures exceeding 28°C. In addition, the presence of the lone actin isoform within this subset provides further evidence towards the proposed heat-induced destabilization of the actin cytoskeletal network, as prolonged heat incubation has been shown to effectively denature actin subunits and increase the number of thin filament aggregates (Levitsky et al., 2008). Given the increasing evidence of temperatures effects on cytoskeletal structural integrity, the high number of cytoskeletal accessory proteins within this cluster might represent the complete of restructuring cytoskeletal domains to protect existent actin thin filaments and prevent filament denaturation.

Typically, actin thin filaments are thought to be static structures, e.g., striated muscle fibers, exhibiting minimal changes in persistent length to support contractile function through the interaction with adjacent myosin thick filaments (Littlefield and Fowler, 2008). The maintenance of thin filament structure is vital to support proper muscle function. Recent evidence has suggested smooth muscle function is primarily regulated through the dynamic restructuring of

thin filaments, a process governed by several major classes of actin-binding proteins (Gunst and Zhang, 2008; Lehman and Morgan, 2012). Interestingly, calponin, filamin-C and tropomyosin, which are all included within this first cluster are all classified as actin-binding proteins and have long been postulated to regulate thin filament architecture and stability (Hodgekinson, 2000; Yu and Ono, 2006; Rozenblum and Gimona, 2008; Gunst and Zhang, 2008).

Calponin displays affinity towards calcium and shows structural homology to the thin-filament regulatory protein troponin (El-Mezgueldi, 1996). Coincidently, calponin orthologs were soon thereafter discovered within smooth muscle tissue of several mussel species, including *M. galloprovincialis*, and were shown to effectively inhibit myosin-mediated cross-bridge cycling (Funabara et al., 2001; Dobrzhanskaya et al., 2013; Sirenko et al., 2013). These results suggest calponin plays a strong role in the regulation of contractile activity within Molluscan smooth muscle. Although calponin's definitive function remains unclear, there have been multiple proposed roles for the proteins hypothesized regulation of smooth muscle contractile dynamics. For instance, Gimona and colleagues suggested calponin confers thin filament conformational stability through interactions with thin filament cross-linking proteins, such as α-actinin, thus providing a more rigid structure to promote torsional stabilization (Gimona et al., 2003). Interestingly, calponin has also been postulated to modulate the availability of F-actin towards additional actin-binding proteins (Lehman and Morgan, 2012) and also exhibits high-affinity towards different thin filament accessory proteins including filamin and tropomyosin (Rozenblum and Gimona 2008; Mendéz-Lopéz, 2012). These findings suggest calponin isoforms display a strong regulatory capacity within smooth muscle cells by regulating thin filament flexural mechanics, structural integrity and influencing F-actin availability towards additional thin filament proteins.

In addition to calponin's proposed regulation of cytoskeletal dynamics, certain isoforms are involved in signaling pathways of smooth muscle (Gunst and Zhang, 2008). Vertebrate calponin isotypes located within submembranous adhesion complexes have exhibited a propensity to interact with multiple signal kinases including mitogen activated protein kinases (MAPKs), extracellular-signal related kinases (ERKs) and protein kinase C (PKC) (A) Kim et al., 2008). Phosphorylation of certain calponin residues by these kinases is thought to induce docking function for multiple effector proteins within the ERK and PKC signaling pathways (A) Kim et al., 2008). For instance, it has been proposed that upon extracellular stimulation, PKC phosphorylates actin-bound calponin causing thin filament dissociation (A) Kim et al., 2008). In turn, phosphorylated calponin serves as signaling scaffold to sequester contractile mediators located within adjacent adhesion complexes near the plasma membrane. Upon membrane dissociation, these large activated protein complexes can translocate between cytoplasmic and cortical actin domains and induce thin filament remodeling parallel to the plasma membrane (A) Kim et al., 2008). The conformational changes among cortical actin thin filaments can then expose myosin binding sites along the filament strand leading to eventual smooth muscle contraction (B) Kim et al., 2008). Thus, calponin may also serve as a downstream mediator within adhesion complexes and promote thin filament remodeling within the adductor muscle in response to heat stress.

Given all the proposed functions of calponin in smooth muscle in addition to the multiple isoforms included within both data sets, it appears these isoforms may regulate critical cytoskeletal functions within the adductor muscle in response to acute heat stress. Another intriguing proposed cellular function of calponin involves the mechanical stability of reconstituted actin thin filament networks (Jensen et al., 2014). These authors found that actin

filament networks decorated with a two-fold increase in calponin exhibited both an increased maximum strain and delayed onset to thin filament strain-stiffening as compared to non-calponin decorated actin thin filaments (Jensen et al., 2014). Interestingly, they attributed these observations towards a decreased persistent length and an overall increased flexural stability of calponin-decorated thin filaments. Thus, in this context, calponin was able to stabilize thin filament structure by making thin filaments more flexible. These results are especially intriguing given the observation heat stress elicits mechanical destabilization of actin filaments through increased kinetic flexibility of the filament strand (Levitsky et al., 2008).

The functional dynamics associated with calponin may also coincide with the increased abundances of filamin-C (FLNC) isoforms at the higher temperature ranges (Fig. 3). Filamin isoforms have previously been identified within the adductor muscle of *M. galloprovincialis*, and exhibited a high affinity association with calponin (Mendéz-Lopéz et al., 2012). FLNC's represent a class of flexible actin-binding proteins which primarily function to interlink submembranous actin thin filament networks (Popowicz et al., 2006). This cross-linking capacity serves a mechanoprotective function by establishing connections between the extracellular matrix and the cortical cytoskeleton, allowing for increased elasticity of cortical thin filaments and resistance to sheer stress (Nakamura et al., 2011). Given the established connections between the plasma membrane and cortical actin cytoskeleton, FLNC's have also been suggested to act as potential mechanotransducers by serving as molecular scaffolds for signaling proteins during responses to extracellular stimuli (Razinia et al., 2012). Considering the multiple proposed functions of calponin and FLNC, it is possible that the upregulation of both proteins in response to acute heat stress may synergistically function to stabilize the actin cytoskeleton via a variety of potential mechanisms. In addition, given that many of these proposed protein functions occur

within adhesion complexes regulating the cortical actin cytoskeleton of smooth muscle, it is also possible the dynamic regulation involving thin filaments within the adductor muscle may also involve the cortical actin domain.

The observed upregulation of both calponin and filamin in response to acute heat stress strongly suggests a cellular response to stabilize the actin cytoskeleton. The final protein within this cluster, i.e., tropomyosin (TPM), may provide the strongest evidence for thin filament stabilization. TPM isoforms represent a large and highly conserved family of dimeric proteins which coil along the length of extended actin filaments to block myosin binding sites and inhibit contraction (Gimona, 2008). Although there have been many reports of multiple tissue-specific TPM isotypes (Gunning et al., 2005), most primarily function as thin filament stabilizers either by increasing the persistent length of actin filaments or by exhibiting antagonistic behavior towards actin depolymerizing factors such as ADF/cofilin and gelsolin (Greenberg et al., 2008; Yu and Ono 2006). TPM isoforms have also been postulated to aid in thin filament polymerization through interactions with tropomodulin, an actin binding protein which caps the barbed end of growing actin thin filaments (Rao et al., 2014). Other reports suggest TPM isoforms may also be involved in cell proliferation, morphogenesis and cytokinesis (Gunning et al., 2015). Many of the proposed cellular functions are affected by the capacity of specific TPM isoforms to regulate thin filament affinity towards accessory actin binding proteins. For instance, overexpression of a certain TPM isoforms elicits a change in the subcellular localization and concomitant increase in the concentration of fascin within murine neuroblast cells (Creed et al., 2011). These results suggest specific TPM isoforms are not only involved in thin filament stabilization, but also with the active recruitment of actin binding proteins to promote thin filament cross-linking and to decrease susceptibility to thin filament severing (Creed, et al.,

2011; Gunning, 2015). Interestingly, basic calponin isoforms in knockout studies have been shown to effect TPM expression, suggesting thin filament regulatory proteins can also alter the transcriptional regulation of alternative actin binding proteins (Rozenblum and Gimona, 2008). Therefore, it appears several thin filament regulatory proteins not only influence mechanical stabilization, but may also affect thin filament dynamics through direct interactions of accessory actin binding proteins. Specifically, the increased expression of calponin, FLNC and TPM in response to increasing temperatures may influence thin filament stabilization within the adductor muscle either through direct interactions with F-actin, or by increasing the recruitment of thin filament cross-linking proteins in order to promote increased flexural stability of existent thin filaments.

Cluster II contains seven proteins which appear to be upregulated at the control temperature (13°C) and downregulated at all the higher temperatures (Fig. 3). These include four isoforms of β-tubulin, an apextrin-like protein, a myosin regulatory light chain (MRLC) and an actin-interacting protein. This pattern of protein downregulation and attenuation of certain cellular functions, may be necessary to reduce energy expenditure from physiological processes which require substantive energy input. For example, muscle contraction is an energetically taxing process, due to the rapid rate of ATP turnover required to fuel myosin Mg^{2+}-ATPase activity and initiate cross-bridge cycling (Hooper, 2008). Interestingly, MRLC is tightly involved in smooth muscle contraction (Kamm and Stull, 1985) and has been shown to be a critical part of smooth muscle regulation within many species of bivalves (Hooper et al., 2008). The downregulation of MRLC could be in response to reduce the energetic demand required to induce contractile processes. In support of this notion, Anestis and colleagues reported decreased oxygen consumption among *M. galloprovincialis* acclimated to immersion temperatures above

24°C (Anestis et al., 2010). The decreases in oxygen availability may also cause a reduction in cross-bridge cycling. The downregulation of MRLC may be associated with the unique physiological properties associated with Molluscan smooth muscle (Galler, 2008). The catch response is exemplified by the formation of transient connections between adjacent thick filaments and thin filaments during extended valve closure events (Butler and Siegman, 2010). During this process, both myosin cross-bridge cycling and ATP turnover rates are drastically reduced, allowing the muscle to relax while these catch linkages remain tethered (Galler, 2008). Therefore, the downregulation in MRLC in response to high temperatures may indicate the attenuation of active contraction and possibly signal the activation of the catch response to maintain valve closure in response to increasing temperatures.

The final protein within this cluster, actin-interacting protein one (AIP1), exhibits cooperation with the thin filament severing protein cofilin (Ono et al., 2003; Okada et al., 2006). The combined actions of these two proteins has been suggested to promote the disassembly of actin thin filaments, possibly as a means to remodel the actin cytoskeleton in anticipation of major cellular events such as cytokinesis and cellular division (Ono et al., 2003; Okada et al., 2006). Although the role of AIP1 in adductor muscle is not well established, the proteins proposed role in thin filament destabilization does offer a unique insight into the possible mechanisms occurring within the cytoskeletal domain during heat stress. Specifically, AIP1 is the only significant actin-binding protein within *M. galloprovincialis* which displays a primary function to destabilize the actin cytoskeleton. In addition, the increases abundances of TPM and other thin filament stabilizing proteins at higher temperatures suggests that actin depolymerizing factors are inhibited during heat stress. Thus, the downregulation of actin depolymerizing factors

during higher temperature exposure provides further evidence for the maintenance of cytoskeletal structures within *M. galloprovincialis*.

Finally, the third and largest cluster contained a total of fifteen proteins, involved in energy metabolism, vesicular trafficking, signal transduction, oxidative stress and regulation of cytoskeletal dynamics (Fig. 3). This cluster was characterized by proteins which exhibited the greatest increase in abundance primarily in response to 24°C (Fig. 3). The substantial amount of proteins within this cluster, in conjunction with the largest assortment of proteins of varying function, suggests significant molecular changes occur within the adductor muscle in response to 24°C as compared to other temperatures. This result was also readily apparent during the investigation of the PCA for *M. galloprovincialis* (Fig. 2A). We hypothesized that 24°C exposure possibly represents the temperature in which the heat shock response is induced. Interestingly, these results are supported from previous experiments as significant increases in the expression of molecular chaperones were reported between acclimation temperatures approaching 24°C -26°C within the gill tissue of *M. galloprovincialis* (Tomanek and Zuzow, 2010; Anestis et al., 2007). Although there was only one molecular chaperone represented in the first cluster, there were several proteins within the third cluster which suggest the occurrence of moderate levels of heat stress during acute exposure to 24°C. Specifically, these include mALDH and NAD-dependent isocitrate dehydrogenase (mICDH) and the TnT isoform (Fig. 3). The increased abundance of both of these proteins in response to acute heat stress has been hypothesized to occur as a result of increased production of ROS, since oxidative stress proteins aid in ROS-sequestration through counter production of reducing equivalents in response to a multitude of environmental stressors (Tomanek and Zuzow, 2010; Tomanek, 2015). Both isoforms in this context are mitochondrial, which suggest that the mitochondria are the possible

source of ROS production within adductor muscle cells during exposure to 24°C. Since many studies have shown a reduction in aerobic metabolism occurring within mussels in response to heat stress (Anestis et al., 2007; Gracey et al., 2008; Sokolova et al., 2012), it is unlikely the increased abundance of NAD-dependent mICDH is due to an increase in aerobic metabolism. However, the increased abundance of mICDH could be representative of a metabolic shunt, possibly to increase anaerobic production of ATP to supplement the increased abundance of thin filament regulatory proteins in response to acute heat stress.

Finally, the last proteins yet to be discussed within this subset are the actin subunits, β-actin and actin-2, which are both located in first and third clusters respectively (Fig. 3). The presence of these different actin isoforms at the higher temperature ranges may indicate different rates of thin filament polymerization in response to increasing temperatures. Monomeric G-actin has a molecular weight of around 42,000-46,000 Daltons (42-46 kDa) and is maintained at relatively stable cytoplasmic ratios to supplement thin filament polymerization in response to many environmental and cellular stimuli (Dugina et al., 2012). Interestingly, the actin-2 isoform present within the third cluster exhibits a molecular weight of 43 kDa, possibly indicating a higher pool of monomeric G-actin in response to 24°C temperature exposure. Therefore, given the substantial amount of actin-binding proteins within the third cluster, 24°C may also signal the formation of specific actin thin filaments. However, perhaps the most intriguing aspect of this potential hypothesis corresponds to the β-actin isoform present upregulated in response to 28°C and 32°C exposure (Fig. 3). This β-actin isoform exhibits a substantial increase in both molecular weight (80 kDa) and the isoelectric point (6.34 pI) as compared to the actin-2 isoform upregulated at 24°C (Fig. 3). Although the variation between actin isoforms present within this subset may be attributed to a PTM, as there are many known PTM's which effect actin

regulation (Terman and Kashina, 2013), it is interesting to note the changes in molecular weights between the actin isoforms in the proposed context of thin filament remodeling. Currently, there are several known classes of smooth muscle actin isoforms, i.e., α-, β- and γ-actin, and the major functional differences between these classes stem from the variation exhibited within the N-terminal region of the actin polypeptide (Dugina et al., 2012). The N-terminal region of actin has been proposed to be a docking site for actin regulatory proteins, given the high number of charged residues conferring increased stability via increased electrostatic interactions (Dugina et al., 2012). Beta-actin has also been postulated to be involved in contractile dynamics and cortical cytoskeletal regulation (Dugina et al., 2012), and also interacts with accessory actin binding proteins such as calponin (Gunst and Zhang 2008). As a result, the variation in actin isoforms in correlation with the increased number of actin binding proteins appears to suggest exposure to higher temperatures elicits substantial changes within the actin cytoskeleton. Specifically, the increased abundance of actin binding proteins and cross-linking proteins in response to the higher temperature exposures may correspond to the increased stabilization of the cortical actin cytoskeleton, possibly as a means to maintain tension development through the increased number of passive linkages formed between the cortical actin cytoskeleton and the contractile domain.

Mytilus trossulus

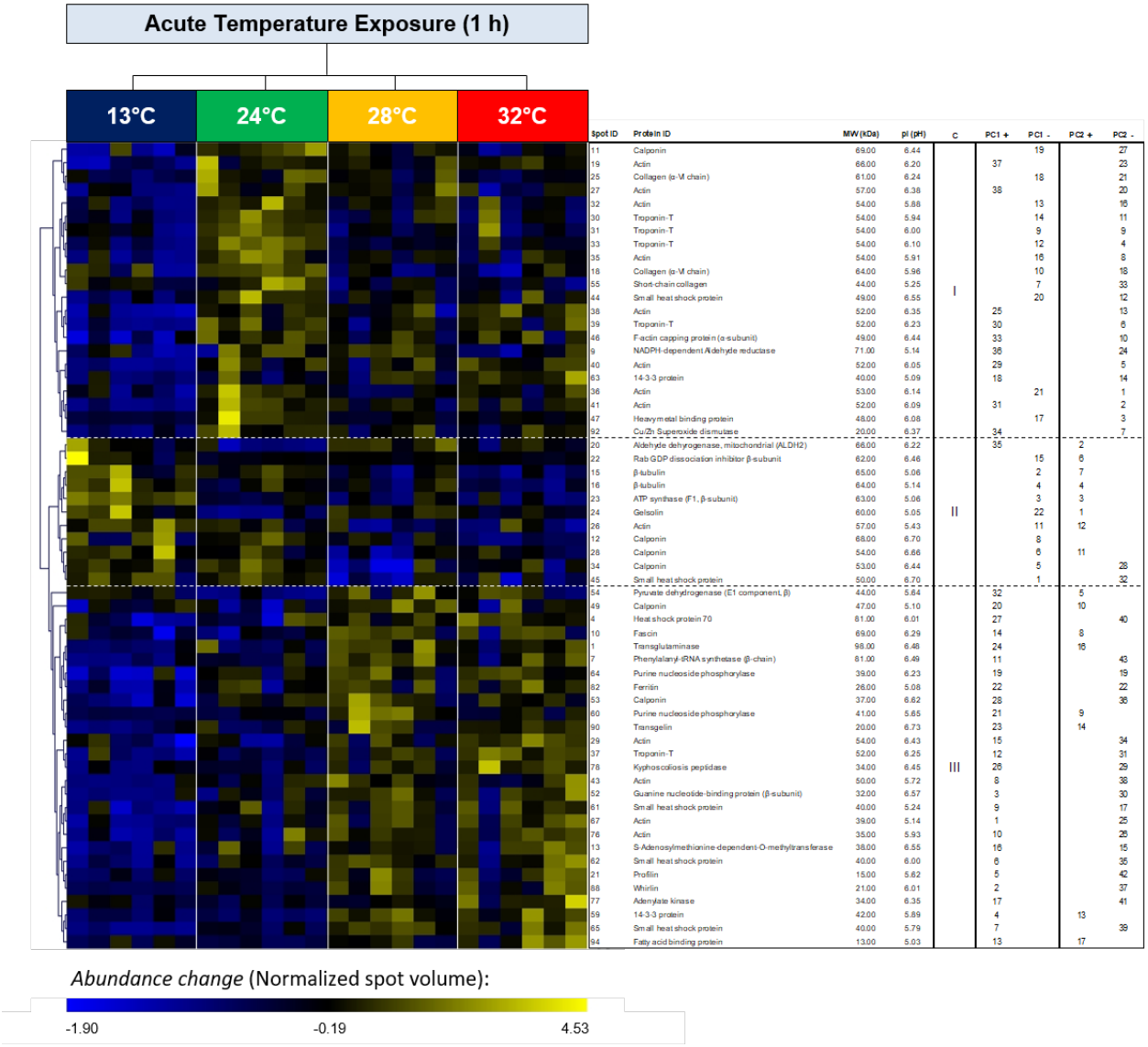

Spot ID	Protein ID	MW (kDa)	pI (pH)	C	PC1 +	PC1 -	PC2 +	PC2 -
11	Calponin	69.00	6.44			19		27
19	Actin	66.00	6.20		37			23
25	Collagen (α-VI chain)	61.00	6.24			18		21
27	Actin	57.00	6.38		38			20
32	Actin	54.00	5.88			13		16
30	Troponin-T	54.00	5.94			14		11
31	Troponin-T	54.00	6.00			9		9
33	Troponin-T	54.00	6.10			12		4
35	Actin	54.00	5.91			16		8
18	Collagen (α-VI chain)	64.00	5.96			10		18
55	Short-chain collagen	44.00	5.25			7		33
44	Small heat shock protein	49.00	6.55	I		20		12
38	Actin	52.00	6.35		25			13
39	Troponin-T	52.00	6.23		30			6
46	F-actin capping protein (α-subunit)	49.00	6.44		33			10
9	NADPH-dependent Aldehyde reductase	71.00	5.14		36			24
40	Actin	52.00	6.05		29			5
63	14-3-3 protein	40.00	5.09		18			14
36	Actin	53.00	6.14			21		1
41	Actin	52.00	6.09		31			2
47	Heavy metal binding protein	48.00	6.08			17		3
92	Cu/Zn Superoxide dismutase	20.00	6.37		34			7
20	Aldehyde dehyrogenase, mitochondrial (ALDH2)	66.00	6.22		35		2	
22	Rab GDP dissociation inhibitor β-subunit	62.00	6.46			15	6	
15	β-tubulin	65.00	5.06			2	7	
16	β-tubulin	64.00	5.14			4	4	
23	ATP synthase (F1, β-subunit)	63.00	5.06			3	3	
24	Gelsolin	60.00	5.05	II		22	1	
26	Actin	57.00	5.43			11	12	
12	Calponin	68.00	6.70			8		
28	Calponin	54.00	6.66			6	11	
34	Calponin	53.00	6.44			5		28
45	Small heat shock protein	50.00	6.70			1		32
54	Pyruvate dehydrogenase (E1 component, β)	44.00	5.84		32		5	
49	Calponin	47.00	5.10		20		10	
4	Heat shock protein 70	81.00	6.01		27			40
10	Fascin	69.00	6.29		14		8	
1	Transglutaminase	98.00	6.48		24		16	
7	Phenylalanyl-tRNA synthetase (β-chain)	81.00	6.49		11			43
64	Purine nucleoside phosphorylase	39.00	6.23		19			19
82	Ferritin	26.00	5.08		22			22
53	Calponin	37.00	6.62		28			36
60	Purine nucleoside phosphorylase	41.00	5.65		21		9	
90	Transgelin	20.00	6.73		23		14	
29	Actin	54.00	6.43		15			34
37	Troponin-T	52.00	6.25		12			31
78	Kyphoscoliosis peptidase	34.00	6.45	III	26			29
43	Actin	50.00	5.72		8			38
52	Guanine nucleoside-binding protein (β-subunit)	32.00	6.57		3			30
81	Small heat shock protein	40.00	5.24		9			17
67	Actin	39.00	5.14		1			25
76	Actin	35.00	5.93		10			26
13	S-Adenosylmethionine-dependent-O-methyltransferase	38.00	6.55		16			15
62	Small heat shock protein	40.00	6.00		6			35
21	Profilin	15.00	5.82		5			42
88	Whirlin	21.00	6.01		2			37
77	Adenylate kinase	34.00	6.35		17			41
59	14-3-3 protein	42.00	5.89		4		13	
65	Small heat shock protein	40.00	5.79		7			39
94	Fatty acid binding protein	13.00	5.03		13		17	

Figure 4. Hierarchal clustering using Pearson's correlation depicting all significantly identified protein spots within *M. trossulus* in response to acute heat stress. Molecular weights (kDa) and isoelectric points (pI) were determined through investigation of the relative locations within corresponding fusion image (Fig. 1B). Principal component loading values are ranked based on the contribution towards separation of temperature treatments (See Fig. 2B).

Similar to *M. galloprovincialis*, hierarchical clustering revealed three clusters which display similar patterns in response to temperature changes. Specifically, each of these clusters depicts proteins exhibiting increased abundance in response to either 13°C, 24°C or both 28°C and 32°C (Fig. 4). Cluster I can best be summarized by proteins which exhibit significant increases in protein abundance in response to 24°C (Fig. 4). This cluster includes 22 proteins, most of which are involved in cytoskeletal regulation, i.e., calponin, eight isoforms of actin, four isoforms of TnT, several collagen fibers and an F-actin capping protein (Fig. 4). There are also several additional functional categories represented within this cluster, including molecular chaperones (sHsp), signal transduction (14-3-3 protein), oxidative stress (NADPH-dependent aldehyde reductase & Cu/Zn SOD) and heavy metal sequestration (heavy metal binding protein).

The protein functional categories represented within this cluster suggests 24°C exposure elicits a moderate cellular stress response which may induce dynamic alterations to the actin cytoskeleton. However, the inclusion of the collagen fibers alludes to a possible mechanism surrounding adhesion complexes and the formation of cortical actin filaments. According to models proposed by Gunst and Zhang, the coordination of smooth muscle contractile stimulation occurs within localized adhesion complexes, which are submembranous macromolecular complexes residing beneath the extracellular matrix (Gunst and Zhang, 2008). These adhesion complexes are highly dynamic structures which actively recruit both cytoskeletal and signaling proteins to the periphery of the cell to regulate the restructuring of the cortical actin cytoskeleton in response to extracellular stimuli (Gunst and Zhang, 2008). This integrative pathway allows for adhesion complexes to promote a comprehensive response to manipulate the cortical actin cytoskeleton to stabilize the plasma membrane and allow force transmission to occur through connections to the cytosolic contractile domain (Gunst and Zhang, 2008). Interestingly, all of the

collagen proteins increased in abundance in response to 24°C and were absent at the high temperature ranges (Fig. 4). Collagen fibers have been shown to be transported via α/β-integrins during cell-mediated contraction and ECM remodeling, and increased expression of collagen fibers has also been associated with increased ECM rigidity (Larsen et al., 2006). In this context, increased ECM rigidity facilitates the formation of adhesion complexes and stimulates contraction via the Rho/ROK pathway (Gunst and Zhang, 2008; Lehman and Morgan, 2012). Although we did not identify any integrin proteins in this study, the upregulation of calponin also supports the possible formation of adhesion complexes during 24°C exposure, as these proteins are actively recruited to adhesion complexes to regulate cortical thin filament dynamics (Gunst and Zhang, 2008; Tojkander et al., 2012). Thus, the increased number of TnT isoforms along with the high number of actin proteins present in the first cluster appears to suggest a coordinated signal to restructure actin thin filaments near adhesion complexes during exposure to 24°C.

In support of this notion, the upregulation pattern of both the 14-3-3 and F-actin capping proteins may provide further evidence for the dynamic remodeling of the cortical thin filament network during temperature increases (Fig. 4). 14-3-3 proteins represent a highly conserved family of protein recruitment scaffolds, which are involved in the coordinated integration of multiple signaling pathways by interacting with effector proteins via phosphorylated serine and threonine residues (van Hemert et al., 2001; Darling et al., 2005). One of the primary proteins which interacts with 14-3-3 proteins in smooth muscle is cofilin, an actin depolymerizing factor, which functions to recycle G-actin and remodel thin filament structures near adhesion complexes (Gunst and Zhang, 2008). The activity of cofilin is also regulated by phosphorylation which inhibits its interaction with F-actin and eliminates the proteins capacity to sever thin filaments (Bernstein and Bamburg, 2010; Breitsprecher et al., 2011). Interestingly, upon phosphorylation,

14-3-3 proteins bind and sequester phospocofilin with high affinity near focal adhesion sites (Gunst and Zhang, 2008). Thus, a significant increased abundance of the 14-3-3 proteins could possibly be in order to sequester and inactivate cofilin, which would indicate an increased rate of thin filament depolymerization occurring during the 24°C exposure.

Interestingly, the upregulation of the sHsp and the F-actin capping proteins within this cluster may provide further support for the occurrence of thin depolymerization in response to 24°C (Fig. 4). Recent evidence suggests some sHsp's may compete with phosphorylated cofilin for 14-3-3 protein binding sites, thus leading to the increased localization of activated cofilin near adhesion complexes (Komalavilas et al., 2008; Gunst and Zhang, 2008). The presence of the F-actin capping protein also potentially suggests increased rates of cortical thin filament turnover, as these proteins bind to the barbed end of newly severed thin filaments and promote the formation of shorter thin filaments (Gunning, 2015). Thus, although we did not identify any cofilin proteins in either species in this study, the function of the F-actin capping proteins indicates the occurrence of thin filament depolymerization mediated by a thin filament depolymerizing factor. Taken together, the increased abundance of all of these proteins in response to 24°C appear to suggest active cytoskeletal rearrangement occurring within the cortical cytoskeleton of the adductor muscle of *M. trossulus*.

Finally, the third cluster is best summarized by proteins which exhibit increased abundances in response to the highest temperatures of 28°C & 32°C (Fig. 4). This cluster contains the greatest assortment of proteins as compared to the previous clusters and includes proteins involved in molecular chaperoning (Hsp70 and three isoforms of sHsp), oxidative stress (ferritin and *S*-adenosyl-O-methyltransferase) signal transduction (guanine nucleotide binding protein β-subunit) energy metabolism (PDH, two isoforms of PNP and adenylate kinase), protein

synthesis (phenylalanyl tRNA synthetase β-chain), thin filament remodeling (fascin, transgelin, profilin, whirlin, 14-3-3 protein, TnT & transglutaminase) and the cytoskeleton (four isoforms of actin) (Fig. 4). The wide range of functional groups present within this cluster was expected, given these temperatures approach the upper physiological thermal tolerance limits of *M. trossulus* (Tomanek and Zuzow, 2010; Lockwood & Somero 2011; Dowd and Somero, 2013).

In a similar response to 24°C, exposure to the higher temperatures appears to facilitate an adaptive response to regulate the restructuring of the cortical actin cytoskeleton given the high number of actin isoforms (four total, Fig. 4). In addition, there are multiple thin filament regulatory proteins included within this cluster which possibly signal the formation of adhesion complexes, including the two isoforms of calponin, profilin, whirlin, a 14-3-3 protein and an additional TnT isoform (Fig. 4). The addition of several proteins within this cluster also potentially indicates the formation of cortical stress fibers during high temperature exposure (Tojkander et al., 2012). For example, certain isotypes of transglutaminase have recently been implicated in cell signaling and been shown to potentiate integrin-dependent signaling leading to stress fiber formation near adhesion complexes (Eckert et al., 2014). Transgelin has also been suggested to stabilize cortical stress fibers (Assinder et al., 2009), while fascin has been suggested to function as an actin bundling protein to assist in stress fiber formation (Tojkander et al., 2012). As such, the increased abundance pattern of actin binding proteins in this context may possible correlate to increased rates of stress fiber formation during temperature increases within *M. trossulus.*

In support of the potential formation of stress fibers during temperature increases, many proteins included within this cluster are involved in the cellular stress response, and the increased abundance of these proteins in response to higher temperatures may be to mitigate damage to the

cytoskeleton. For instance, there were a higher number of molecular chaperones present within this cluster, including several sHsp's and an Hsp70 isoform, which possibly indicate a higher accumulation of denatured thin filaments and misfolded proteins occurring at this temperature range (Fig. 4). As a result, the increased abundance of molecular chaperones during acute exposure to higher temperatures may evoke a severe thermal stress response within the adductor muscle, which could also explain the concomitant rise in the abundance of oxidative stress proteins (Fig. 4). For example, ferritin gene transcripts and protein isoforms have been shown to increase in response to high temperature exposure within the liver of both white shrimp, *Litopenaeus vannamei* (Zhou et al., 2014) and the snakehead fish, *Channa striatus* (Mahanty et al., 2016) respectively. All ferritin protein isoforms have a ferrioxidase epicenter which primarily sequesters and neutralizes highly reactive ferrous radicals (Arosio and Levi, 2002). Recent studies have also shown a high correlation between increased expression of ferritin isoforms and heavy-metal induced ROS production (Arosio and Levi, 2010). As such, ferritin has been proposed to be included among the primary responsive thermal tolerance elements to acute heat stress (Mahantay et al., 2016).

In addition to ferritin, the effects of thermally induced oxidative stress are also implicated by the abundance patterns of both the *S*-adenosyl-O-methyltransferase (SAM) and the fatty acid binding protein (FABP) (Fig. 4). Heat-induced ROS production evokes substantial increases in the formation of lipid peroxides, which may elicit adverse effects on membrane fluidity (Ellis, 2007). Thus, an increase in the abundance of FABP's may be required to sequester reactive fatty acids to prevent further damage to the membrane in response to temperature increases. Since many of the proposed changes occurring within the adductor muscle appear to involve regulation surround the cortical actin cytoskeleton, it is possible the continual restructuring of

submembranous cortical thin filament may also require an increased abundance of proteins to stabilize the cellular membrane. Interestingly, this may also provide rationale for the observed increased abundance of SAM isoforms. *S*-adenosyl-methionine (AdoMet) is a primary carbon source utilized by methyltransferases during a variety of cellular processes including DNA and protein repair, signal transduction and energy metabolism (Schubert et al., 2003). Specifically, SAM isoforms catalyze the conversion of AdoMet to S-adenosyl-homocysteine (AdoHcy), which is the required precursor for the biosynthesis of the amino acid cysteine (Schubert et al., 2003). Cysteine is a required precursor for the synthesis of glutathione (Tchantchou et al., 2008), which sequesters ROS radicals and has been implicated in the thermally-induced oxidative stress response within mussel gill tissue (Tomanek, 2015). Recent proteomic analysis have also shown a significant increase in AdoMet levels in response to thermal stress within the gill tissue of pacific oyster, *Crassostrea gigas* (Zhang et al., 2014). Interestingly, these authors also postulated increases in AdoMet may also confer cellular protection from thermal stress through increased phospholipid synthesis and molecular chaperone gene regulation (Zhang et al., 2014). Therefore, the protein abundance pattern exhibited among molecular chaperones and oxidative stress proteins within the third cluster suggests acute exposure to temperatures exceeding 28°C elicits a severe cellular stress response within *M. trossulus* possibly to ameliorate thermally induced oxidative damage to cortical thin filaments and the cellular membrane.

The final proteins yet to be discussed within this cluster subset are all involved in energy metabolism. These include one isoform of PDH, two isoforms of PNP and an adenylate kinase (AK) isoform. The primary energetic role for the AK enzyme is the catalytic interconversion of adenine nucleotides between intracellular compartments as a means to monitor ATP homeostasis (Dzeja and Terzic, 2009). Since many energetic enzymes are allosterically regulated by adenine

nucleotides, AK isoforms can effectively monitor the changes in energy balance to cause a metabolic shunt from ATP consumption to ATP production (Dzeja and Terzic, 2009). As a result, AK isoforms have also been observed to be upregulated within organisms during carbon starvation responses (Dzeja and Terzic, 2009). This observation coincides with the upregulation of the SAM oxidative stress protein, as the activity of the methyltransferase may limit the availability of carbon precursors for biosynthesis during temperature increases (Schubert et al., 2003). However, ribose phosphates can be utilized as a preferred energy or carbon source and can be converted through the action of nucleoside phosphorylases (Tozzi et al., 2006). Specifically, PNP isoforms generate ribose-1-phosphate (Rib-1-P) through the addition of a phosphate to the ribose moiety of adenine or guanine. The newly synthesized Rib-1-P can then enter catabolic pathways, e.g., glycolysis and the TCA cycle, through a series of reactions to increase ATP production (Tozzi et al., 2006). As such, the increase in these specific energetic proteins appears to suggest an acute increase in energetic demand in response to high temperatures, possibly to fuel cellular stress response mechanisms. Coincidentally, the inclusion of the phenylalanyl tRNA synthetase at the higher temperature range may support this notion, as protein synthesis exhibits high rates of ATP turnover (Nelson and Cox, 2008).

In summary, acute exposure to increasing immersion temperatures appears to elicit a more severe stress response within the adductor muscle *M. trossulus*, as evidenced by the increased abundance of cytoprotective proteins and molecular chaperones at each of the higher temperatures, which may impede the dynamic restructuring of cortical thin filaments. Thus, higher temperature exposure may limit the passive connections between the cortical cytoskeleton domain and the contractile apparatus, possibly resulting in adductor muscle dysfunction.

Protein Expression Profiles: *Post-hoc* Analyses

In the previous sections, several major hypotheses were generated with respect to each species towards the effects of acute heat stress on the adductor muscle proteome. Many of the hypotheses generated for both species specifically focused on the dynamic restructuring of cortical thin filaments during temperature increases, possibly as a means to increase the connections between the cortical cytoskeleton and the contractile apparatus to maintain adductor muscle function. Since each of these hypotheses is based on the changes occurring within orthologous homologs, it is difficult to make direct comparisons between species based on relative protein abundance changes (Tomanek and Zuzow, 2010). Therefore, the aim of this final section is to potentially identify key mechanistic differences occurring within the adductor muscle in response to acute heat stress between the two species.

These protein functional groups were based in part through interpretation from previous data sets (See Tomanek & Zuzow 2010; Garland et al. 2015). However, functional group classification is meant to encompass the broad range of cellular processes possible. Furthermore, in order to highlight key differences, we have included proteins which were identified but were not found to significantly change in abundance in response to acute heat stress. However, not all the proteins identified are depicted in the preceding sections; proteins which are not mentioned can be referenced in the supplement.

Proteins were separated into the following categories: molecular chaperones, oxidative stress, signal transduction and cytoskeletal elements. Due to the expansive subset of proteins evident within both data sets, the cytoskeletal category required additional classification. Cytoskeletal proteins were further divided into thin-filament regulation and proteins involved in the regulation about the actin-myosin binding complex. Several protein functional categories

were also omitted from this section, due to the lack of overlap in orthologous homologs between the congeners.

Molecular Chaperones-

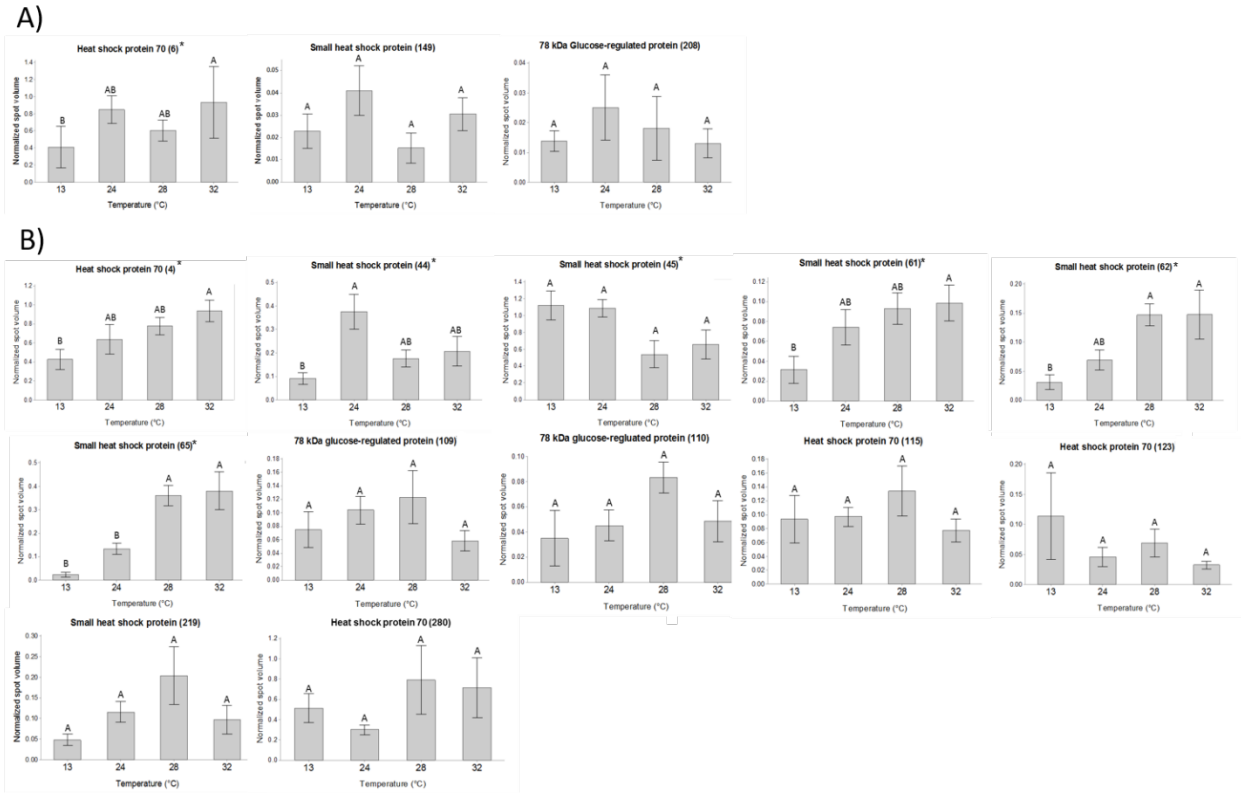

Figure 5. Changes in protein abundance (normalized spot volume) among molecular chaperones identified within A) *M. galloprovincialis* & B) *M. trossulus* in response to acute heat shock. Spot volumes were obtained by normalizing against the volume of all the protein spots across all gels and treatments, and exhibit means + 1 S.E.M. Within each protein expression profile, spot volumes which do not share a letter exhibit significant changes in protein abundance between the corresponding temperature treatments (Tukey pairwise comparison, $p<0.05$). Spot numbers are shown in parentheses, and correspond to the respected composite image of species origin (See Fig(s). 1A & 1B). "*" refers to protein spots which were found to exhibit significant changes in mean protein abundance in response to acute heat shock (One-way permutation ANOVA, $p < 0.05$).

Interestingly, of the 31 significantly identified proteins within the adductor muscle of *M. galloprovincialis*, only one chaperone was included within this functional category (Fig. 5A). Increased abundance of Hsp70 was observed at the highest temperature of 32°C as compared to the 13°C control. However, two additional molecular chaperones, i.e., sHsp & 78 kDa glucose-related protein (GRP-78), were identified but did not exhibit significant changes in abundance in response to heat stress (Fig. 5A). Although the temperature treatments used in this study exceed the heat shock induction temperature range reported in *M. galloprovincialis*, it appears exposure to the higher temperatures did not elicit as a robust stress response as was predicted. The non-significant sHsp isoform also suggests acute exposure did not cause a substantive increase among the rapid response molecular chaperones, suggesting there may not have been as high accumulation of thermally-denatured proteins as compared to *M. trossulus* (Fig. 5B). In addition, the non-significant GRP-78 isoform suggests acute heat stress did not elicit an unfolded protein response, as this protein has become a hallmark for stress within the endoplasmic reticulum and ROS-related apoptosis (Lai et al., 2007; Gu et al., 2016). Therefore, the identification of the non-significant molecular chaperones may provide further evidence for cortical thin filament stabilization and maintenance of adductor muscle cytoskeletal integrity during acute heat stress within *M. galloprovincialis*.

In contrast, however, seven of the sixty significantly identified proteins within *M. trossulus* were characterized as molecular chaperones (Fig. 5B), supporting a greater overall magnitude of heat-induced stress occurring within the adductor muscle of *M. trossulus*. One molecular chaperone, Hsp70, observed significant increases at the highest temperature compared to the 13°C control similar to the pattern exhibited in *M. galloprovincialis*. However, there were three total Hsp70 isoforms, which did not observe significant changes in abundance with respect

to temperature (Fig. 5B). Therefore, the greatest changes exhibited among molecular chaperones appear to be associated with the regulation of sHsp's within *M. trossulus*.

The wide range of sHsp expression within *M. trossulus* in response to increasing temperatures highlights one of the greatest interspecific differences between the congeners. The variation in molecular chaperone abundance has also been described to occur within gill tissue (Tomanek and Zuzow, 2010) and was suggested to be one of the most prevalent adaptive physiological responses to acute heat stress. These authors also reported changes in sHsp abundance tended to occur in a rather stepwise fashion, in which greater increases in molecular chaperones were observed with subsequent increases in temperature, i.e., a Q_{10} effect. Tomanek and colleagues also reported increased synthesis of sHsp isoforms within *M. trossulus* at much lower temperatures as compared to *M. galloprovincialis* (Tomanek, 2012). The increased abundance patterns of sHsp's in this context suggests acute heat stress causes a greater detrimental effect on the actin cytoskeletal within *M. trossulus*. Specifically, the greater magnitude of low-weight molecular chaperones along with the significantly higher number of actin isoforms identified within *M. trossulus*, suggests the increased occurrence of thin filament destabilization and thin filament turnover. Thus, thin filaments within the adductor muscle of *M. trossulus* may be more susceptible to temperature increases as compared to *M. galloprovincialis*.

Oxidative Stress-

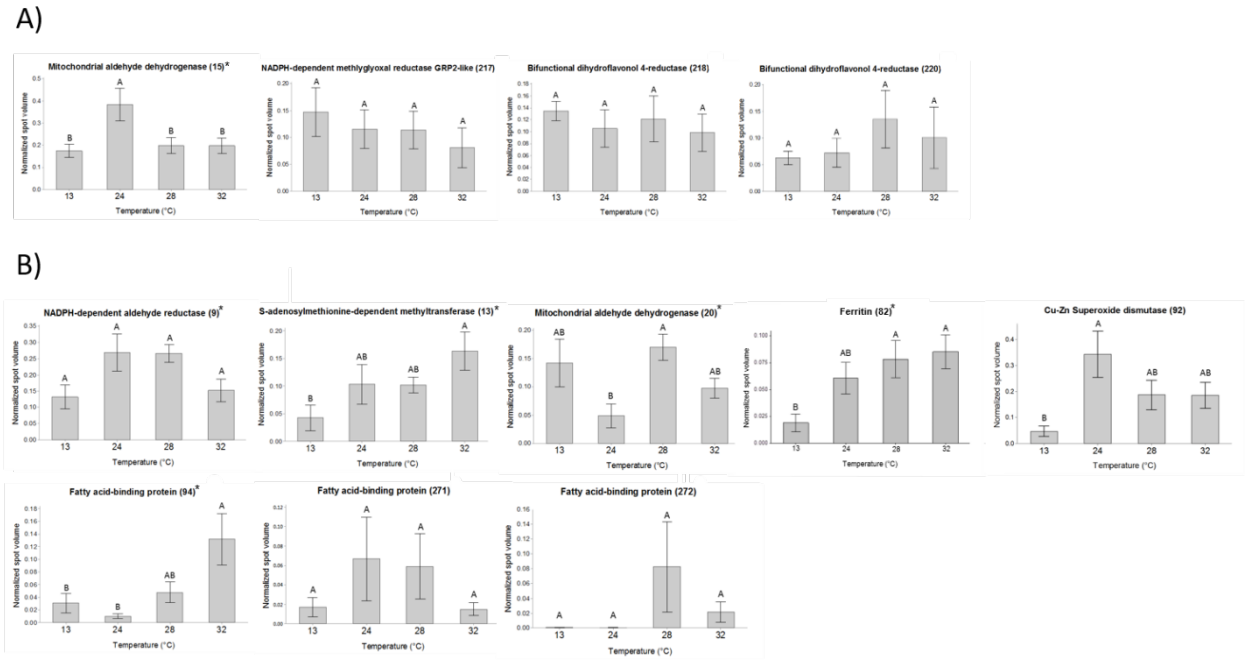

Figure 6. Changes in protein abundance among oxidative stress proteins identified within the adductor muscle A) *M. galloprovincialis* & B) *M. trossulus* in response to acute heat shock

Only one significantly identified protein, i.e., mALDH, was included in this category for *M. galloprovincialis* (Fig. 6A). This protein exhibited significant increases during exposure to 24°C, possibly reflecting the induction of the heat shock response. While the role of mALDH in this context remains unclear, the observed increased abundance may possibly indicate alterations to the mitochondrial membrane which require reactive aldehyde sequestration (Singh et al., 2013; Stephens-Camacho et al., 2015). However, another intriguing aspect within this functional category is the identification of several aldose reductase enzymes which did not exhibit significant changes in abundance (Table S3, Fig. 6A). These enzymes are important regulators in catalyzing the breakdown of reactive carbonyls, such as methylglyoxal, which are by-products of major energetic pathways including glycolysis, amino-acid metabolism and lipid peroxidation

(Hoon et al., 2011). Taken together, in addition to the low number of molecular chaperones, it appears acute heat stress did not elicit as a severe cellular stress response within the adductor muscle of *M. galloprovincialis* as compared to *M. trossulus*.

There were five significantly identified proteins associated within *M. trossulus* which were included within the oxidative stress category (Fig. 6B). Similar to *M. galloprovincialis*, a mALDH ortholog was included within this category and exhibited significant increases in response to 28°C exposure as compared to all other temperatures (Fig. 6B). In contrast to *M. galloprovincialis*, however, this mALDH ortholog exhibited a more cyclic pattern of abundance change in response to the different temperatures (Fig. 6A). The variation exhibited within this isoform appears to suggest a phasic increase in ROS-induced lipid peroxidation, which possibly occurs concurrently with the dynamic changes occurring within the cortical cytoskeleton domain during temperature increases. This may also explain the abundance pattern of the NADPH-dependent aldehyde reductase isoform (Fig. 6B). Therefore, the patterns exhibited by both proteins appears to suggest an increase in the abundance of specific ROS intermediates during temperature fluctuations.

Coincidentally, the Cu-Zn SOD isoform was observed to significantly increase at the 24°C exposure as compared to 13°C (Fig. 6B). This protein also showed a high positive component loading value contributing towards the separation of the higher temperatures from the 13°C control (Table 1, Fig. 2B). Therefore, it is possible multiple ROS-scavenging pathways are induced during acute heat stress, possibly to mitigate the effects of heat-induced oxidative stress within *M. trossulus*. Likewise, this also suggests accumulation of different sources of ROS in response to temperature increase, e.g., peroxides. As a result, further increases in temperature may exacerbate the production of ROS, as exemplified by the FABP and SAM isoforms at the

higher temperature ranges (Fig. 6B). In addition, the significant increases in one of the three FABP isoforms along with the ferritin and SAM proteins at 32°C (Fig. 6B), suggests this temperature range may approach the critical temperature threshold for *M. trossulus*. While the upregulation of FABP may be to sequester lipid ROS intermediates, upregulation of the SAM isoform may be in response to activate alternative ROS-scavenging pathways, i.e., the glutathione pathway. Taken together, the evidence suggests acute exposure to temperatures as low as 24°C is sufficient to cause a rise in transitory ROS intermediates, thus prompting an oxidative stress response within the adductor muscle during exposure to higher temperatures. The abundance patterns displayed by these proteins are indicative of major cellular ROS-scavenging pathways and may also represent the primary response to ameliorate heat-generated ROS within certain bivalves (Tomanek, 2015). Therefore, higher temperature exposure appears to produce a greater increase in ROS, prompting a more robust cellular stress response within *M. trossulus* as compared to *M. galloprovincialis*.

Signal Transduction-

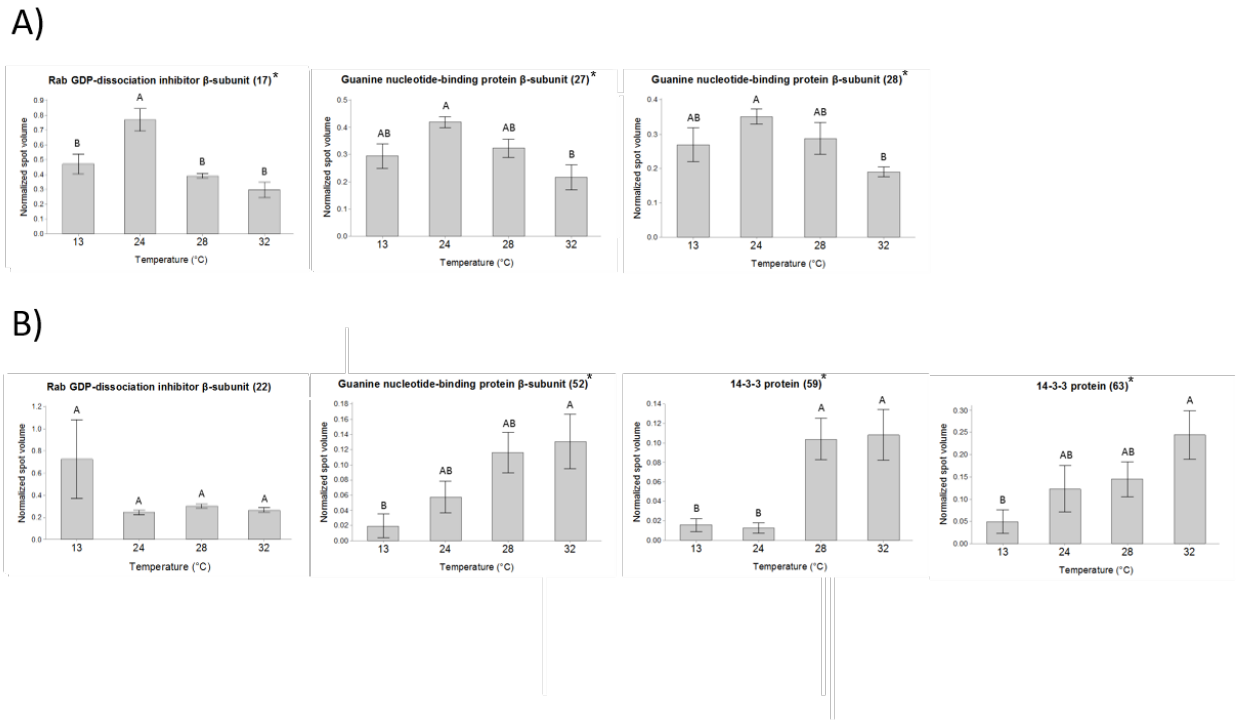

Figure 7. Changes in protein abundance among signal transduction proteins identified within the adductor muscles of A) *M. galloprovincialis* & B) *M. trossulus* in response to acute heat shock.

The evidence presented within both data sets continue to suggest thermal stress imposes physiological constraints on the adductor muscle which appear to induce a dynamic restructuring of both the contractile and cortical actin cytoskeletal domains. In order to implement cellular restructuring, however, these mechanistic changes require coordinated signaling pathways to connect the cytoskeletal domains to the extracellular network. While it is still unclear as to the specific molecular pathways which orchestrate these structural changes, a growing body of evidence suggests extracellular stimuli are converted into intracellular responses through the active coordination of signaling proteins and actin regulatory proteins found within submembranous adhesion complexes (Gunst and Zhang, 2008). Integrated downstream signaling pathways from these adhesion complexes are also postulated to converge upon specific signaling

cascades, e.g., RhoA/RHOK pathway, which ultimately act upon effector proteins to stimulate cortical actin remodeling and cortical thin filament polymerization (Gunst and Zhang, 2008).

Coincidentally, the same signaling proteins were identified in both congeners, i.e., guanine nucleotide binding protein β-subunit and Rab-GDI, suggesting certain stress response signaling pathways are evolutionarily conserved within the *M. edulis* complex (Fig. 7). However, these protein orthologs also exhibited substantial variation in terms of their overall patterns of abundance. For instance, the G-protein subunits for *M. galloprovincialis* exhibited significant increased abundance in response to 24°C as compared to 32°C (Fig. 7A). In contrast, the protein ortholog for *M. trossulus* exhibited significant increased abundance in response to 32°C as compared to 13°C (Fig. 7B). This suggests *M. galloprovincialis* is able to detect and possibly respond to thermal perturbations at lower temperature thresholds as compared to *M. trossulus*. The preceding abundance changes among signaling proteins may also facilitate the downstream changes in thin filament restructuring within both species, as many thin filament regulatory proteins appear to be upregulated at temperatures preceding significant increases in signaling proteins (See below; Fig(s) 8-10). In addition, the capacity to detect acute thermal changes at a lower temperature range may allow *M. galloprovincialis* to coordinate a more adaptive response to stabilize connections between the cytoskeletal domains, thus providing greater rigor capacity and tensile strength among contractile fibers.

Another prominent difference exhibited between the congeners is represented within the variation in abundance between the 14-3-3 scaffolding proteins (Fig. 7B). In this context, two isoforms were only identified in *M. trossulus*, and were observed to significantly increase in abundance in response to the higher temperatures of 28°C and 32°C (Fig. 7B). Given the proteins multi-functional role and isolation within *M. trossulus*, it suggests more dynamic responses

within adhesion complexes occurring within *M. trossulus* in response to the highest temperature range. Therefore, both congeners appear to exhibit conserved signaling pathways to coordinate the dynamic restructuring of the actin cytoskeleton in response to temperature increases. However, given the increased abundance pattern of signaling proteins in response to lower temperature, the adductor muscle of *M. galloprovincialis* may be better able to detect and modify thin filament architecture during temperature increases as compared to *M. trossulus*.

Thin Filament Regulation-

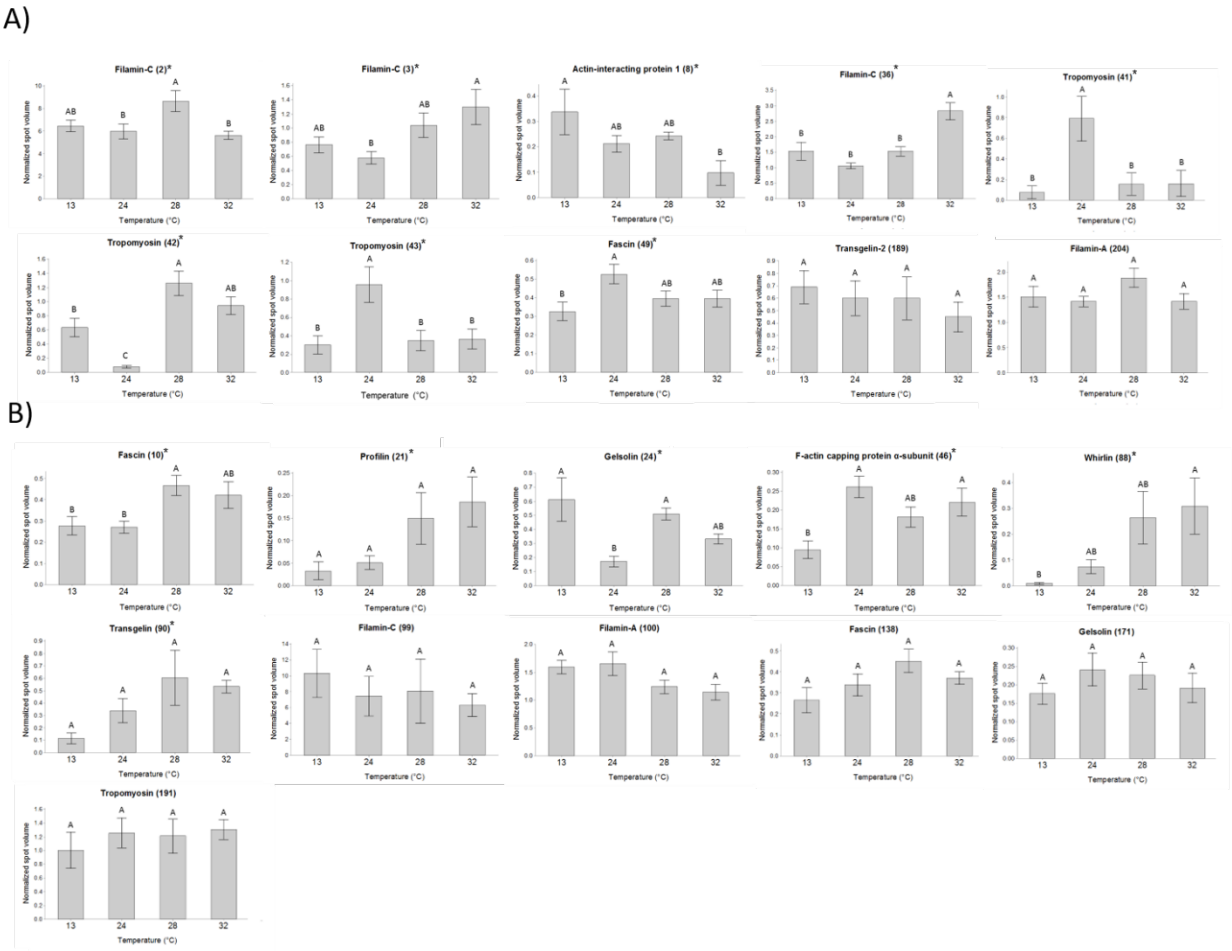

Figure 8. Changes in protein abundance among proteins involved in thin filament regulation identified within the adductor muscles of A) *M. galloprovincialis* & B) *M. trossulus* in response to acute heat shock.

The potential changes occurring within the actin cytoskeleton during acute heat stress are perhaps necessary to execute proper adductor muscle function, given the established connections between cytoskeletal fibers and the development of muscle tension. For instance, force production, tension development and cross-bridge mediated contractile dynamics are all dependent upon the connections between actin thin filaments and myosin thick filaments

(Hooper, 2008). Passive linkages formed between thick and thin filaments are orchestrated by specific adapter proteins, i.e., twitchin, which are essential in maintaining prolonged valve closure events in response to external stressors (Galler, 2008). Thus, alterations to the thin filament architecture through increased abundance of thin filament regulatory proteins may not only be vital to coordinate smooth muscle function, but may also represent an adaptive molecular response to regulate the catch response during acute thermal stress.

Of the 31 significantly identified proteins within *M. galloprovincialis*, eight proteins were associated with the thin filament regulation category (Fig. 8A). These included three isoforms of FLNC, AIP1, three isoforms of TPM and an isoform of fascin. There was also an isoform of transgelin and FLNA included within this functional category which did not exhibit significant changes in abundance with respect to temperature treatment (Fig. 8A). The most prominent feature displayed within this functional category is each of the thin filament regulatory proteins, apart from AIP1, exhibits significant increases in response to at least one of the higher temperature treatments. For example, each of the FLNC isoforms exhibits the greatest increases in abundance at either 28°C & 32°C as compared to the lower temperatures (Fig. 8A). One of the primary functions of FLN isoforms is to establish cross-linkages between cortical and cytoskeletal thin filaments, as these connections may facilitate increased stability to mechanical stress. In addition, FLN isoforms exhibit binding affinity with other actin binding proteins such as calponin (Dobrzhanskaya et al., 2013), which has also been hypothesized to mediate dynamic restructuring of cortical thin filaments (Rozenblum and Gimona, 2008). Therefore, FLN isoforms may regulate thin filament flexibility and stabilization during acute heat stress.

Similar to the proposed functions of FLN, TPM isoforms are also well-known thin filament stabilizers which inhibit the action of specific actin depolymerizing factors (Marston

and El-Mezgueldi, 2008; Gunning et al., 2015). However, further evidence suggests the variation in TPM isoforms also affects the affinity and active recruitment of specific actin binding proteins towards actin thin filaments (Gunning et al., 2015). Thus, specific TPM isoform may actually determine the functional role of a nascent actin thin filament. The variation exhibited in thin filament subtypes may then possibly effect tension development, stabilize different cytoskeletal domains or alter the cellular morphology in response to stress (Gunning et al., 2015). Although we were unable to determine the specific TPM isotype, each of the three TPM isoforms within this data set exhibited dramatic increases in abundance with respect to a specific higher temperature (Fig. 8A). Specifically, two isoforms exhibit significant increases in abundance in response to the 24°C exposure as compared to all other temperatures, whereas the third isoform exhibits the greatest increase in response to 28°C & 32°C as compared to 24°C (Fig. 8A). Since 24°C may represent the heat shock induction temperature range for *M. galloprovincialis*, it is possible the significant increases in TPM abundance during 24°C exposure may also correspond to the active generation of specific actin thin filaments to regulate and stabilize the cortical cytoskeleton. This result may also explain the increased abundance of both significant actin isoforms at the higher temperature range (Fig. 8A). Therefore, the increased abundance of TPM isoforms within *M. galloprovincialis* may signal the generation of specific actin thin filaments, which may also actively recruit additional actin binding proteins to promote thin filament stability and maintain the structural integrity of the cortical actin cytoskeleton in response to acute heat stress.

In contrast to *M. galloprovincialis*, six proteins were included within the thin filament category for *M. trossulus* (Fig. 8B). These included fascin, profilin, gelsolin, an F-actin capping protein, whirlin, and transgelin (Fig 8B). There were also two FLN isoforms, i.e., FLNC &

FLNA, as well as a fascin, gelsolin and a TPM isoform which did not exhibit significant changes in protein abundance in response to acute heat stress (Fig. 8B; Table S4).

The most prominent distinction between *M. galloprovincialis* and *M. trossulus* with respect to the thin filament regulatory category appears to be the regulation of actin polymerization factors at higher temperatures. Specifically, these involved the contributions of fascin, F-actin capping protein and whirlin at the higher temperature range (Fig. 8B). Although much of the research regarding whirlin comes from observations of thin filament dynamics in stereocilia of cochlear hair cells (Rzadzinska et al., 2004; Mburu et al., 2006), it is important to note that the cytoskeletal architecture of these sensory cells is pivotal for their roles in auditory function (Brown et al., 2008). Since increased abundance of whirlin proteins is associated with elongated actin filaments near the apical membrane, whirlin appears to actively recruit thin filaments to specific cellular domains (Wang et al., 2011; Green et al., 2013). In this context, the increased abundance of whirlin proteins at the higher temperature range may also serve to recruit further thin filament proteins during formation of adhesion complexes near the muscle membrane. In addition, the increased abundance of fascin and F-actin proteins suggests increased reorganization and cross-linking of shorter submembranous cortical thin filaments (Breitsprecher et al., 2011; Tojkander et al., 2012; Gross, 2013). Although profilin and transgelin did not exhibit significant changes in mean abundance in response to temperature exposure during *post-hoc* analysis, their inclusion within this subcategory provides further evidence for cortical thin filament reorganization and stress fiber formation during heat stress (Gunst and Zhang, 2008; Tojkander et al., 2012).

Another key difference exhibited between these species is exemplified by the variation among the non-significant proteins included within this category. Specifically, this involves the

non-overlap of specific isoforms of FLNC and TPM, in which *M. galloprovincialis* displays significant increases of both of these thin filament stabilizers, whereas *M. trossulus* did not exhibit any significant increases in either protein in response to acute heat stress (Fig. 8). Interestingly, this variation may reflect differential responses involving stress fiber formation, as certain actin stress fibers which are linked to adhesion complexes are decorated with TPM isoforms which function to further stabilize the cortical cytoskeleton (Tojkander et al., 2012). During the formation of these stress fibers, adjacent TPM-decorated thin filaments are linked together via cross-linking proteins (Tojkander et al., 2012). Therefore, the increased abundance of FLNC may be in response to link adjacent TPM-decorated thin filaments within the nascent stress fibers and further stabilize the cortical cytoskeleton of *M. galloprovincialis* but not *M. trossulus*.

In summary, although both species appear to induce stress fiber formation within the adductor muscle in response to heat stress, the increased abundance of thin filament stabilizing and cross-linking proteins appears to suggest the cortical thin filament cytoskeletal network is more stable in *M. galloprovincialis* during temperature increases. In contrast, *M. trossulus* exhibits increased abundances of actin regulatory proteins involved in thin filament bundling, thin filament polymerization and the formation of shorter actin thin filaments. As a consequence, the increased restructuring of the cortical cytoskeletal network within *M. trossulus* may limit the number of cytoskeletal connections and decrease the function of the adductor muscle in response to temperature increases.

Regulation of the acto-myosin complex-

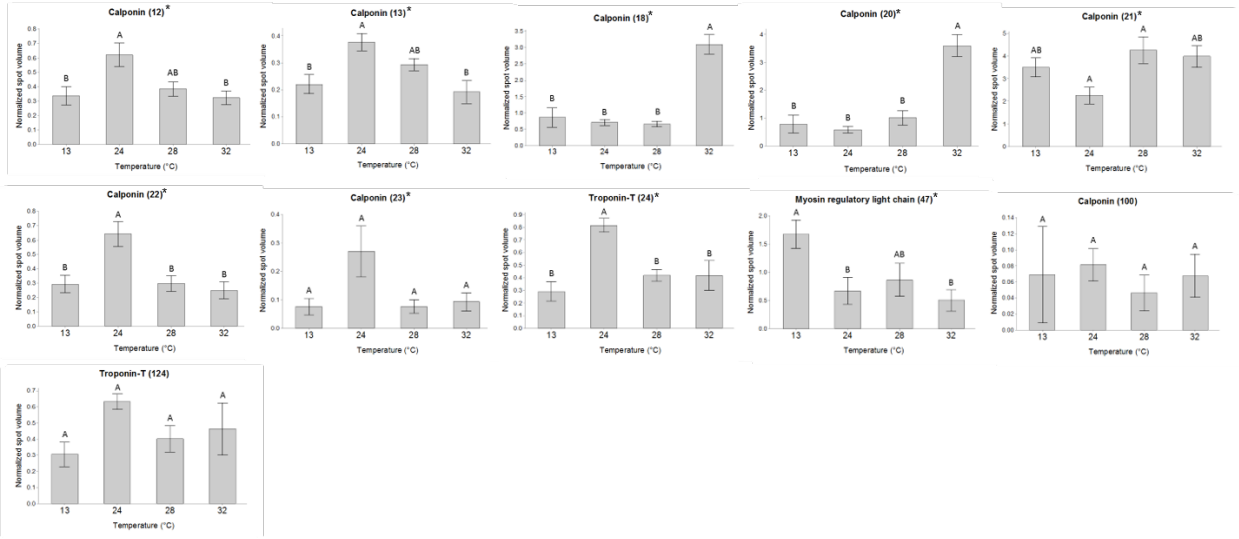

Figure 9. Changes in protein abundance (normalized spot volume) among identified proteins involved in regulation of the actin-myosin binding complex within the adductor muscle of *M. galloprovincialis* in response to acute heat shock.

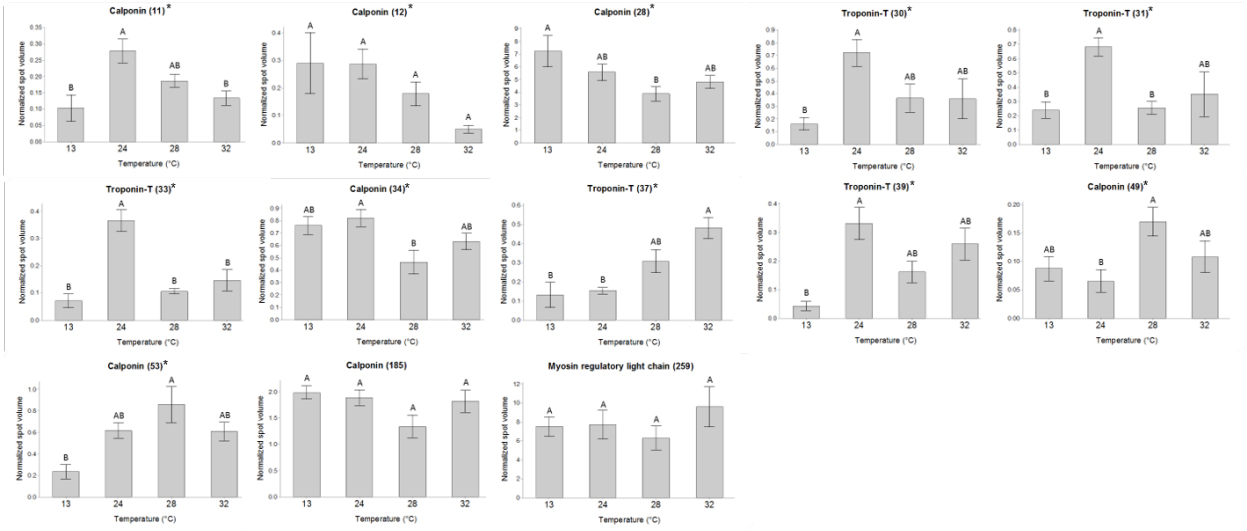

Figure 10. Changes in protein abundance (normalized spot volume) among identified proteins involved in regulation of the actin-myosin binding complex within the adductor muscle of *M. trossulus* in response to acute heat shock.

In this final section, we discuss regulation of the acto-myosin complex, specifically regarding the interactions associated between actin thin filaments and myosin thick filaments. Although there are multiple proteins which comprise invertebrate thick filaments, e.g., paramyosin and myorod, and aid in the invertebrate catch response, i.e., twitchin, all of these proteins are relatively large suggesting we were unable to detect them as they may have exceeded the dynamic molecular weight range used during 2D gel separation (Fig(s) 1A & 1B; Hooper, 2008; Galler, 2008). Therefore, future investigations should consider the high molecular weights of thick filament proteins. However, this category included the greatest assortment of proteins with respect to both species, as eleven proteins were included for *M. galloprovincialis* as well as thirteen total proteins were included for *M. trossulus* (Fig(s). 9 & 10 respectively). The majority of both data sets consisted of multiple isoforms of calponin and TnT. However, the major distinction between the species involves the greater presence of TnT isoforms included within the *M. trossulus* data set as compared to *M. galloprovincialis* (Fig. 10).

Of the eleven significant proteins included within this functional category, only nine proteins exhibited variation in abundance across temperature treatments within *M. galloprovincialis* (Fig. 9). These included seven isoforms of calponin as well as a single isoform of TnT and MRLC (Fig. 9). Interestingly, each of the seven calponin isoforms displayed the greatest increases in abundance with respect to at least one of the higher temperatures. Specifically, three isoforms exhibited the greatest increase in response to 24°C exposure, another was observed to increase in response to the 28°C exposure and two isoforms increased at the highest temperature of 32°C (Fig. 9). The abundance pattern displayed by the calponin isoforms suggests a cyclic increase in calponin abundance during exposure to high temperatures. This fluctuating pattern may also be reminiscent of the adductor muscle's ability to respond to acute

temperature change in a temporal manner, owing to a potential capacity to adjust to temperature increases through increased calponin synthesis or modification to existing calponin isoforms. Given the latter hypothesis, the variation in MW and pI exhibited among the identified calponin isoforms could possibly indicate potential PTM's (Fig. 3). For instance, certain calponin isoforms exhibit increased binding affinity to F-action upon increased phosphorylation of specific residues (Rozenblum and Gimona, 2008). However, calponin has also been suggested to be involved in signal transduction (Rozenblum and Gimona, 2008), by serving as a signaling scaffold which increases the localization of actin binding proteins to adhesion complexes during cortical thin filament assembly (Kim et al., 2008; Gunst and Zhang, 2008). The increased abundances of calponin during high temperature exposure may then signal the formation of stress fibers near adhesion complexes to strengthen the cortical actin cytoskeleton. Thus, the increased abundance of multiple calponin isoforms may confer greater stability to the actin cytoskeleton during acute heat stress.

Similar to *M. galloprovincialis*, there were six significantly identified isoforms of calponin within the subset for *M. trossulus* (Fig. 10). Of these calponin homologs, at least one isoform exhibited the greatest increase in abundance in response to exposure to either 13°C, 24°C or 28°C. This suggests the adductor muscle within both species displays a conserved response to upregulate calponin isoforms in response to temperature increases. In contrast to *M. galloprovincialis*, none of these isoforms exhibited increased abundance in response to 32°C (Fig. 10). The decreased abundance of calponin isoforms at the highest temperature range may indicate the thermal tolerance limits of *M. trossulus*, as there are no substantial increases in the abundance of calponin isoforms to temperatures exceeding 28°C (Fig. 10). These results may also coincide with the hypothesized increases in thin filament polymerization and thin filament

turnover occurring at the higher temperature range. Therefore, 32°C may impose physiological constraints on the adductor muscle within *M. trossulus*, as it is possible the pathways associated with thermal sensitization are inhibited during exposure to temperatures exceeding 28°C.

Another staunch contrast between the species represented within this functional category is the considerable variation exhibited in TnT isoform abundance. Only one TnT isoform was identified within *M. galloprovincialis* and it increased in abundance in response to 24°C (Fig. 9). In contrast, there were four TnT isoforms observed to increase abundance in response to 24°C exposure within *M. trossulus* (Fig. 10). In addition, there was a fifth isoform which increased in abundance during exposure to 32°C (Fig. 10). Since the increased abundance of TnT orthologs is most prevalent in response to 24°C within both congeners, it suggests a possible conserved cytoskeletal response within the adductor to thermal stress. The variation observed in TnT abundance is possibly related to the restructuring of specific actin thin filaments, as many of the rapid alterations to actin filaments in response to extracellular stimuli occur within cortical actin filaments (Gunst and Zhang, 2008; Galler 2008). Since the cortical actin cytoskeleton functions to transmit contractile stimuli between the plasma membrane and the contractile apparatus, it is possible the changes observed in both TnT and calponin isoforms may correspond to the advanced restructuring of cortical stress fibers (Tojkander et al., 2012). Specifically, the increased number of TnT isoforms may represent the formation of specific cortical stress fibers during acute heat stress.

While the restructuring of cortical actin thin filaments is unlikely to be attributed to an increase in contraction rates, the dynamic restructuring may be necessary to maintain elastic connections between thick and thin filaments to maintain the muscle function during temperature increases (Hooper, 2008; Galler, 2008). This notion is supported from the functional

relationships associated between TnT and its inhibitory effects on the other troponin isoforms, i.e., I and C, which reduces cross-bridge cycling (Hooper et al., 2008). Therefore, the increased abundance in TnT isoforms may also represent a reduction in contractile activity. Furthermore, the increased abundance of TnT isoforms within *M. trossulus* may also signal consistent remodeling of thin filament architecture, possibly limiting the number of catch connections between cytoskeletal structures. Since only one TnT isoform was exhibited to increase in response to 24°C within *M. galloprovincialis*, it is also possible the catch connections are more stable within *M. galloprovincialis* given the increased abundance of thin filament stabilizing proteins and thin filament recruitment proteins in response to higher temperature exposure. As a result, the cytoskeletal connections maintaining the catch response and cytoskeletal integrity of the adductor muscle may be weakened during higher temperature exposure within *M. trossulus* as opposed to *M. galloprovincialis.*

Conclusions

Given the substantial number of proteins present within both data sets in response to acute heat stress, many of the hypothesized mechanisms occurring within the adductor muscle of both species require further testing. However, we are confident in our interpretation of the observed protein abundance patterns and their potential implications towards adductor muscle function during acute heat stress. Both congeners appear to share conserved signaling pathways in response to acute heat stress as evidenced by the increased abundances of Rab GDI, g-proteins and calponin. These molecular signaling pathways might be conserved within Blue mussels to mitigate the effects of heat stress within the adductor muscle through the integrative rearrangement of major cytoskeletal domains. However, there were major interspecific

differences which also appeared to revolve around cytoskeletal rearrangement and adjustments to cortical thin filament architecture. In this context, smooth muscle cytoskeletal networks may be potentially subdivided into three primary molecular domains: membrane adhesion complexes, cortical actin networks and the contractile apparatus located towards the interior of the cell (Gunst and Zhang, 2008; Lehman and Morgan, 2012). Together, these domains may induce adaptive contractile dynamics in response to extracellular stimulation via formation of transient cortical thin filaments and membrane adhesion complexes which connect the membrane and the contractile apparatus (Gunst and Zhang, 2008). Thus, the cortical actin cytoskeleton may represent an adaptive domain to regulate contractile function through acute reorganization of cortical thin filament structures in response to heat stress. This also represents an innovative strategy to coordinate adaptive contractile responses within the muscle, as it would allow thin filament polymerization to occur mainly within the cortical actin cytoskeleton whereby minimizing changes to the contractile apparatus. Interestingly, this notion is further supported through recent evidence associated with the formation of cortical stress fibers as these actomyosin bundles can actively recruit actin-binding proteins, polymerize near adhesion complexes and strengthen connections with myosin decorated thick filaments (Tojkander et al., 2012). Therefore, it is plausible the formation of stress fibers may provide further passive connections between the plasma membrane and the contractile apparatus which thereby influence the contractile efficacy of the adductor muscle in response to heat stress.

Given the potential contribution of cortical actin thin filaments towards regulating contractile dynamics in response to acute heat stress, the variation observed within cytoskeletal structures appears to mirror thermal tolerance windows exhibited for both species. Specifically, the proteins upregulated within *M. galloprovincialis* in response to the higher temperature

exposures appear to suggest greater recruitment of proteins involved in cortical thin filament stabilization and maintenance which strengthen connections between cytoskeletal networks. The maintenance of these actin cytoskeletal networks may be necessary to retain passive linkages between the contractile domains, which are essential in order to sustain the catch response and maintain valve closure. Thus, the maintenance of the cortical actin cytoskeleton may be vital to control the function of the adductor muscle within *M. galloprovincialis* during acute heat stress.

In contrast, acute heat stress appears to induce greater proteomic changes within the adductor muscle of *M. trossulus*, as indicated by the greater magnitude of significant proteins upregulated in response to acute heat stress. Specifically, the increased abundances exhibited among molecular chaperones and oxidative stress protein isoforms suggests acute heat stress invokes a more severe cellular stress response which may also trigger greater rates of cortical thin filament turnover. The greater thermal sensitivity of actin cytoskeletal structures within *M. trossulus* may also induce the increased formation of actin stress fibers in order to sustain passive linkages within the contractile domain. Coincidentally, the cytoskeletal architecture within *M. trossulus* may be more susceptible to thermal denaturation, thin filament destabilization and therefore a reduced propensity to maintain passive cytoskeletal linkages as a result of temperature increases. Together, these results indicate that the function of the adductor muscle of *M. trossulus* may be weakened when exposed to higher temperatures, which may also inhibit valve closure. Thus, alterations to the actin cytoskeletal architecture of the adductor muscle may, in part, contribute towards the thermal tolerance limitations observed between the two mussel species.

Although future increases in mean sea surface temperatures may continue to impose thermal tolerance constraints, it is important to note the changes in biogeographic range shifts are

compounded upon a variety of abiotic factors as a result of global climate change. For instance, the variation observed in gape behavior owing to adductor muscle function in response to acute heat stress may also be attributed to alternative physiological constraints, e.g., oxygen availability, which may also necessitate adaptive alterations to the adductor muscle during heat stress. Likewise, the severity and duration of exposure to abiotic stressors within the intertidal varies widely between temporal and spatial scales, which may also drastically effect mussel populations. There are also many other environmental factors, e.g., food availability, predator-prey responses, niche competition, etc., which may influence mussel distribution.

In addition to environmental factors, there are also technical limitations which limit our interpretation, including the detection of low abundance proteins and integral membrane proteins. Future studies investigating the proteomic responses within the adductor muscle should also take into consideration the proteins present within invertebrate thick filaments and their relatively high molecular weights, which may have been excluded from our analysis given the restrictions of 2D gel analysis. In particular, this would allow for greater interpretations towards the effects of acute heat stress on the invertebrate catch response. Finally, since many of the proposed hypotheses generated within this data set involve actin thin filament regulation and actin binding proteins, it would be pertinent to conduct a time course analysis of specific proteins which are thought to contribute towards the rearrangement of the cortical actin cytoskeleton in response to acute heat stress. Specifically, this would provide further evidence as to whether the changes occurring within the actin cytoskeleton in response to acute heat stress are occurring within the peripheral cortical domain or the interior contractile domain.

However, given all of these technical restraints, the changes observed within the adductor muscle are vital towards determining the impacts of environmental stress on important sentinel

species such as *M. galloprovincialis* and *M. trossulus*. These results also compliment recent findings investigating the effects of acute heat stress on gill tissue by providing the cellular responses of alternative tissues, which may contribute to the overall physiological and behavioral responses occurring at the level of the whole organism. For example, these results also suggest oxidative stress is a concomitant stressor of thermal stress and may attenuate the contractile responsiveness within the adductor muscle of *M. trossulus* during temperature increases. Thus, by incorporating a system based perspective and comparing the proteomic responses observed between *Mytilus* congeners within multiple tissues, it may allow for further elucidation as to the specific physiological mechanisms governing adaptive radiation among intertidal invertebrates in response to global climate change.

References

Abele, D. Heise, K., Pörtner, H. O., and Puntarulo. S. (2002). Temperature-dependence of mitochondrial function and production of reactive oxygen species in the intertidal mud clam *Mya arenaria*. *J. Exp. Biol.*, **205**, 1831-1841.

Adams, J. C. (2004). Fascin protrusions in cell interactions. *TCM*. **14** (6), 221-226.

Akhmanova, A., and Steinmetz M.O. (2008) Tracking the ends: a dynamic protein network controls the fate of microtubule tips. *Nat. Rev. Mol. Cell Biol.* **9**, 309–322

Alberts, B., Johnson, A., Lewis, J., Raff, M., Roberts, K., and Walter. P. (2008). Molecular biology of the cell. In *The Cytoskeleton*: *The Tubulin and Actin Subunits Assemble Head-to-Tail to Create Polar Filaments* (ed. M. Anderson and S Granum), pp. 904-921. New York: Garland Science.

Allen, D. G., Lamb, G. D., and Westerblad, H. (2008). Skeletal muscle fatigue: cellular mechanisms. *Physiol Rev*. **88**, 287-332.

Anacleto, P., Maulvault, A. L., Lopes, V. M., Repolho, T., Diniz, M., Nunes, M. L., Marques, A., and Rosa. R. (2014). Ecophysiology of native and alien-invasive clams in an ocean warming context. *Comp. Comparative Biochemistry and Physiology, Part A.* **156**, 28-37.

Anestis, A., Lazou, A., Pörtner, H.O., and Michaelidis, B. (2007). Behavioral, metabolic, and molecular stress responses of marine bivalve *Mytilus galloprovincialis* during long-term acclimation at increasing ambient temperature. *Am J Physiol Regul Inegr Comp Physiol*. **293**, R911-R921.

Anestis, A., Pörtner, H.O., Karagiannis, D., Angelidis, P., Staikou, A., Michaelidis, B. (2010). Response of *Mytilus galloprovincialis* (L.) to increasing seawater temperature and to marteliosis: metabolic and physiological parameters. *Comparative Biochemistry and Physiology, Part A.* **156**, 57-66.

Apple, F. S., and Collinson P. O. (2012). Analytical characteristics of high-sensitivity cardiac troponin assays. *Clinical Chemistry* **58**, 54-61.

Arosio, P., and Levi, S. (2002). Ferritin, iron homeostasis, and oxidative damage. *Free Radical Biology & Medicine* **33**, 457-463.

Arosio, P., and Levi, S. (2010). Cytosolic and mitochondrial ferritins in the regulation of cellular iron homeostasis and oxidative damage. *Biochemical et Biophysica Acta* 1800: 783-792.

Assinder, S. J., Stanton, J. L., and Prasad, P. D. (2009). Transgelin: an actin-binding protein and tumour suppressor. *The International Journal of Biochemistry and Cell Biology.* **41**, 482-486.

Bennett, A. F. (1984). Thermal dependence of muscle function. *Am. J. Physiol. Reg. Int. Comp. Physiol.* **247**, R217-R229.

Bernhardt, J. R., and Leslie, H. M. (2013). Resilience to climate change in coastal marine ecosystems. *Annu. Rev. Mar. Sci.* **5**, 371-392.

Bernstein, B. W., and Bamburg, J. R. (2010). ADF/Cofilin: a functional node in cell biology. *Trends in Cell Biology*. **20**, 187-195.

Braby, C. E., and Somero, G. N. (2006). Following the heart: temperature and salinity effects on heart rate in native and invasive species of blue mussels (genus *Mytilus*). *Jour. Exp. Bio*. **209**, 2554-2566.

Breitsprecher, D., Koestler, S. A., Chizhov, I., Nemethova, M., Mueller, J., Goode, B. L., Small, J. V., Rottner, K., and Faix, J., (2011). Cofilin cooperates with fascin to disassemble filopodial actin filaments. *Cell Science*. **124**, 3305-3318.

Brown, S. M. D., Hardisty-Hughes, R. E., and Mburu, P. (2008). Quiet as a mouse: dissecting the molecular and genetic basis of hearing. *Nature*. **9**, 277-290.

Buchberger, A., Bukau, B., and Sommer, T. (2010). Protein quality control in the cytosol and the endoplasmic reticulum: brothers in arms. *Molecular Cell* **40**, 238-252.

Bucki, R., Levental, I., Kulakowska, A., Jammey, P. A. (2008). Plasma Gelsolin: function, prognostic value, and potential therapeutic use." *Current Protein and Peptide Science*. **9**, 541-551.

Buckley, B. A., Owen, M.-E. and Hofmann, G. E. (2001). Adjusting the thermostat: the threshold induction temperature for the heat-shock response in intertidal mussels (genus *Mytilus*) changes as a function of thermal history. *Journal of Experimental Biology*. **204**, 3571-3579.

Buckley, B. A., Gracey, A. Y., and Somero, G. N. (2006). The cellular response to heat stress in the goby *Gillichthys mirabilis*: a cDNA microarray and protein-level analysis. *Journal of Experimental Biology*. **204**, 2660-2677.

Burrows, M. T., Schoeman, D. S., Buckley, L. B., Moore, P., Poloczanska, E. S., Brander, K. M., Brown, C., Bruno, J. F., Duarte, C. M., Halpern, B. S., Holding, J., Kappel, C. V., Kiessling, W., O'Connor, M. I., Pandolfi, J. M., Parmesan, C., Schwing, F. B., Sydeman, W. J., Richardson, A. J. (2011). The pace of shifting climate in marine and terrestrial ecosystems. *Science*. **334**, 652-655.

Butler, T. M., and Siegman, M. J. (2010). Mechanism of catch force: tethering of thick and thin filaments by twitchin. *Journal of Biomedicine and Biotechnology*. **2010**, 1-19

Carlier, M. F. and Pantaloni, D. (2007). Control of actin assembly dynamics in cell motility. *Journal of Biological Chemistry*. **282**, 23005-23009

Cevallos. M., Riha, G. M., Wang, X., Yang, H., Yan, S., Li. M., Chai, H., Yao, Q., and Chen, C. (2006). Cyclic strain induces expression of specific smooth muscle cell markers in human endothelial cells. *Differentiation* **74**, 552-561.

Cipolla, M. J., Gokina, N. I., and Osol, G. (2002). Pressure-induced actin polymerization in vascular smooth muscle as a mechanism underlying myogenic behavior. *FASEB J.* 16, 72-76.

Clarke, A., and Pörtner, H. O. (2010). Temperature, metabolic power and the evolution of endothermy. *Biological Reviews.* 2-22.

Coyle, P., Philcox, J. C., Carey, L. C., Rofe, A. M. (2002). Metallothionein: the multipurpose protein. *Cell. Mol. Life Sci*. **59**, 627-647.

Creed, S. J., Desouza. M., Bamburg, J. R., Gunning, P., and Stehn, J. (2011). Tropomyosin isoform 3 promotes the formation of filopodia by regulating the recruitment of actin-binding proteins to actin filaments. *Exp Cell Res* **317**, 249-261.

Dalle-Donne, I., Rossi, R., Giustarini, D., Colombo, R., Milzani, A. (2003). Actin *S*-glutathionylation: evidence against a thiol-disulphide exchange mechanism. *Free Radical Biology & Medicine*. **35**, 1185-1193.

Darling, D. L., Yinglin, J., and Wynshaw-Boris, A. (2005). Role of 14-3-3 proteins in eukaryotic signaling and development. *Current Topic in Developmental Biology*. **68**, 281-315.

Davies, M. J. (2005). The oxidative environment and protein damage. *Biochemica et Biophysica Acta*. **1703**, 93-109.

Decostre, V., Bianco, P., Lombardi, V., and Piazzesi, G. (2005). Effect of temperature on the working stroke of muscle myosin. *PNAS.* **102**, 13927-13932.

de Nooij, J. C., Simon, C. M., Simon, A., Doobar, S., Steel, K. P., Banks, R. W., Mentis, G. Z., Bewick, G. S., and Jessell T. M. (2015). The PDZ-domain protein whirlin facilitates mechanosensory signaling in mammalian proprioceptors. *The Journal of Neuroscience*. **35**, 3073-3084.

Dheilly, N. M., Haynes, P. A., Bove, U., Nair, S. V., and Raftos, D. A. (2010). Comparative proteomic analysis of a sea urchin (*Heliocidaris erythrogramma*) antibacterial response revealed the involvement of apextrin and calreticulin. *Journal of Invertebrate pathology* **106**, 223-229.

Diz, A. P., Martínez-Fernández, M., and Rolán-Alvarez, E. (2012). Proteomics in evolutionary ecology: linking the genotype with the phenotype. *Mol. Ecology* **21**, 1060-1080.

Dobrzhanskaya, A., Vyatchin, I. G., Lazarev, S. S., Matusovsky, O. S., Shelud'ko, N. S. (2013). Molluscan smooth catch muscle contains calponin but not caldesmon. *J. Muscle Res. Cell Motil*. **34**, 23-33.

Doney, S. C., Ruckelshaus, M. J., Duffy, E., Barry, J. P., Chan, F., English, C. A., Galindo, H. M., Grebmeier, J. M., Hollowed, A. B., Knowlton, N., Polovina, J., Rabalais, N. N., Sydeman, W. J., and Talley, L. D. (2012). Climate change impacts on marine ecosystems. *Annu. Rev. Mar. Sci.* **4**, 11-37.

Dos Remedios, C. G., Chhabra, D., Kekic, M., Dedova, I. V., Tsubakhara, M., Berry, D. A., and Nosworthy, N. J. (2003). Actin binding proteins: regulation of cytoskeletal microfilaments. *Physiology Review*. **84**, 433-473.

Dowd, W. W., and Somero, G. N. (2013). Behavior and survival of *Mytilus* congeners following episodes of elevated body temperature in air and seawater. *Journal of Experimental Biology* **216**, 502-514.

Dráber, P., and Dráberová, E. (2012). Microtubules. In *Part I Basics of the Cytoskeleton: Cytoskeleton and Human Disease* (ed. M. Kavallaris), pp. 29-33. New York: Springer Science-Business Media, LLC.

Drinkwater, K. F., Beaugrand, G., Kaeriyama, M., Kim, S., Ottersen, G., Perry, R. I., Pörtner, H. O., Polovina, J. J., and Takasuka, A. (2010). On the processes linking climate to ecosystem changes. *Journal of Marine Systems.* **79**, 374-388.

Dugina, V., Arnoldi, R., Janmey, P. A., Chaponnier, C. (2012). Chapter 1: ACTIN. *In Cytoskeleton and Human Disease* (ed. M. Kavallaris), pp 3-29. New York: Springer Science+Business Media, LLC.

Dzeja, P., and Terzic, A. (2009). Adenylate kinase and AMP signaling networks: metabolic monitoring, signal communication and body energy sensing. *Int. J. Mol. Sci*. **10**, 1729-1772.

Eckert, R. L., Kaartinen, M. T., Nuriminskaya, M., Belkin, A. M., Colak, G., Johnson, G. V. W., Mehta, K. (2014). Transglutaminase regulation of cell function. *Physiol. Rev*. **94**, 383-417.

Eisen, M. B., Spellman, P. T., Brown, P. O., Botstein, D. (1998). Cluster analysis and display of genome-wide expression profiles. *Proc. Natl. Acad. Sci.* **95**, 14863-14868.

Ellis, E. M. (2007). Reactive carbonyls and oxidative stress: potential for therapeutic intervention. *Pharmacology Therapeutics* **115**, 1017-1031.

Elliott, J., Holmes, K., Chambers, R., Leon, K., and Wimberger, P. (2008). Differences in morphology and habitat use among the native mussel *Mytilus trossulus*, the non-native *M. galloprovincialis*, and their hybrids in Puget Sound, Washington. *Mar. Biol.* **156**, 39-53.

El-Mezgueldi, M. (1996). Calponin. *Int. J Biochem. Cell Bio*. **28**, 1185-1189.

Estévez-Calvar, N., Romero, A., Figueras, A., and Novoa B. (2011). Involvement of pore-forming molecules in immune defense and development of the Mediterranean mussel (*Mytilus galloprovincialis*). *Developmental and Comparative Immunology* **35**, 1015-1029.

Farah, C. S., and Reinach, F. C. (1995). The troponin complex and regulation of muscle contraction. *FASEB* **9**, 755-767.

Fields, P. A., Rudomin, E. L., and Somero, G. N. (2006). Temperature sensitivities of cystolic malate dehydrogenases from native and invasive species of marine mussels (genus *Mytilus*): sequence-function linkages and correlations with biogeographic distribution. *The Journal of Experimental Biology* **209**, 656-667.

Fields, A. P., Zuzow, M. J., Tomanek, L. (2011). Proteomic responses of blue mussels (Mytilus) congeners to temperature acclimation. *The Journal of Experimental Biology* **215**, 1106-1116.

Franzellitti, S., and Fabbri, S. (2005). Differential HSP70 gene expression in the Mediterranean mussel exposed to various stressors. *Biochemical and Biophysical Research Communications* **336**, 1157-1163.

Funabara, D., Nakaya, M., and Watabe, S. (2001). Isolation and characterization of a novel 45 kDa calponin-like protein from anterior byssus retractor muscle of the mussel *Mytilus galloprovincialis*. *Fisheries Science*. **67**, 511-517.

Funabara, D., Kanoh, S., Siegman, M. J., Butler, T. M., Hartshorne, D. J., and Watabe, S. (2005). Twitchin as a regulator of catch contraction in molluscan smooth muscle. *Journal of Muscle Research and Cell Motility*. **26**, 455-460.

Galler, S. (2008). Molecular basis of catch state in molluscan smooth muscles: a catchy challenge. *J. Muscle Res Cell Motil*. **29**, 73-99.

Galtsoff, P. S. (1964). The American oyster *Crassostrea virginica Gmelin*. In *The Adductor Muscle: Effect of Temperature*, pp. 172-175. Washington, D. C.: U.S. Government Printing Office.

Garland, M. A., Stillman, J. H., and Tomanek, L. (2015). The proteomic response of cheliped myofibril tissue in the eurythermal porcelain crab *Petrolisthes cintipes* to heat shock following acclimation to temperature fluctuations. *Journal of Experimental Biology*. **218**, 388-403.

Geller, J. B. (1999). Decline of a native mussel masked by sibling species invasion. *Conservation Biology* **13**, 661-664.

Gimona, M., Kaverina, I., Resch, G. P., Vignal, E., and Brugstaller, G. (2003). Calponin repeats regulate actin thin filament stability and formation of podosomes in smooth muscle cells. *Molecular Biology of the Cell* **14**, 2482-2491.

Gimona, M. (2008). Dimerization of tropomyosins. In *Tropomyosin* (ed. P. Gunning), pp. 73-82. New York: Landes Bioscience and Springer Science+Business Media, LLC.

Gosling, E. (2015). *Marine Bivalve Molluscs*. Second Ed., Wiley-Blackwell.

Green, J. A., Yang, J., Grati, M., Kachar, B., and Bhat, M. A. (2013). Whirlin, a cytoskeletal scaffolding protein, stabilizes the paranodal region and axonal cytoskeleton in myelinated axons. *BMC Neuroscience* **14**, 96

Greenberg, M. J., Wang, C. L. A., Lehman, W., and Moore, J. R. (2008). Modulation of actin mechanics by caldesmon and tropomyosin. *Cell Motility and the Cytoskeleton*. **65**, 56-164.

Gross, S. R. (2013). Actin binding proteins their ups and downs in metastatic life. *Cell Adhesion & Migration* **7**, 199-213.

Gunning, P. W., Schevzov, G., Kee, A. J., and Hardeman, E. C. (2005). Tropomyosin isoforms: divining rods for actin cytoskeleton function. *TRENDS in Cell Biology*. **15**, 333-341.

Gunning. P. W., Hardeman, E. C., Lappalainen, P., and Mulvihill D. P. (2015). Tropomyosin-master regulator of actin filament function in the cytoskeleton. *Cell Science* **128**, 2965-2974.

Gunst, S. J., and Zhang, W. (2008). Actin cytoskeletal dynamics in smooth muscle: a new paradigm for the regulation of smooth muscle contraction. *Am J Physiol Cell Physiol.* **295**, C576-C587.

Halayko, A. J., and Stelmack, G. L. (2005). The association of caveolae, actin, and the dystrophin-glycoprotein complex; a role in smooth muscle phenotype and function. *Can. J. Physiol. Pharmacol.* **83**, 877-981.

Harley, C. D. G., Hughes, A. R., Hultgren, K. H., Miner, B. G., Sorte, C. J. B., Thornber, C. S., Rodriguez, L. F., Tomanek, L., and Williams, S. L. (2006). The impacts of climate change in coastal marine ecosystems. *Ecology Letters* **9**, 228-241.

Haslbeck, M., Franzmann, T., Weinfurtner, D., and Buchner, J. (2005). Some like it hot: the structure and function of small heat-shock proteins. *Nature Structural and Molecular Biology* **12**, 842-846.

Helbig, A. O., Heck, A. J. R., and Slijper, M. (2010). Exploring the membrane proteome-challenges and analytical strategies. *Journal of Proteomics*. **73**, 868-878.

Helmuth. B. (2009). From cells to coastlines: how can we use physiology to forecast the impacts of climate change. *Jour. Exp. Bio*. **212**, 753-760.

Helmuth, B., Broitman, B. R., Blanchette, C. A., Gilman, S., Halpin, P., Harley, C. D. G., O'Donnell, M. J., Hofmann, G. E., Menge, B., and Strickland, D. (2006). Mosaic patterns of thermal stress in the rocky intertidal zone: implications for climate change. *Ecological Monographs*. **76**, 461-479.

van Hemert, M. J. Steensma, H. Y., and van Heusden, G. P. H. (2001). 14-3-3 proteins: key regulators of cell division, signaling and apoptosis. *BioEssays* **23**, 936-946.

Hodgkinson, J. L. (2000). Actin and the smooth muscle regulatory proteins: a structural perspective. *Journal of Muscle and Cell Motility.* **21**, 115-130.

Hofmann, G. E., and Somero, G. N. (1996). Interspecific variation in thermal denaturation of proteins in the congeneric mussels Mytilus trossulus and M. galloprovincialis: evidence from the heat-shock response and protein ubiquitination. *Marine Biology*. **126**, 65-75.

Hofmann, G. E., and Todgham, A. E. (2010). Living in the now: physiological mechanisms to tolerate a rapidly changing environment. *Annu. Rev. Physiol.* **72**, 127-145.

Hoon, S., Gebbia, M., Costanzo, M., Davis, R. W., Giaver, G., and Nislow, C. (2011). A global perspective of the genetic basis for carbonyl stress resistance. *G3: Genes Genomes Genetics* **1**, 219-231.

Hooper S. L., and Thuma, J. B. (2005). Invertebrate muscles: muscle specific genes and proteins. *Physiol Rev*. **85**, 1001-1060.

Hooper, S. L., Hobbs, K. H., and Thuma, J. B. (2008). Invertebrate muscles: thin and thick filament structure; molecular basis of contraction and its regulation, catch and asynchronous muscle. *Progress in Neurobiology*. **86**, 72-127.

Ioannou, S., Anestis, A., Pörtner, H. O., and Michaelidis, B. (2009). Seasonal patterns of metabolism and the heat shock response (HSR) in farmed mussels Mytilus galloprovincialis. *Journal of Experimental Marine Biology and Ecology* **381**, 136-144.

IPCC, 2014: *Climate Change 2014: Synthesis Report*. Contribution of working groups I, II and III to the fifth assessment report of the Intergovernmental panel on climate change [Core Writing Team, R.K. Pachauri and L.A. Meyer (eds.)]. IPCC, Geneva, Switzerland, 151 pp.

Jensen, M. H., Watt, J., Hodgkinson, J. L., Gallant, C., Appel, S., El-Mezgueldi, M., Angelini, T. E., Morgan, K. G., Lehman, W., and Moore, J. R. (2012). Effects of basic calponin on the flexural mechanics and stability of F-actin. *Cytoskeleton* **69**, 49-48.

Jensen, M. H., Morris, E. J., Gallant, C. M., Morgan, K. G., Weitz, D. A., Moore, J. R. (2014). Mechanism of calponin stabilization of cross-linked actin networks. *Biophysical Journal*. **106**, 793-800.

Jones, S. J., Lima, F. P., Wethey, D. S. (2010). Rising environmental temperatures and biogeography: poleward range contraction of the blue mussel, *Mytilus edulis* L., in the western Atlantic. *J. Biogeogr*. **37**, 2243-2259.

Kamm K. E., and Stull, J. T. (1985). The function of myosin and myosin light chain kinase phosphorylation in smooth muscle. *Annual Review of Pharmacology and Toxicology*. **25**, 593-620.

Karaki, H., Ozaki, H., Hori, M., Mitsui-Saito, M., Amano, K. I., Harada, K. I., Miyamoto, S., Nakazawa, H., Won, K. J., and Sato, K. (1997). Calcium movements, distribution and function in smooth muscle. *Pharmacological Reviews*. **49**, 157-230.

Kardos, R., Nevalainen E., Nyitrai, M., and Hild. G. (2013). The effect of ADF/cofilin and profilin on the dynamics of monomeric actin. *Biochemica et Biophysica Acta* **1834**, 2010-2019.

Kim, Y. E., Hipp, M. S., Bracher, A., Hayer-Hartl. M., and Hartl, U. F. (2013). Molecular chaperone functions in protein folding and proteostasis. *Annu. Rev. Biochem.* **82**, 322-355.

A) Kim, H. R., Appel, S., Vetterkind, S. Gangopadhyay, S. S., and Morgan, K. G. (2008). Smooth muscle signaling pathways in health and disease. *J. Cell Mol. Med.* **12**, 2165-2180.

B) Kim, H. R., Gallant, C., Leavis, P. C., Gunst, S. J., and Morgan K. G. (2008). Cytoskeletal remodeling in differentiated vascular smooth muscle is actin isoform dependent and stimulus dependent. *Am J Physiol* **295**, C768-C778.

Komalavilas, P., Penn, R. B., Flynn, C. R., Thresher, J., Lopes, L. B., Furnish, E., Guo, M., Pallero, M. A., Murphy-Ulrich, J. E., and Brophy, C. M. (2008). The small heat shock-related protein, HSP20, is a cAMP-dependent protein kinase substrate that is involved in airway smooth muscle relaxation. *Am. J. Physiol. Lung Cell Mol. Physiol.* **294**, L69-L78.

Kültz, D. (2005). Molecular and evolutionary basis of the cellular stress response. *Annu. Rev. Physiol.* **67**, 225-257.

Larsen, M., Artym, V. V., Green, J. A., Yamada, K. M. (2006). The matrix reorganized: extracellular matrix remodeling and integrin signaling. *Current Opinion in Cell Biology*. **18**, 463-471.

Lavatelli, F., Albertini, R., Di Fonzo, A., Palladini, G., and Mertini, G. (2014). Biochemical markers in early diagnosis and management of systemic amyloidoses. *Clin Chem Lab Med* **52**, 1517-1531.

Lehman, W., and Morgan K. G. (2012). Structure and dynamics of the actin-based smooth muscle contractile and cytoskeletal apparatus. *J Muscle Res Cell Motility*. **33**, 461-469.

Levitsky, D. I., Pivovarova, A. V., Mikhailova, V., and Nikolaeva, O. P. (2008). Thermal unfolding and aggregation of actin stabilization and destabilization of actin filaments. *FEBS* **275**, 4280-4295.

Linehan, C. M. (1982). The effect of temperature on the tension responses of the anterior byssal retractor muscle (ARBM) of *Mytilus edulis*. *J. exp. Biol*, **97**, 375-384.

Littlefield, R. S., and Fowler, V. M. (2008). Thin filament length regulation in striated muscle sarcomeres: pointed-end dynamics go beyond a nebulin ruler. *Seminars in Cell and Developmental Biology* **19**, 511-519.

Lockwood, B. L., Sanders, J. G., and Somero, G. N. (2010). Transcriptomic responses to heat stress in invasive and native blue mussels (genus *Mytilus*): molecular correlates of invasive success. *Journal of Experimental Biology* **213**, 3458-3558.

Lockwood, B. L., and Somero, G. N. (2011). Invasive and native blue mussels (genus Mytilus) on the California coast: The role of physiology in a biological invasion. *Jour. Exp. Mar. Bio. and Ecol.* **400**, 167-174.

Lovrić, J. (2011). Introducing proteomics: from concepts to sample separation, mass spectrometry and data analysis. John Wiley & Sons. West Sussex, UK.

Mahanty, A., Purohit, G. K., Banerjee, S., Karunakaran, D., Mohanty, S. and Mohanty B. P. (2016). Proteomic changes in the liver of *Channa striatus* in response to high temperature stress. *Electrophoresis* **3**, 1704-1707.

Marchitti, S. A., Brocker, C., Stagos, D., and Vasilou, V. (2008). Non-P450 aldehyde oxidizing enzymes: the aldehyde dehydrogenase superfamily. *Expert Opin Drug Metab Toxicol*. **4**, 697-720.

Marden, J. H., Fitzhugh, G. H., Girgenrath, M., Wolf, M. R., and Girgenrath, S. (2001). Alternative splicing, muscle contraction and intraspecific variation: associations between troponin T transcripts, Ca^{2+} sensitivity and the force and power output of dragonfly flight muscles during oscillatory contraction. *Journal of Experimental Biology* **204**, 3457-4370.

Marston, S., and Mezgueldi, E. (2008). Role of tropomyosin in the regulation of contraction in smooth muscle. *In Tropomyosin* (ed. P. Gunning), pp. 110-120. New York, Springer Science+Business Media, LLC Landes Bioscience

Matés, J. M., and Sánchez-Jiménez, F. M. (2000). Role of reactive oxygen species in apoptosis: implications for cancer therapy. *Int Jour Biochem & Cell Bio* **32**, 157-170.

Mayer, M. P., and Bakau, B. (2005). Hsp70 chaperones: cellular functions and molecular mechanism. *Cell. Mol. Life. Sci* **62**, 670-684.

Mburu, P., Kikkawa, Y., Townsend, S., Romero, R., Yonekawa, H., and Brown S. M. D. (2006). Whirlin complexes with p55 at the stereocilia tip during hair cell development. *PNAS.* **103**, 10973-10978.

McDonagh, B., and Sheehan, D. (2007). Effect of oxidative stress on protein thiols in the blue mussel *Mytilus edulis*: proteomic identification of target proteins. *Proteomics* **7**, 3395-3403.

McDonald, J. H., and Koehn, R. K. (1988). The mussels *Mytilus galloprovincialis* and *M. trossulus* on the Pacific coast of North America. *Marine Biology*. **99**, 111-118.

Méndes-López, L., Hellman, U., Ibarguren, I., and Villamarín, J. A. (2012). Filamin isoforms in molluscan smooth muscle. *Biochimica et Biophysica Acta.* **1824**, 1334-1341.

Meunier, B., Dumas, E., Piec, I., Béchet, D., Hébraud, M., Hocquette, J. F. (2007). Assessment of hierarchical clustering methodologies for proteomic data mining. *Journal of Proteome Research*. **6**, 358-366.

Nakamura, F., Stossel, T. P., and Hartwig, J. H. (2011). The filamins organizers of cell structure and function. **5**, 160-169.

Nakamoto, H., and Vigh, L. (2007). The small heat shock proteins and their clients. *Cell. Mol. Life. Sci*. **64**, 294-306.

Neer, E. J. (1995). Heterotrimeric G proteins: organizers of transmembrane signals. *Cell* **80**, 249-257.

Nelson, D. L., and Cox, M. M. (2008). Lehninger. Principles of biochemistry. In *The Citric Acid Cycle: Reactions of the Citric Acid Cycle* (ed. K. Ahr, R. Rossignol, P. Shriner, P. McCaffrey, E. Geller, and B. Moscatelli), pp. 616-626. New York: W. H. Freeman and Company.

Nicastro, K. R., Zardi, G. I., McQuaid, C. D., Stephens, L., Radloff, S., and Blatch, G. L. (2010). The role of gaping behavior in habitat partitioning between coexisting intertidal mussels. *BMC ecology*. **10**, 17.

Okada, K., Ravi, H., Smith, E. M., and Goode, B. L. (2006). Aip1 and cofilin promote rapid turnover of yeast actin patches and cables: a coordinated mechanism for severing and capping filaments. *Molecular Biology of the Cell.* **17**, 2855-2868

Olson, J. M., and Marsh. R. L. (1993). Contractile properties of the striated adductor muscle in the bay scallop *Argopecten irradians* at several temperatures. *J. exp. Biol*. 176: 175-193.

Ono, S. (2003) Regulation of actin filament dynamics by actin depolymerizing factor/cofilin and actin-interacting protein 1: new blades for twisted filaments. *Biochemistry* **42**, 13363-13370.

Perry, S. V. (1998). Troponin T: genetics, properties and function. *Journal of Muscle Research and Cell Motility*. **19**, 575-602.

Perry, A. L., Low, P. J., Ellis, J. R., and Reynolds, J. D. (2005). Climate change and distribution shifts in marine fishes. *Science* **308**, 1912-1915.

Pfeffer, S. R., Barbara Dirac-Svejstrup, A., and Soldati, T. (1995). Rab GDP dissociation inhibitor: putting Rab GTPases in the right place. *Journal of Biological Chemistry*. **270**, 17057-17059.

Piano, A., Valbonesi, P., and Fabbri, E. (2004). Expression of cytoprotective proteins, heat shock protein 70 & metallothioneins, in tissues of *Ostrea edulis* exposed to heat and heavy metals. *Cell Stress & Chaperones*. **9**, 134-142.

Pivovarova, A. V., Chebotareva, N. A., Chernik, I. S., Gusev, N. B., and Levitsky, D. I. (2007). Small heat shock protein Hsp27 prevents heat-induced aggregation of F-actin by forming soluble complexes with denatured actin. *FEBS* **274**, 5937-5948

Pollard, T. D. and Borisy, G. G. (2003). Cellular motility driven by assembly and disassembly of actin filaments. *Cell*. **112**, 453-465.

Popowicz, G. M., Schleicher, M., Noegel A. A., and Holak T. A. (2006). Filamins: promiscuous organizers of the cytoskeleton. *Trends in Biochemical Science*. **31**, 411-419.

Pörtner, H. O. (2009). Oxygen- and capacity-limitation of thermal tolerance: a matrix for integrating climate-related stressor effects in marine ecosystems. *Journal of Experimental Biology*. **213**, 881-893.

Pörtner, H. O. (2012). Integrating climate-related stressor effects on marine organisms: unifying principles linking molecule to ecosystem-level changes. *Mar. Ecol. Prog. Ser.* **470**, 273-290.

Pörtner, H. O., and Knust., R. (2007). Climate change affects marine fishes through the oxygen limitation of thermal tolerance. *Science*. **315**, 95-97.

Pörtner, H. O., Langenbuch, M., and Michaelidis B. (2005). Synergistic effects of temperature extremes, hypoxia and increases in CO_2 on marine animals: from Earth history to global change. *Journal of Geophysical Research* **110**, 1-15.

Prosser, H. M., Rzadzinska, A. M., Steel, K. P., Bradley. (2008). Mosaic complementation demonstrates a regulatory role for myosin VIIa in actin dynamics of stereocilia. *Molecular and cellular biology.* **28**, 1702-1712.

Rao, J. N., Madasu, Y, and Dominguez, R. (2014). Mechanism of actin filament pointed-end capping by tropomodulin. *Science* **345**, 463-467.

Ray, P. D., Huang, B.W., and Tsuji, Y. (2012). Reactive oxygen species (ROS) homeostasis and redox regulation in cellular signaling. *Cellular Signaling.* **24**, 981-990.

Raychaudhuri, S., Stuart, J. M., and Altman R. B. (2000). Principal components analysis to summarize microarray experiments: application to sporulation time series. *Pac. Symp. Biocomput*: 455-466.

Razinia, Z., Mäkelä. T., Ylänne, J., Calderwood, D. A. (2012). Filamins in mechanosensing and signaling. *Annu. Rev. Biophys*. **41**, 227-246.

Ringnér, M. (2008). What is principal component analysis? *Nature Biotechnology*. **26**, 303-304.

Rocher, B., Bultelle, F., Chan, P., Le Foll, F., Letendre, J., Monsinjon, T., Olivier, S., Péden, R., Poret, A., Vaudry, D., and Knigge, T. (2015). 2-DE mapping of the blue mussel gill proteome: the usual suspects revisited. *Proteomes*. **3**, 3-41.

Ron, D., and Walter, P. (2007). Signal integration in the endoplasmic reticulum unfolded protein response. *Nature*. **8**, 519-529.

Rosado, C. J., Kondos, S., Bull, T. E., Kuiper, M. J., Law, R. H., Buckle, A. M., Voskoboinik, I., Bird, P. J., Trapani, J. A., Whisstock, J. C., and Dunstone, M. A. (2008). The MACPF/CDC family of pore-forming toxins. *Cellular Microbiology* **10**, 1765-1774.

Rozenblum, G.T., Gimona, M. (2008). Calponins: adaptable modular regulators of the actin cytoskeleton. *International Journal of Biochemistry and Cell Biology*. **40**, 1990-1995.

Rzadzinska, A. K., Schneider, M. E., Davies, C., Riordan, G. P., Kachar., B. (2004). An actin molecular treadmill and myosins maintain stereocilia functional architecture and self-renewal. *Journal of Cell Biology.* **164**, 887-897.

Salinthone, S., Tyagi, M., and Gerthoffer, W. T. (2008). Small heat shock proteins in smooth muscle. *Pharmacology & Therapeutics* **119**, 44-54.

Schneider, K. R. (2008). Heat stress in the intertidal: comparing survival of an invasive and native mussel under a variety of thermal conditions. *Biol. Bull.* **215**, 253-264.

Schneider, K. R., and Helmuth. B. (2007). Spatial variability in habitat temperature may drive patterns of selection between an invasive and native mussel species. *Mar. Ecol. Prog. Ser.* **339**, 157-167.

Schubert, H. L., Blumenthal, R. M., Cheng, X. (2003). Many paths to methyltransfer: a chronicle of convergence. *TRENDS in Biochemical Sciences* **28**, 329-335

Sena, L. A., and Chandel, N. S. (2012). Physiological roles of mitochondrial reactive oxygen species. *Molecular Cell*. **48**, 158-167

Shinen, J. S., and Morgan, S. G. (2009). Mechanisms of invasion resistance: competition among intertidal mussels promotes establishment of invasive species and displacement of native species. *Mar. Ecol. Prog. Series.* **383**, 187-197.

Singh, S., Brocker, C., Koppaka, V., Chen, Y., Jackson, B. C., Matsumoto, A., Thompson, D. C., and Vasiliou, V. (2013). Aldehyde dehydrogenases in cellular responses to oxidative/electrophilic stress. *Free Radical Biology and Medicine*. **56**, 89-101.

Sinha, K., Das, J., Pal, P. B., and Sil, P. C. (2013). Oxidative stress: the mitochondria-dependent and mitochondria-independent pathways of apoptosis. *Arch. Toxicol*. **87**, 1157-1180.

Sirenko, V. V., Simonyan, A. H., Dobrzhanskaya, A. V., Shelud'ko, N. S., and Borovikov, Y. S. (2013). 40-kDa Protein from thin filaments of the mussel *Crenomytilus grayanus* changes the conformation of F-actin during the ATPase cycle. *Biochemistry* (Moscow). **78**, 273-281.

Sokolova, I. M., Frederich, M., Bagwe, R., Lanning, G., Sukhotin, A. A. (2012). Energy homeostasis as an integrative tool for assessing limits of environmental stress tolerance in aquatic invertebrates. *Mar. Env. Res*. **79**, 1-15.

Somero, G. N. (2002). Thermal physiology and vertical zonation of intertidal animals: optima, limits, and the cost of living. *Integ. And Comp. Biol.* **42**, 780-789.

Somero, G. N. (2010). The physiology of climate change: how potentials for acclimatization and genetic adaptation will determine 'winners' and 'losers'. *Journal of Experimental Biology*. **213**, 912-920.

Somero, G. N. (2011). Comparative physiology: a "crystal ball" for predicting consequences of global climate change. *Am J Physiol Regul Integr Comp Physiol.* **301**, R1-R14.

Somero, G. N. (2012). The physiology of global climate change: linking patterns to mechanisms. *Annu. Rev. Mar. Sci*. 4: 39-61.

Somlyo, A. P., and Somlyo, A. V. (1994). Signal transduction and regulation in smooth muscle. *Nature*. 372(17): 231-236.

Somlyo, A. P., and Somlyo, A. V. (2003). Ca^{2+} sensitivity of smooth muscle and nonmuscle myosin II: modulated by g proteins, kinases, and myosin phosphatase. *Physiol. Rev.* 83: 1325-1358.

Sorte, C. J. B., Jones, S. J., and Miller, L. P. (2011). Geographic variation in temperature tolerance as an indicator of potential population responses to climate change. *Jour. Exp. Mar. Bio and Ecol.* 400: 209-217.

Stephens-Camacho, N.A., Muhlia-Almazan, A., Sanchez-Paz, A., and Rosas-Rodriguez, J.A. (2015). Surviving environmental stress: the role of betaine aldehyde dehydrogenase in marine crustaceans. *ISJ*. **12**, 66-74.

Stenmark, H. and Olkkonen, V. (2001). The Rab GTPase family. *Genome Biology*. **2**, 3007.1-3007.7.

Sun, Y., and MacRae, T. H. (2005). Small heat shock proteins: molecular structure and chaperone function. *Cell. Mol. Life. Sci*. **62**, 2460-2476.

Sunday, J. M., Bates, A. E., Dulvy, N. K. (2012). Thermal tolerance and the global redistribution of animals. *Nature Climate Change* **2**, 686-690.

Tabas, I., and Ron, D. (2011). Integrating the mechanisms of apoptosis induced by endoplasmic reticulum stress. *Nature*. **13**, 184-190.

Tchantchou, F., Graves, M., Falcone, D., and Shea T. B. (2008). S-Adenosylmethionine mediates glutathione efficacy by increasing glutathione-S-transferase activity: implications for S-adenosyl methionine as a neuroprotective dietary supplement. *Journal of Alzheimer's disease.* **14**, 323-328.

Tojkander, S., Gateva, G., and Lappalainen, P. (2012). Actin stress fibers – assembly, dynamics and biological roles. *Journal of Cell Science*. **125**, 1855-1864.

Tomanek, L., and Somero, G. N. (1999). Time course and magnitude of synthesis of heat-shock proteins in congeneric marine snails (genus *Tegula*) from different tidal heights. *Physiological and Biochemical Zoology* **73**, 249-256.

Tomanek, L. (2008). The importance of physiological limits in determining biogeographical range shifts due to global climate change: the heat-shock response. *Physiological and Biochemical Zoology*. **81**, 709-717.

Tomanek, L. (2009). Variation in the heat shock response and its implication for predicting the effect of global climate change on species' biogeographical distribution ranges and metabolic costs. *Journal of Experimental Biology.* **213**, 971-979.

Tomanek, L., Zuzow, M. J. (2010). The proteomic response of the mussel congeners *Mytilus trossulus* and *M. galloprovincialis* to acute heat stress: implications for thermal tolerance and metabolic costs of thermal stress. *Journal of Experimental Biology.* **213**, 3559-3574.

Tomanek, L. (2011). Environmental proteomics: changes in the proteome of marine organisms in response to environmental stress, pollutants, infection, symbiosis and development. *Ann. Rev. Mar. Sci.* **3**, 14.1-14.27.

Tomanek, L., Zuzow, M. J., Hitt, L., Serafini, L., and Valenzuela J. (2012). Proteomics of hyposaline stress in blue mussel congeners (genus *Mytilus*): implications for biogeographic range limits in response to climate change. *Journal of Experimental Biology* **215**, 3905-3916.

Tomanek, L. (2012). Environmental proteomics of the mussel *Mytilus*: implications for tolerance to stress and change in limits of biogeographic ranges in response to climate change. *Integrative and Comparative Biology*. **52**, 648-664.

Tomanek, L. (2014). Proteomics to study adaptations in marine organisms to environmental stress. *Journal of Proteomics.* **105**, 92-106.

Tomanek, L. (2015). Proteomic response to environmentally induced oxidative stress. *Journal of Experimental Biology* **218**, 1867-1869.

Tozzi, M. G., Camici, M., Mascia, L., Sgarella, F., and Ipata, P. (2006). Pentose phosphates in nucleoside interconversion and catabolism. *FEBS* **273**, 1089-1101.

Treman, J. R., Kashina, A. (2013). Post-translational modification and regulation of actin. *Curr Opin Cell Biol*. **25**, 30-38.

Twarog, B. M. (1967). Factors influencing contraction and catch in *Mytilus* smooth muscle. *J. Physiol*. **192**, 847-856.

Wang, L. Zou, J., Shen, Z., Song, E., and Yang, J. (2012). Whrilin interacts with espin and modulates its actin-regulatory function: an insight into the mechanism of Usher syndrome type II. *Human Molecular Genetics* **21**, 692-710.

Wettstein, G., Bellaye, P. S., Micheau, O., and Bonniaud, P. H. (2012). Small heat shock proteins and the cytoskeleton: an essential interplay for cell integrity? *The International Journal of Biochemistry and Cell Biology*. **44**, 1680-1686.

Yu, R., and Ono, S. (2006) Dual roles of tropomyosin as an F-actin stabilizer and a regulator of muscle contraction in *Caenorhabditis elegans* body wall muscle. *Cell Motility and the Cytoskeleton*. **63**, 659-672.

Zerebecki, R. A., and Sorte, C. J. B. (2011). Temperature tolerance and stress proteins as mechanisms of invasive species success. *PLoS ONE* **6**, e14806.

Zhang, Y., Sun, J., Huawei, M., Li, J., Zhang, Y., Xu, F., Xiang, Z., Qian, P. Y., Qiu, J. W., and Yu, Z. (2014). Proteomic basis of stress responses in the gills of the pacific oyster *Crassostrea gigas*. *Journal of Proteome Research.* **14**, 304-317.

Zhou, J., Wang, L., Xin, Y., Wang, W. N., He, W. Y., Wang A. L., and Liu, Y. (2010). Effect of temperature on antioxidant enzyme gene expression and stress protein response in white shrimp, *Litopenaeus vannamei. Journal of Thermal Biology*. **25**, 284-289.

Materials and Methods

Animal collection, maintenance and experimental design

Mytilus trossulus (Gould 1850) and *M. galloprovincialis* (Lamarck 1819) were collected from subtidal locations in Newport, OR, USA (44°38’25’’N, 124°03’10’’W) and Santa Barbara, CA, USA (34°24’15’’N, 119°41’30’’W) respectively. In a separate study, PCR was used to confirm that only a single species occupied each location (Lockwood et al., 2010). Mussels collected from both location sites were transferred to the Environmental Proteomics Lab (California Polytechnic State University, San Luis Obispo, CA, USA) and held under constant immersion within a recirculating seawater tank. These mussels were maintained at constant garden temperature of 13°C and fed a daily phytoplankton diet for an acclamatory period of four weeks prior to the investigation.

The experimental design was previously outlined in a prior investigation (Tomanek and Zuzow, 2010). To outline the experiment, however, acclimated mussels (*N*=48 total; *N*=24 per species) were transferred to an initial temperature controlled ice-chest set at 13°C. This control ice-chest was maintained with circulating seawater and held under constant aeration to minimize the effect of hypoxia. Mussels from both species were then randomly selected (N=36 total; *N*=18 per species) and placed into a second experimental temperature controlled ice-chest set at 13°C. However, the temperature within the experimental chest was gradually increased by a factor of $6°C \cdot h^{-1}$, beginning with the initial acclimation temperature of 13°C and steadily raised to one of three desired peak temperature treatments: I) 24°C; II) 28°C; and III) 32°C respectively. At the time point in which these target temperatures were reached, mussels from both species were randomly selected (*N*=6 per temperature treatment) and transferred to a third separate temperature controlled ice-chest which was maintained at one of the three respective peak

temperature treatments for duration of 1 h. Following the acute temperature exposure, mussels were then subsequently brought back to the 13°C control chest and allowed to recover for a period of 24 h. The recovery period was designed to provide sufficient time in order for appropriate protein expression levels to occur within target tissues in response to acute heat stress. Immediately following the recovery period gill, posterior adductor muscle and mantle tissues were sampled across temperature treatment groups (g=4) and were subsequently flash-frozen using liquid nitrogen. Tissues were then stored at -80°C until sample preparation was conducted (See Homogenization).

Target temperature regimes were based on acclimatization temperatures required for the induction of the heat shock response within the cold-adapted *Mytilus trossulus* ranging from the initial threshold temperature of 23°C to 28°C (Buckley et al. 2001). The highest temperature of 32°C approaches the temperature threshold required to inhibit protein synthesis among several species of *Mytilus* (Roberts et al. 1997), in addition to the critical heart rate temperatures exhibited among both *M. trossulus* and *M. galloprovincialis* (Petes et al. 2007; Lockwood and Somero, 2011). It is also noteworthy to mention that the latter temperature extreme has been recorded within mussels during peak seasonal variations in temperature (Harley et al. 2008).

Homogenization

In addition to the experimental design, sample preparation and separation procedures were followed in accordance with a prior investigation (Tomanek and Zuzow, 2010). Briefly, adductor tissue was lysed using homogenization buffer [7 mol l^{-1} urea, 2 mol l^{-1} thiourea, 1% amidosulfobetaine (ASB)-14, 40 mmol l^{-1} Tris-base, 0.5% immobilized pH 4-7 gradient (IPG) buffer (GE Healthcare, Piscataway, NJ, USA) and 40 mmol l^{-1} dithiothreitol] at a ratio of 1:4

(tissue (g): buffer (mL)). Following centrifugation at 20°C for 30 min at 16,100 ***g***, the proteins were precipitated by adding four volumes of ice-cold 10% trichloroacetic acid in acetone and incubating the solution at -20°C overnight. The following morning, the precipitate was centrifuged at 4°C for 15 min at 18,000 ***g***, the resulting supernatant was decanted and discarded, and the protein pellet was washed with 100% ice-cold acetone and centrifuged again at 4°C. After allowing the pellet to air-dry, the pellet was re-suspended in rehydration buffer [7 mol l^{-1} urea, 2 mol l^{-1} thiourea, 2% cholamidopropyl-dimethylammonio-propanesulfonic acid (CHAPS), 2% nonyl phenoxylpolyethoxylethanol (NP-40), 0.002% Bromophenol Blue, 0.5% IPG buffer and 100 mmol l^{-1} dithioerythritol] through repeated vortexing at room temperature (20°C). Finally, the samples were centrifuged at 20°C for 10 min at 16,100 ***g***. The supernatant was retained, and the protein concentration was determined using the 2-D Quant kit (GE Healthcare), according to the manufacturer's instructions.

Two-dimensional gel electrophoresis

Proteins were diluted to an optimal concentration (2µg•µl^{-1}) using rehydration buffer to equate to a total volume of 200µL, which was then loaded onto 1st-dimention IPG strips (pH 4-7, 11 cm; GE Healthcare) to separate the proteins according to their isoelectric point (pI). Protein samples were separated using a isoelectric focusing cell (BioRad, Hercules, CA, USA) *via* the following focusing program: 5 h of passive rehydration, 12 h of active rehydration (50 V), followed by rapid mode (under maximum current of 50 µA) in which voltages were steadily increased by 500 V for 1 h, 1000 V for 1 h and 8000 V for 2. 5 h. The IPG strips were then immediately removed from the focusing cell and subsequently frozen at -80°C. It should be noted that an initial sample run utilizing a representative protein concentration from each

treatment was run to ensure the proper elution of rehydrated protein samples. Since several of the samples exhibited improper migration through the 1D IPG strips (i.e., indicative of incomplete elution of samples) all adductor protein samples across all four treatments were then re-precipitated using the aforementioned techniques, to ensure proper protein migration and separation had been achieved (see homogenization).

In order to prepare solutions for further separation in the second-dimension using SDS-PAGE electrophoresis, resultant IPG strips were immersed in equilibration buffer [375 mmol l^{-1} Tris-base, 6 mol l^{-1} urea, 30% glycerol, 2% sodium dodecyl sulfate (SDS) and 0.002% Bromophenol Blue] for two 15 min intervals: first with 65 mmol l^{-1} dithiothreitol and second with 135 mmol l^{-1} iodoacetamide. This step was performed to deter any unwanted protein aggregation from occurring prior to separation. IPG strips were then placed on top of 11.8% polyacrylamide gels, which were then run (Criterion Dodeca; BioRad) at 200 V for 55 min at 10°C. Following separation, gels were subsequently removed and stained using colloidal Coomassie Blue (G-250) overnight and later destained through repeated washes using Milli-Q water (Millipore, Billerica, MA, USA) for an additional 48 h. The resulting gel images were scanned with an Epson 1280 transparency scanner (Epson, Long Beach, CA, USA).

Gel image analysis and primary statistical analysis

Digitized images of two-dimensional (2-D) gels were analyzed using Delta2D software program (version 4.3, Decodon, Greifswald, Germany) (Berth et al., 2007). Both species were analyzed separately. Gels within peak temperature treatment groups were warped to a representative treatment group gel image using match vectors, while gels across treatments were warped to a master control group gel image (i.e., 13°C) using a group-warping strategy. Once

match vector analysis was complete, all gel images were then fused to create an average composite image (See Figure(s) 1A & 1B), indicative of all gels across all treatments. This composite image (i.e. proteome map) was then used to detect spot boundaries and generate a consensus spot pattern (Berth et al., 2007). Careful diligence was taken to ensure that these spot boundaries were separated into individual protein spots and any questionable spot patterns thereof, e.g., dimensional smearing, air bubbles, etc., were omitted from statistical analysis. This was achieved through utilization of specific gel diagnostic tools, e.g., three-dimensional rotation tool, available on Delta 2D software. After background subtraction following transfer of the generated consensus spot pattern, the relative amount of protein in each spot, i.e. spot volume and/or pixel density, was quantified by normalizing against total spot volume of all proteins within the gel image.

In order to determine which spots changed significantly in response to acute immersed heat stress (24°C, 28°C and 32°C), we used a one-way ANOVA ($p<0.05$) with temperature as the main effect. We generated a null distribution for the one-way ANOVA based on 1,000 permutations to account for the unequal variance and non-normal distributions of the response variables, i.e., protein abundance. This test was utilized to minimize the false-discovery rate associated with multiple hypotheses testing using data gathered from two-dimensional gel images (Delta 2D). Significantly identified proteins were further separated into the following functional categories: I) molecular chaperones, II) oxidative stress, III) signal transduction, IV) thin filament regulation, and V) regulation of the acto-myosin complex. Due to the overabundance of cytoskeletal proteins, the latter two categories were subdivided into thin filament regulation and regulation of the acto-myosin complex. Due to the limited overlap between the composite images of the two congeners, as well as the uncertainty associated with

overlapping proteins potentially being orthologous or paralogous homologs, a two-way ANOVA comparing species was not feasible. Following the one-way ANOVA, Tukey's *post hoc* analysis ($p<0.05$) in Minitab (version 15, Minitab, State College, PA, USA) was used to assess the variation associated with individual significant identified protein abundance changes across the different peak temperature treatments.

Mass spectrometry

Proteins that were observed to change in abundance in response to acute temperature acclimation were excised from gels using the generated proteome maps and were subsequently prepared for mass spectrometry (MS) in accordance with previously published protocols (Fields et al., 2012; Tomanek and Zuzow 2010).

We obtained peptide mass fingerprints (PMFs) using a matrix-assisted laser desorption ionization tandem time-of-flight mass spectrometer (Ultraflex II, Bruker Daltonics, Billerica, MA, USA). We selected a minimum of twelve peptides, whose charge state was assumed to be +1 to conduct tandem MS, in order to obtain enough information about the b- and y-ions of the peptide sequence to make a strong enough identification.

We used flexAnalysis (version 3.4; Bruker Daltonics Inc.) to analyze and internally calibrate the mass spectra. The TopHat algorithm was used for baseline subtraction, the Savitzky Golay analysis was used for smoothing (with: 0.2 m/z; number of cycles=1), and the SNAP algorithm was used to detect peaks (with a signal-to-noise ratio of 6 for MS and 1.5 for MS/MS). Porcien trypsin (Promega, Madison, WI, USA) was used for internal mass calibration.

To identify proteins, we used Mascot (version 2.2; Matric Science Inc., Boston, MA, USA) and combined PMFs and tandem mass spectra in a search against two databases. The first

database search was an EST library that contained sequence information for *Mytilus edulis*, which contained approximately 26,000 entries, representing 12,961 and 1,688 different gene sequences for *M. californianus* and *M. galloprovincialis*, respectively (Lockwood et al., 2010). If the latter search did not yield significant results, a second search through NCBI (Metazoa) was conducted. Oxidation of methionine and carbamidomethylation of cysteine were included as variable modifications. Our search allowed one missed cleavage during trypsin digestion. For tandem mass spectrometry we used the default setting of a precursor-ion mass tolerance of 0.6 Da. The molecular weight search (MOWSE) score that indicated a significant hit was dependent on that database: scores higher than 41 and 45 were significant ($p<0.05$) for a search in the *Mytilus edulis* EST library and NCBI respectively. In addition, we only accepted positive identifications that included at least two matched peptides regardless of MOWSE score.

Exploratory statistical analysis

Aforementioned, in order to determine the effect of acute heat shock during seawater immersion on the posterior adductor muscle proteome between the two congeneric species of mussel within the genus *Mytilus*, we conducted a One-way ANOVA ($p<0.05$) based on 1,000 permutations. Protein spots determined to exhibit significantly different variations in protein expression, i.e., protein abundance patterns, among individual adductor muscle gels across temperature treatments were then compared using average-linkage clustering utilizing a Pearson correlation metric (Berth et al., 2007). Hierarchical clusters generated from this analysis were then implemented to group significant proteins which were observed to share similar patterns in protein expression across temperature treatments (Eisen et al., 1998). In order to determine and better understand the contribution of specific significant proteins to the variation observed

between the different temperature treatments, we conducted principal component analyses (PCA) (Delta 2D). Protein spot intensities within all gel images were transformed into vector components and used to plot each adductor gel image along principal component axes. These principal components are projections of spot intensities within a two-dimensional space, which explain the percent variation that exists between the different temperature treatments with respect to protein abundance. Significant identified proteins were then assigned component loading values, i.e., eigenvalues. These values are numeric representations of the relative magnitude to which a particular protein contributes to sample, i.e., gel image, separation along a given component. Boundaries were made in order to enclose all samples within a temperature treatment. Temperature treatment groups which exhibited a high degree of overlap were suggested to confer similar changes in protein abundance patterns in response to immersed heat stress (Tomanek and Zuzow, 2010).

References

Berth, M., Moser, F. M., Kolbe, M. Bernhardt, J. (2007). The state of the art in the analysis of two-dimensional gel electrophoresis images. *Applied Microbiology Biotechnology*. **76**, 1223-1243.

Buckley, B. A., Owen, M.-E. and Hofmann, G. E. (2001). Adjusting the thermostat: the threshold induction temperature for the heat-shock response in intertidal mussels (genus *Mytilus*) changes as a function of thermal history. *Journal of Experimental Biology*. **204**, 3571-3579.

Eisen, M. B., Spellman, P. T., Brown, P. O., and Botstein, D. (1998). Cluster analysis and display of genome-wide expression patterns. *Proc. Natl. Acad. Sci. USA. Genetics*. **95**, 14863-14868.

Fields, A. P., Zuzow, M. J., Tomanek, L. (2011). Proteomic responses of blue mussels (Mytilus) congeners to temperature acclimation. *The Journal of Experimental Biology* **215**, 1106-1116.

Harley, C. D. G. (2008). Tidal dynamics, topographic orientation, and temperature-mediated mass mortalities on rocky shores. *Marine Ecology Progress Series*. **371**, 37-46.

Lockwood, B. L., Sanders J. G. and Somero, G. N. (2010). Transcriptomic responses to heat stress in invasive and native blue mussels (genus *Mytilus*): molecular correlates of invasive success. *Journal of Experimental Biology*. **213**, 3548-3558.

Lockwood, B. L., and Somero, G. N. (2011). Invasive and native blue mussels (genus *Mytilus*) on the California coast: The role of physiology in biological invasion. *Journal of Experimental Marine Biology and Ecology* **400**, 167-174.

Lovrić, J. (2011). Introducing proteomics: from concepts to sample separation, mass spectrometry and data analysis. John Wiley & Sons. West Sussex, UK.

Petes, L. E., Menge, B. A. and Murphy, G. D. (2007). Environmental stress decreases survival growth, and reproduction in New Zealand mussels. *Journal of Experimental Marine Biology and Ecology*. **351**, 81-91.

Roberts, D. A., Hofmann, G. E. and Somero, G. N. (1997). Heat-shock protein expression in *Mytilus californianus*: acclimatization (seasonal and tidal-height comparisons) and acclimation effects. *Biology Bulletin* **192**, 309-320.

Tomanek, L., Zuzow, M. J. (2010). The proteomic response of the mussel congeners *Mytilus trossulus* and *M. galloprovincialis* to acute heat stress: implications for thermal tolerance and metabolic costs of thermal stress. *Journal of Experimental Biology.* **213**, 3559-3574.

Supplemental Information

Table S1. Identification of proteins exhibited to significantly change abundance within the adductor muscle of *Mytilus galloprovincialis*, in response to acute heat shock under seawater immersion (One-way permutation ANOVA, $p < 0.05$). Estimated molecular weights (MW) and isoelectric points (pI) were quantified utilizing the corresponding fusion gel image (See Figure 12A). Predicted molecular weights and isoelectric points were obtained through expressed sequence tag database searches of orthologous protein matches (SIB Swiss Institute of Bioinformatics). For clarity, proteins have been further grouped into separate categories based on molecular function. "*" corresponds to proteins which were not found to exhibit significant changes in abundance through post-hoc analysis (Tukey pairwise comparison, $p < 0.05$. See Figures 5-10).

Spot ID	Protein ID	Estimated MW (kDa)	Estimated pI	Predicted MW (kDa)	Predicted pI	GenBank ID	Mascot Score	Peptide Matches	Sequence Coverage(%)	Functional Category
12	Calponin	68.00	6.48	44.51	6.85	gi14422379	72	4	6	Actin-Myosin Binding Complex
13	Calponin	68.00	6.61	43.35	6.84	gi405975242	185	5	16	Actin-Myosin Binding Complex
18	Calponin	60.00	6.83	44.51	6.85	gi14422379	92	4	8	Actin-Myosin Binding Complex
20	Calponin	54.00	6.83	44.51	6.85	gi14422379	84	4	12	Actin-Myosin Binding Complex
21	Calponin	55.00	6.90	44.51	6.85	gi14422379	434	9	14	Actin-Myosin Binding Complex
22	Calponin	54.00	6.62	44.51	6.85	gi14422379	70	3	10	Actin-Myosin Binding Complex
23	Calponin	54.00	6.51	44.51	6.85	gi14422379	90	3	4	Actin-Myosin Binding Complex
24	Troponin-T	52.00	6.43	20.66	5.00	gi405965308	49	4	6	Actin-Myosin Binding Complex
31	Calponin	23.00	5.78	44.51	6.85	gi14422379	85	4	4	Actin-Myosin Binding Complex
47	Myosin regulatory light chain	18.00	4.45	19.55	4.68	gi405964694	86	3	8	Actin-Myosin Binding Complex
7	β-Actin	80.00	6.34	41.86	5.30	gi341579620	118	4	11	Cytoskeletal
37	β tubulin	67.00	5.05	50.00	4.73	gi390349564	272	7	11	Cytoskeletal
38	β tubulin	67.00	5.09	50.00	4.73	gi390349564	63	3	6	Cytoskeletal
39	β tubulin	67.00	5.07	50.00	4.76	gi405959361	106	5	9	Cytoskeletal
40	β tubulin	67.00	5.17	50.00	4.73	gi390349564	204	6	11	Cytoskeletal
46	Actin-2	43.00	5.19	41.77	5.30	gi405973339	62	3	7	Cytoskeletal
25	NAD-dependent-isocitrate dehydrogenase mitochondrial (α-subunit)	52.00	5.85	39.63	5.44	gi405968311	86	2	2	Energy Metabolism
29	Apextrin-like protein	38.00	6.27	24.39	8.42	gi339785142	66	2	7	Immune Response
6	Heat shock protein 70	81.00	6.08	69.69	5.50	gi405964548	325	6	26	Molecular Chaperone
15	Aldehyde dehydrogenase (mitochondrial)	66.00	6.29	56.93	6.18	gi405965075	109	3	3	Oxidative Stress
27	Guanine nucleotide-binding protein (β-subunit)	46.00	5.80	37.31	5.62	gi405963261	106	5	4	Signal Transduction
28	Guanine nucleotide-binding protein (β-subunit)	47.00	5.98	37.31	5.62	gi405963261	251	5	4	Signal Transduction
2	Filamin-C	96.00	6.20	32.35	5.54	gi405962873	391	10	6	Thin Filament Regulation
3	Filamin-C	97.00	6.68	32.35	5.54	gi405962873	143	4	4	Thin Filament Regulation
8	Actin-interacting protein 1	77.00	6.82	65.32	6.68	gi405966870	141	5	3	Thin Filament Regulation
36	Filamin-C	98.00	6.90	32.35	5.54	gi405962873	56	2	2	Thin Filament Regulation
41	Tropomyosin	53.00	4.66	33.00	4.57	gi219806594	96	5	14	Thin Filament Regulation
42	Tropomyosin	52.00	4.70	32.71	4.48	gi290794772	157	5	14	Thin Filament Regulation
43	Tropomyosin	49.00	5.18	32.65	4.57	gi83715932	158	5	14	Thin Filament Regulation
49	Fascin	68.00	6.36	55.57	6.21	gi405961655	192	6	8	Thin Filament Regulation
17	Rab GDP-dissociation inhibitor (β)	62.00	6.54	50.00	5.57	gi405976470	75	4	6	Vessicle Trafficking/Signal Transduction

Table S2. Identified proteins which exhibited significant abundance changes in response to acute heat stress while under seawater immersion within the adductor muscle tissue of *Mytilus trossulus* (One-way permutation ANOVA' $p < 0.05$). "*" corresponds to proteins which were not found to exhibit significant changes in abundance through post-hoc analysis (Tukey pairwise comparison, $p < 0.05$. See Figures 5-10).

Spot ID	Protein ID	Estimated MW (kDa)	Estimated pI (pH)	Predicted MW (kDa)	Predicted pI	GenBank ID	Mascot Score	Peptide Matches	Sequence Coverage(%)	Functional Category
11	Calponin	69.00	6.44	44.51	6.85	gi14422379	103	3	12	Actin-Myosin Binding Complex
12	Calponin	68.00	6.70	43.35	6.84	gi405975242	69	2	7	Actin-Myosin Binding Complex
28	Calponin	54.00	6.66	44.51	6.85	gi14422379	317	8	17	Actin-Myosin Binding Complex
30	Troponin-T	54.00	5.94	20.66	5.00	gi405965308	170	5	7	Actin-Myosin Binding Complex
31	Troponin-T	54.00	6.00	20.66	5.00	gi405965308	140	4	7	Actin-Myosin Binding Complex
33	Troponin-T	54.00	6.10	20.66	5.00	gi405965308	100	3	6	Actin-Myosin Binding Complex
34	Calponin	53.00	6.44	44.51	6.85	gi14422379	217	4	9	Actin-Myosin Binding Complex
37	Troponin-T	52.00	6.25	20.66	5.00	gi405965308	140	4	6	Actin-Myosin Binding Complex
39	Troponin-T	52.00	6.23	20.66	5.00	gi405965308	115	3	6	Actin-Myosin Binding Complex
49	Calponin	47.00	5.10	44.51	6.85	gi14422379	115	3	4	Actin-Myosin Binding Complex
53	Calponin	37.00	6.62	44.51	6.85	gi14422379	88	3	4	Actin-Myosin Binding Complex
15	β-tubulin	65.00	5.06	49.96	4.74	gi45598623	132	5	8	Cytoskeletal
16	β-tubulin	64.00	5.14	49.96	4.74	gi45598623	422	12	13	Cytoskeletal
18	Collagen (α-VI chain)	64.00	5.96	206.00	5.81	gi405958346	135	3	7	Cytoskeletal
19	Actin	66.00	6.20	41.77	5.29	gi32816054	57	3	7	Cytoskeletal
25	Collagen (α-VI chain)	61.00	6.24	206.00	5.81	gi405958346	123	3	8	Cytoskeletal
26	Actin-2	57.00	5.43	41.71	5.30	gi18565104	460	7	19	Cytoskeletal
27	Actin-2	57.00	6.38	41.77	5.30	gi405973339	56	2	5	Cytoskeletal
29	Actin	54.00	6.43	41.74	5.30	gi405964579	304	5	12	Cytoskeletal
32	Actin	54.00	5.88	41.74	5.30	gi405964579	92	3	7	Cytoskeletal
35	Actin	54.00	5.91	41.78	5.29	gi238683607	172	4	10	Cytoskeletal
36	Actin	53.00	6.14	41.74	5.30	gi405964579	214	4	10	Cytoskeletal
38	Actin-2	52.00	6.35	41.77	5.30	gi405973339	179	5	13	Cytoskeletal
40	Actin-2	52.00	6.05	41.77	5.30	gi405973339	170	4	10	Cytoskeletal
41	Actin	52.00	6.09	41.74	5.30	gi405964579	128	4	8	Cytoskeletal
43	Actin	50.00	5.72	17.20	5.20	gi338808655	80	2	18	Cytoskeletal
55	Short-chain collagen	44.00	5.25	25.01	7.02	gi405969715	205	5	9	Cytoskeletal
67	Actin	39.00	5.14	41.77	5.29	gi32816054	76	4	8	Cytoskeletal
76	Actin	35.00	5.93	17.19	5.20	gi338808655	84	2	18	Cytoskeletal
1	Transglutaminase	98.00	6.48	82.84	5.92	gi19702209	52	3	4	Energy Metabolism
23	ATP synthase (F1, β-subunit)	63.00	5.06	55.07	5.33	gi307181472	339	10	20	Energy Metabolism
54	Pyruvate dehydrogenase (E1 component, β)	44.00	5.64	39.39	6.03	gi225707590	69	3	5	Energy Metabolism
60	Purine nucleoside phosphorylase	41.00	5.65	36.22	6.67	gi405969123	228	4	12	Energy Metabolism
64	Purine nucleoside phosphorylase	39.00	6.23	36.22	6.67	gi405969123	176	6	17	Energy Metabolism
77	Adenylate kinase	34.00	6.35	99.78	8.57	gi405972862	49	2	2	Energy Metabolism
47	Heavy metal binding protein	48.00	6.08	26.86	5.09	gi38635428	102	3	11	Heavy Metal Transport (Cations)
82	Ferritin	26.00	5.08	18.96	5.12	gi343455265	42	2	7	Iron Storage
4	Heat shock protein 70	81.00	6.01	69.69	5.50	gi405964548	131	5	15	Molecular Chaperone
44	Small heat shock protein	49.00	6.55	21.36	5.79	gi301070146	76	3	14	Molecular Chaperone
45	Small heat shock protein	50.00	6.70	21.66	5.76	gi399894425	92	3	14	Molecular Chaperone
61	Small heat shock protein	40.00	5.24	28.52	5.61	gi347545633	83	3	7	Molecular Chaperone
62	Small heat shock protein	40.00	6.00	28.52	5.61	gi347545633	64	3	7	Molecular Chaperone
65	Small heat shock protein	40.00	5.79	28.52	5.61	gi347545633	236	7	17	Molecular Chaperone
78	Kyphoscoliosis peptidase	34.00	6.45	24.01	7.64	gi405970056	110	3	13	Myofibril Development
9	NADPH-dependent Aldehyde reductase	71.00	5.14	41.19	5.51	gi340375086	118	4	3	Oxidative Stress
13	S-adenosylmethionine-dependent methyltransferase	38.00	6.55	35.93	8.34	gi405953767	178	3	19	Oxidative Stress
20	Aldehyde Dehydrogenase (mitochondrial)	66.00	6.22	563.40	7.00	gi178390	70	3	5	Oxidative Stress
92	Cu-Zn Superoxide dismutase	20.00	6.37	15.77	5.85	gi215263232	69	2	3	Oxidative Stress
94	Fatty acid-binding protein	13.00	5.03	14.92	4.98	gi405951541	85	2	8	Oxidative Stress
7	Phenylalanyl-tRNA synthetase (β-chain)	81.00	6.49	66.11	5.06	gi56090156	57	4	4	Protein Synthesis
52	Guanine nucleotide-binding protein (β-subunit)	32.00	6.57	37.31	5.62	gi405963261	52	3	2	Signal Transduction
59	14-3-3 protein	42.00	5.89	28.85	4.78	gi324506362	119	4	3	Signal Transduction
63	14-3-3 protein	40.00	5.09	28.85	4.78	gi324506362	102	3	3	Signal Transduction
10	Fascin	69.00	6.29	55.57	6.21	gi405961655	141	5	7	Thin Filament Regulation
21	Profilin	15.00	5.62	15.27	6.10	gi47551153	116	3	7	Thin Filament Regulation
24	Gelsolin	60.00	5.05	42.00	5.22	gi41349563	200	5	9	Thin Filament Regulation
46	F-actin capping protein (α-subunit)	49.00	6.44	21.36	5.79	gi301070146	132	4	19	Thin Filament Regulation
88	Whirlin	21.00	6.01	16.65	6.40	gi405968329	67	4	8	Thin Filament Regulation
90	Transgelin	20.00	6.73	22.47	6.35	gi405967947	219	4	12	Thin Filament Regulation
22	Rab GDP dissociation inhibitor (β)	62.00	6.46	50.00	5.57	gi405976470	285	6	6	Vessicle Trafficking/Signal Transduction

Table S3. Identification of proteins which did not exhibit significant changes in terms of protein abundance, in response to acute heat shock while under seawater immersion within the adductor muscle of *Mytilus galloprovincialis* (One-way permutation ANOVA; $p < 0.05$).

Spot ID	Protein ID	MW (kDa) Estimated	pI Estimated	MW (kDa) Predicted	pI Predicted	GenBank ID	Mascot Score	Peptide Matches	Sequence Coverage(%)	Functional Category
100	Calponin-like protien	44.51	6.85	64.00	6.72	gi14422379	68	1	5	Actin-Myosin Binding Complex
103	Actin 2	32.04	5.66	57.00	5.78	gi18565104	194	3	11	Cytoskeletal
108	Calponin-like protein	44.51	6.85	58.00	6.63	gi14422379	122	4	16	Actin-Myosin Binding Complex
112	Calponin-like protein	44.51	6.85	54.00	6.58	gi14422379	142	4	17	Actin-Myosin Binding Complex
114	Actin 2	41.72	5.30	54.00	6.25	gi18565104	82	2	8	Cytoskeletal
115	Actin 2	41.72	5.30	54.00	6.42	gi18565104	117	2	8	Cytoskeletal
118	Actin 2	41.72	5.30	54.00	6.12	gi18565104	155	2	8	Cytoskeletal
119	Actin 2	41.72	5.30	54.00	6.02	gi18565104	104	2	8	Cytoskeletal
120	Troponin-T	20.66	5.00	53.00	6.33	gi40596530	72	3	13	Actin-Myosin Binding Complex
122	Tubulin alpha 1C chain	50.01	4.94	53.00	6.26	gi405965638	171	4	17	Cytoskeletal
124	Troponin-T	20.66	5.00	52.00	6.14	gi40596530	79	3	13	Actin-Myosin Binding Complex
125	Troponin-T	20.66	5.00	52.00	6.22	gi40596530	157	4	13	Actin-Myosin Binding Complex
126	Troponin-T	20.66	5.00	53.00	6.54	gi2541910	59	4	13	Actin-Myosin Binding Complex
127	Troponin-T	38.42	5.20	52.00	5.99	gi2541910	82	2	9	Actin-Myosin Binding Complex
128	Troponin-T	20.66	5.00	51.00	5.75	gi40596530	94	3	13	Actin-Myosin Binding Complex
130	Troponin-T	20.66	5.00	52.00	5.92	gi40596530	100	3	13	Actin-Myosin Binding Complex
133	Cystolic malate dehydrogenase	36.39	6.02	49.00	6.19	gi73656362	75	3	6	Energy Metabolism
134	Fructose-1,6-bisphosphatase	36.76	6.25	49.00	5.91	gi405966541	65	3	10	Energy Metabolism
135	Cystolic malate dehydrogenase	36.39	6.02	48.00	6.46	gi73656362	145	3	9	Energy Metabolism
141	Uncharazterized protein yfeX	39.57	5.96	43.00	6.59	gi405970525	144	3	12	Unknown
149	small heat shock protein 24.1	28.52	5.61	41.00	6.42	gi347545633	85	3	19	Molecular Chaperone
189	Transgelin-2	22.47	6.35	22.00	6.70	gi405967947	133	2	10	Thin Filament Regulation
204	Filamin-A	90.71	6.15	97.00	6.79	gi405975785	89	1	7	Thin Filament Regulation
205	Filamin-A	90.71	6.15	97.00	6.86	gi405975785	100	1	7	Thin Filament Regulation
208	78 kDa Glucose-regulated protein	72.98	5.02	87.00	5.10	gi405968607	101	2	11	Molecular Chaperone
210	Collagen-Alpha-5(VI) chain	206.00	5.81	80.00	5.24	gi402861601	200	3	19	Cytoskeletal
213	Collagen-Alpha-5(VI) chain	206.00	5.81	79.00	5.18	gi402861601	145	3	19	Cytoskeletal
217	NADPH-dependent methlyglyoxal reductase GRP2-like	27.23	5.41	73.00	5.13	gi390363789	72	3	12	Oxidative Stress
218	bifunctional dihydroflavonol 4-reductase/flavanone 4-reductase-like	52.51	6.45	73.00	5.17	gi39035321	103	3	12	Oxidative Stress
220	bifunctional dihydroflavonol 4-reductase/flavanone 4-reductase-like	52.51	6.45	73.00	5.20	gi39035321	99	3	12	Oxidative Stress
222	tubulin alpha chain	40.45	6.20	70.00	5.25	gi568249318	99	3	17	Cytoskeletal
223	Actin	32.03	5.66	68.00	5.43	gi523569569	232	5	18	Cytoskeletal
225	tubulin alpha chain	40.45	6.20	69.00	5.29	gi568249318	156	4	17	Cytoskeletal
226	Actin 2	41.72	5.30	67.00	5.38	gi18565104	112	2	8	Cytoskeletal
237	Actin	32.03	5.66	57.00	5.45	gi523569569	389	7	30	Cytoskeletal
239	Actin	25.21	5.18	57.00	5.25	gi167683056	143	3	11	Cytoskeletal
240	Beta-actin	29.32	4.99	57.00	5.20	gi312106932	242	5	18	Cytoskeletal
242	Actin	53.00	6.02	57.00	5.14	gi385145402	65	2	8	Cytoskeletal
265	Collagen-Alpha-5(VI) chain	247.90	5.94	82.00	5.30	gi405975735	158	3	22	Cytoskeletal
270	Actin	32.03	5.66	57.00	5.66	gi523569569	324	5	18	Cytoskeletal

Table S4. Identification of proteins which did not exhibit significant changes in terms of protein abundance, in response to acute heat shock while under seawater immersion within the adductor muscle of *Mytilus trossulus* (One-way permutation ANOVA; $p < 0.05$).

Spot ID	Protein ID	MW (kDa) Estimated	pI Estimated	MW (kDa) Predicted	pI Predicted	GenBank ID	Mascot Score	Peptide Matches	Sequence Coverage(%)	Functional Category
98	Kyphoscoliosis peptidase	32.94	5.86	34.00	6.81	gi405955275	165	6	27	Myofibril Development
99	Filamin-C	323.54	5.54	98.00	6.12	gi405962873	63	3	12	Thin Filament Regulation
100	Filamin-A	90.71	6.15	101.00	6.67	gi405975785	130	3	2	Thin Filament Regulation
101	Filamin-A	90.71	6.15	101.00	6.61	gi405975785	169	4	3	Thin Filament Regulation
105	Filamin-A	90.71	6.15	101.00	6.93	gi405975785	56	2	5	Thin Filament Regulation
109	78 kDa glucose-regulated protein	72.98	5.02	84.00	5.13	gi405968607	205	5	6	Molecular Chaperone
110	78 kDa glucose-regulated protein	72.98	5.02	85.00	5.11	gi405968607	74	3	4	Molecular Chaperone
115	Heat Shock Protein 70	69.69	5.50	82.00	6.10	gi405964548	71	2	8	Molecular Chaperone
123	Heat Shock Protein 70	75.70	6.12	82.00	6.23	gi66766196	124	3	4	Molecular Chaperone
131	Actin-interacting protein 1	64.84	5.99	78.00	6.76	gi524883288	95	4	3	Thin Filament Regulation
138	Fascin	55.57	6.21	68.00	6.40	gi405961655	132	5	9	Thin Filament Regulation
139	Actin	41.90	5.30	70.00	6.06	gi47116419	88	3	7	Cytoskeletal
141	Fascin	55.58	6.21	69.00	6.49	gi405961655	119	3	6	Thin Filament Regulation
142	Actin	41.84	5.36	68.00	5.77	gi47116422	125	3	7	Cytoskeletal
143	Actin	41.84	5.36	70.00	6.08	gi47116422	110	4	10	Cytoskeletal
146	Dihydrolipyl dehydrogenase (mitochondrial)	53.75	7.97	68.00	6.56	gi657550813	92	2	4	Energy Metabolism
148	Tubulin alpha chain	57.07	5.29	66.00	5.34	gi674261674	225	7	10	Cytoskeletal
152	Collagen alpha-4(VI) chain	49.62	6.03	66.00	5.41	gi524882700	161	6	11	Cytoskeletal
157	Tubulin beta chain	49.96	4.74	64.00	6.01	gi459182867	110	6	11	Cytoskeletal
158	Actin	17.96	5.20	66.00	5.77	gi338808655	97	2	18	Cytoskeletal
159	Enolase	47.70	5.99	64.00	6.16	gi332025671	182	5	3	Glycolysis
162	Tubulin alpha 1a	27.64	5.03	66.00	5.31	gi669687871	70	2	13	Cytoskeletal
163	Tubulin alpha	20.78	5.30	65.00	5.35	gi72533710	75	1	13	Cytoskeletal
171	Gelsolin	42.63	7.18	60.00	6.36	gi390348627	85	3	4	Thin Filament Regulation
175	Actin	41.82	5.30	60.00	5.95	gi113273	334	6	14	Cytoskeletal
178	Isocitrate dehydrogenase (NADP-dependent)	50.40	7.10	58.00	6.63	gi385268559	70	3	14	Energy Metabolism
179	Actin	41.84	5.36	61.00	6.00	gi47116422	332	6	14	Cytoskeletal
182	Actin	41.84	5.36	56.00	5.34	gi47116422	272	6	14	Cytoskeletal
183	Actin	41.83	5.30	57.00	6.25	gi3421457	207	6	14	Cytoskeletal
185	Calponin	44.51	6.85	53.00	6.49	gi14422379	113	5	9	Actin-Myosin Binding Complex
187	Actin	41.82	5.30	54.00	6.07	gi113273	134	3	7	Cytoskeletal
191	Tropomyosin	32.75	4.62	51.00	4.69	gi6647862	296	6	16	Thin Filament Regulation
196	Cystolic malate dehydrogenase	36.37	6.02	48.00	6.37	gi73656269	92	2	6	Energy Metabolism
198	Heavy Metal Binding Protein	26.86	5.09	47.00	5.18	gi38635428	86	2	7	Heavy Metal Transport (Cations)
205	Malate dehydrogenase (Mitochondrial)	36.29	7.63	46.00	6.64	gi524878973	144	5	7	Energy Metabolism
207	Uncharacterized protein yfeX	30.30	5.04	44.00	5.37	gi405970525	64	2	9	Unknonwn
210	Actin	41.74	5.30	44.00	5.03	gi325297142	59	2	9	Cytoskeletal
215	Uncharacterized protein yfeX	39.57	5.96	43.00	6.50	gi405978693	121	4	14	Unknonwn
216	Actin	41.72	5.30	42.00	5.20	gi405964580	99	2	5	Cytoskeletal
219	small heat shock protein 24.1	28.52	5.61	41.00	5.88	gi347545633	92	2	5	Molecular Chaperone
221	Adenylate kinase Isoenzyme 1	23.32	6.01	40.00	4.82	gi405972863	85	2	11	Energy Metabolism
244	Heterongenous nuclear ribonucleoprotein 27C	58.88	8.32	30.00	5.86	gi405977312	64	4	16	mRNA Transport
259	Myosin regulatory light chain	19.74	4.64	17.00	4.49	gi524878458	111	6	15	Actin-Myosin Binding Complex
268	Heterongenous nuclear ribonucleoprotein (A/B)	36.83	5.00	13.00	5.38	gi22364910	170	3	13	mRNA Transport
271	Fatty acid-binding protein	14.92	4.98	11.00	4.95	gi405951541	118	4	16	Oxidative Stress
272	Fatty acid-binding protein	14.92	4.98	10.00	5.19	gi405951541	108	3	11	Oxidative Stress
276	Filamin-A	90.71	6.15	101.00	6.56	gi405975785	141	4	3	Thin Filament Regulation
280	Heat Shock Protein 70	69.47	5.36	82.00	5.86	gi76780606	89	3	3	Molecular Chaperone
282	Calponin	44.51	6.85	59.00	6.88	gi14422379	80	3	16	Actin-Myosin Binding Complex

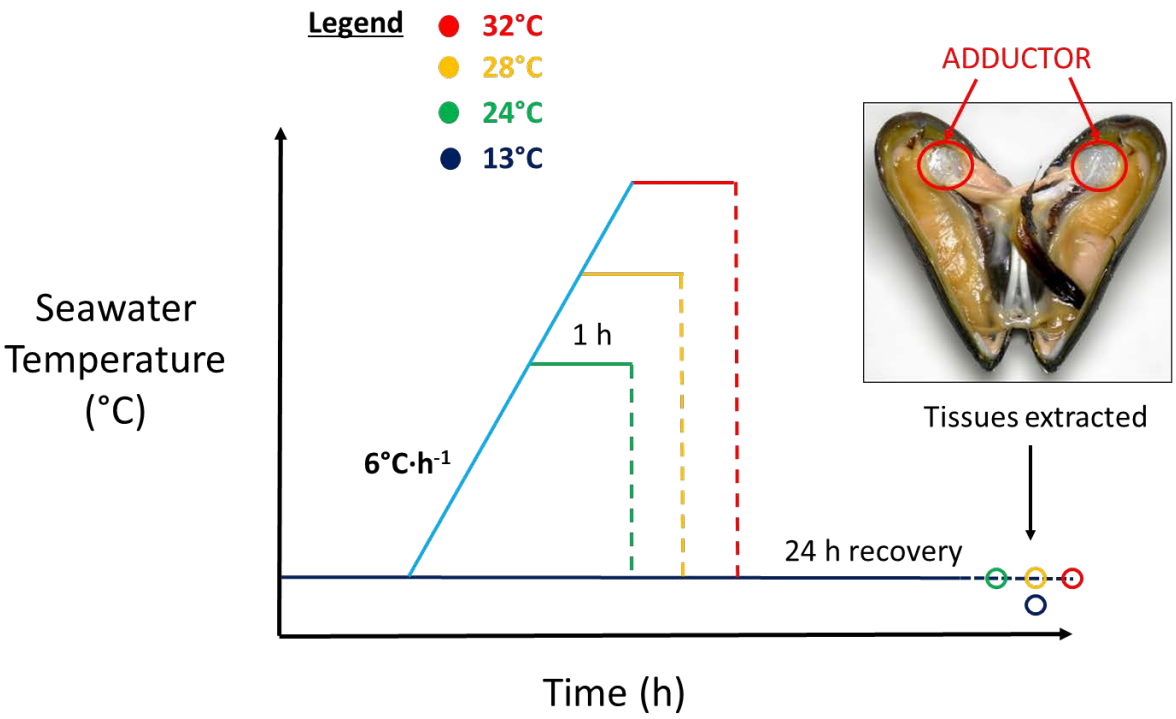

Figure S1. Experimental design. Following acclimation to 13°C, mussels were exposed to 24°C, 28°C and 32 °C (at a heating rate of 6C/h), kept mussels at the temperature for 1 h and then added a 24-h recovery period at 13°C. Adductor mussel samples were then extracted and flash-frozen for subsequent proteomic analysis.